A Framework for Vibration based Damage Detection of Bridges under Varying Temperature Effects using Artificial Neural Networks and Time Series Analysis

by

Branislav Kostić

A thesis submitted in partial fulfillment of the requirements for the degree of

Master of Science

in

Structural Engineering

Department of Civil and Environmental Engineering

University of Alberta

Abstract

Structural Health Monitoring (SHM) has become a very important area in civil engineering for evaluating the performance of critical civil infrastructure systems such as bridges. One of the most important issues with continuous SHM is the environmental effects (such as temperature, humidity, wind) on the measurement data, which can produce bigger effects in the response of the structures than the damage itself. Damage detection is considered as one of the most important components of SHM and without appropriately considering the environmental factors in the damage detection process, the efficiency and accuracy of this process may be questionable for practical applications. Temperature is considered as one of the most important and influential environmental effects on structures, especially in bridges. In this study, an artificial neural network based approach integrated with a sensor clustering based time series analysis is employed for damage detection under the temperature effects. Damage features from the time series analysis method (will be referred as DF_{ARX}) can indicate the damage, if there is no presence of detrimental temperature effect. However, if present, temperature effect can lead to false indication of the damage existence in the structure. Neural network damage features (DF_{ANN}) are used to compensate these effects. Final damage features (DF) are computed as absolute difference between these two damage features. The proposed methodology is applied to a footbridge finite element model and it is demonstrated that the method can successfully determine the existence, location and extent of the damage for different types of damage cases under environmental temperature variability, and with different levels of the noise. Finally, recommendations for the future work, as well as the limitations of the proposed methodology are addressed.

Acknowledgements

First of all, I would like to thank my supervisor, Dr. Mustafa Gül, for his sincere mentorship and guidance throughout my study and research. His passion for research was a big help through all stages of my thesis.

I would like to thank the members of my examining committee, Dr. J.J. Roger Cheng and Dr. Robert Driver, for their time in reviewing this thesis and their valuable suggestions.

Many thanks to all of the members of SHM group at the University of Alberta for their support and friendship: Ngoan Do Tien, Jianfeng Gu, Qipei Mei, Aimee De Laurentiis, Saeideh Fallah Nafari, Lihua Zhang, Haiyang Zhang and Lomere Mori.

I would like to thank my parents and my sister for believing in me, and for giving me the opportunity to study at the University of Alberta.

Finally, I wish to give my special thanks to my wife Nataša, for her endless support, understanding and patience, and to my son Marko, who was my main motivation through this research.

Table of Contents

List of Tables

List of Figures

List of Symbols

$y(t)$	Output of ARX model
$u(t)$	Input of ARX model
$e(t)$	Error term of ARX model
C	Damping Matrix
M	Mass matrix
K	Stiffness Matrix
$x_i(t)$	Displacement of the i^{th} degree of freedom
$\dot{x}_i(t)$	Velocity of the i^{th} degree of freedom
$\ddot{x}_i(t)$	Acceleration of the i^{th} degree of freedom
$n^{k+1}(i)$	Net input to unit I in layer k+1 of in Backpropagation algorithm
$a^{k+1}(i)$	Output of unit i in Backpropagation algorithm
J	Jacobian Matrix
FR	Fit Ratio of ARX model
DF_{ARX}	Damage Feature from the ARX model
DF_{ANN}	Damage Feature from the Neural Network
DF	Final Damage Feature

CHAPTER 1:INTRODUCTION

1.1 Introduction to Structural Health Monitoring

Due to the complex and progressing problem of deterioration of aging civil infrastructure, Structural Health Monitoring (SHM) has become a very important area in civil engineering for assessing the performance of civil infrastructure systems. SHM is considered to be one of the most critical components of civil infrastructure management for providing an objective, versatile, and innovative decision-making support tool for infrastructure owners and decision-makers to increase the safety and reliability of our infrastructure system. Bridges are among the most critical infrastructures and most of them are reaching or have already reached their life span. In Canada one-third of 75,000 highway bridges are with structural or functional deficiencies (NRCC 2013). Similarly, the most recent Report Card for America's Infrastructure (2013) graded the US infrastructure with a D+, and C+ for bridges (one in nine of the nation's bridges are rated as structurally deficient).

Although the SHM is a relatively new concept in bridge engineering community, testing of bridge structures dates before 1900s (ISIS Canada 2001). SHM methodology can be very effective in complementing the visual inspection techniques for determination of condition of structures. Condition of the bridge network can be improved by continuous evaluation of bridges using SHM systems. Continuous monitoring of bridges improves safety, reduces response time and it has economic impact on the bridge maintenance practices. Besides the regular continuous monitoring of the structures, SHM can be utilized after the incidental events, such as earthquakes. SHM can then provide relevant information on the new condition of the structure, and determine its operational safety.

Structural Health Monitoring (SHM) term can be defined in many ways. For example, Wenzel (2009) indicates that *"SHM is the implementation of a damage identification strategy to the civil engineering infrastructure"*. Karbhari and Ansari (2009) define SHM as *"an attempt at deriving knowledge about the actual condition of a structure"*. According to Sohn and Farrar (2000), "*SHM is best studied in the context of a statistical pattern recognition paradigm*", composed of the following components:

1. Operational Evaluation;

2. Data Acquisition;

3. Feature Extraction;

4. Statistical Model Development.

Operational Evaluation comprises several steps of SHM process. Data acquisition system is specified based on the adopted methodology. Also, damage features are defined for damage detection algorithm.

In *Data Acquisition* part, response of the structure is recorded and transmitted. Cleansing process can also be performed. If necessary, compression of data and data fusion from multiple sources can be conducted. Data is either archived or used simultaneously with the process. Deciding on excitation method is also an important part of data acquisition process. Forced excitation can be used in the form shakers, or other impacting devices. Another option is to use ambient excitation of the structures – pedestrian or vehicular traffic for the bridge structures, wind load, etc.

Feature extraction process determines features that indicate the presence of damage in a structure. Sets of data measured on the structure are transformed to a different form, which can indicate the damage. As an example, damage features in vibration based models can take different forms: coherence functions, modal strain energy, modal assurance criteria, etc.

Final step includes use of *statistical models* in order to separate damage features from damaged and undamaged states. Considering that the damage features can be sensitive to other factors than the damage, normalization can be conducted.

If damage detection methodology includes input data and desired output data, that type of learning is considered supervised learning. Unsupervised learning refers to methodologies with input data only. For bridge structures, it is usually very impractical to retrieve desired output data, therefore unsupervised learning is preferred.

Another classification of methods can be done depending on whether the physical models or models based on data are used (Aktan et al. 1999; Worden and Manson 2007). Former group of methods belongs to the model-based methods, and the latter one to data-driven

methods. For example, finite element based models belong to the first group, considering that they are based on physical properties of the structure. On the other side, data-driven methods depend on data from the measurements only. Considering that there is no knowledge needed on structural system in second group of methods, these methods are more practical for continuous monitoring of bridges, even though model-based methods may provide more information in certain cases.

1.2 Damage Detection under Varying Environmental Conditions

Considering that all materials contain some defects (Worden et al. 2007) that can propagate during the lifetime of the structure, detecting these defects is of major importance for safe and proper service of the structures. Therefore, damage detection is considered as one of the most important components of SHM. In damage detection methods, global or local techniques can be used. The issue with the local techniques is that the approximate location of the damage should be known in advance, which is not always practical. On the other hand, such issues are minimized with vibration based global monitoring methods. These methods have been employed for a few decades (Doebling et al. 1996; Farrar and Jauregui 1998; Guan 2006; Fan and Qiao 2011; Brownjohn et al. 2011). They are based on the fact that modal characteristics of the structure are related to the physical characteristics of the structure (stiffness, mass, damping) and that any change in these characteristics would cause change in modal properties, causing the change in dynamic response of the structure. Vibration response of the structure is usually measured at several locations, and this data is then used for determination of modal parameters of the structure (or other damage features based on the dynamic characteristics of the structure), which can then be used for damage detection process.

One of the most important issues with vibration based continuous SHM is the environmental effects on the measurement data. This is especially true for civil infrastructure systems, such as bridges, where environmental factors, such as temperature, humidity and wind, can produce bigger effects in the response of the structure than the damage itself (Sohn 2007; Sohn and Oh 2009). Considering that the real damage can be masked by the environmental effects, this can lead to false conclusions on the damage. In

order to compensate environmental effects, one can use the measurements of the environmental data, or perform the analysis without direct measurement of these parameters. If measured, parameters should be determined from a wide range of different environmental conditions in order to comprehensively define baseline condition of the structure (Sohn 2007).

Temperature is considered the most significant and influential environmental effect on bridges. Temperature variation alters dynamic characteristics, such as natural frequencies, of the structure (Sohn et al. 1999), and affects the performance of the vibration based methodologies. As an example, Cornwell et al. (1999) presented that for the single span bridge structure, modal frequencies varied up to 6% over a 24-hour period. Temperature changes mainly affect the stiffness of the structure (Wood 1992; Khanukhov et al. 1986; Sabeur et al. 2007), and support conditions (Moorty and Roeder 1992; Sohn 2007; Siddique et al. 2007). Besides these two effects, temperature effects can cause additional thermal stresses in structures, which can also alter the vibration response of the structure. Without appropriately considering the environmental factors in the damage detection process, the efficiency and accuracy of this process may be questionable for practical applications.

Another difficulty for assessing the temperature effects on modal properties of structures is the non-uniform distribution of temperature in the structure, especially bridges. Bridges are usually designed as unique structures, with specific boundary conditions, geometry, location and types of loads (Wenzel 2009). Temperature distribution in bridges depends on orientation, shape and environment of the bridge structure. Therefore, this distribution will also be specific for different bridges. Moreover, surface temperatures are usually different compared to the inner temperature of the elements, because of the thermal inertia effect. It is also determined that temperature gradients provided in the codes are usually smaller than the measured temperature gradients for stiff structures (Wenzel 2009). All of these effects contribute to the randomness of the temperature distribution in the structure. Besides the environmental effects, operational effects, such as traffic, can have disturbing effect on the vibration measurements. However, changes in the operational conditions, and other environmental variable parameters, such as humidity

and wind, have not been considered in this study. These conditions can be included as future steps within the framework study presented here.

1.3 Objectives and Scope

As discussed above, vibration based damage detection methods can experience detrimental effects from variable environmental factors, since change in these factors influences dynamic response of the structure, and therefore alters the measured data. Therefore, in order to successfully perform damage detection process, these effects must be minimized. Temperature is considered as one of the most common and influential environmental effect. Thus, the objective of this thesis is to develop a damage detection framework based on the vibration response of the structure, where temperature effects on damage detection process are compensated. The developed framework uses a sensor clustering based time series analysis method for damage detection (Gül 2011) along with artificial neural networks for temperature compensation. After discussing the theoretical developments, the methodology is tested using the finite element of a footbridge.

1.4 Organisation of the Thesis

This thesis comprises following chapters:

- Chapter 2 includes literature review of relevant structural health monitoring research. Firstly, a variety of publications regarding the damage detection methods are discussed. Then, papers that consider the effect of environmental factor on bridges and damage detection methodologies are presented. Final publications presented in this chapter are the publications where compensation of these effects is discussed.
- In Chapter 3, time series analysis and backpropagation neural networks are briefly explained. Then, a novel methodology using these two components for compensation of temperature effects within damage detection algorithm is presented.
- Chapter 4 describes the footbridge model used for verification of the developed methodology, along with the analysis steps performed. Also, damage cases and temperature distribution used in the model are introduced.

- Chapter 5 includes damage detection analysis of the finite element footbridge model under variable temperature effects. Five damage cases are applied to the footbridge model under different temperature scenarios. The results of the proposed methodology are then presented.
- Chapter 6 presents conclusions about most relevant issues discussed in the thesis, and recommendations for the future work.

CHAPTER 2:LITERATURE REVIEW

Literature review of the most relevant structural health monitoring publications is presented in this chapter. Considering that this thesis focuses on temperature effect compensation in damage detection processes, papers regarding the damage detection methodologies are presented first. Following are the papers which analyze the environmental effects on bridges and damage detection methods. Finally, publications investigating compensation of environmental effects are presented.

2.1 Literature Review of Methods for Damage Detection

Damage detection is considered as one of the most important components of SHM. A variety of damage detection methods is presented in this section. According to Rytter (1993), damage detection methods can be used for different levels of assessment:

Level 1: Is there damage in the system (existence)?

Level 2: Where is the damage in the system (location)?

Level 3: How severe is the damage (extent)?

Level 4: How much useful (safe) life remains (prognosis)?

Pandey et al. (1991) analyzed cantilever and simply supported beam models, and concluded that changes in curvatures of the mode shapes can indicate the location of the damage. Hamey et al. (2004) confirmed that damage detection process can be conducted with curvature of the modes, which can be measured by the piezoelectric sensors.

Nakamura et al. (1998) investigated the application of neural-networks for damage detection process in a steel building structure. The structure was damaged under earthquake loads in Kobe, Japan in 1995. Vibration measurements were performed after the damage, and also after the repairs. State of the structure after the repairs was used as a baseline state. Neural-network based methodology was able to successfully identify locations of the damages that were subsequently repaired afterwards.

Lamb waves, as non-destructive methods, have also been used for damage detection algorithms. Lamb waves are used along with the piezoelectric sensors, which are power

efficient. Monnier et al. (2000) analyzed a plate-like composite structure for localization of flaws. They indicated that sensitivity of lamb waves with regards to the type of the damage can be improved with adjusting the excitation of the sensor. Kessler (2002) indicated that lamb waves are more sensitive to local damage, compared to the frequency response methods. It was also concluded that the shortcoming of these methods is that they require a mechanism for wave propagation. Sohn et al. (2003) successfully detected delamination damage case on composite plate with variable temperature effects and boundary conditions.

Yam et al. (2003) investigated a damage detection methodology applied to composite sandwich plate structures with crack damage. The methodology employed vibration data, wavelet transform and artificial neural networks (ANN). Damage features were based on the energy variation of wavelet signals before and after the damage, where neural networks were used for statistical pattern recognition. It was indicated that excitation signals should be consistent for the baseline and damaged case, and should contain sufficient number of frequency components.

Giraldo et al. (2006) analyzed an analytical model of a benchmark structure using the vibration data along with the applied noise. Structural properties were obtained from this data, and principal component analysis (PCA) was then applied. Damage indicator in this method is based on the residual error of PCA method. Damage was simulated in the analytical model as a loss of stiffness. It was concluded that particular damage detection techniques may not be applicable to all types of damages in different structures.

Bakhary et al. (2007) employed an ANN algorithm along with the substructure technique, in order to adapt the algorithm to be more sensitive to local damage in two span concrete slab model. With this method, ANN models were defined for each part of the substructure, and all of the substructure parts were analyzed progressively. ANN used modal frequencies and shapes as an input data. Eventually, the method successfully detected the damage, which was applied as a reduction of the local stiffness along the slab.

Mehrjoo et al. (2008) used a backpropagation neural network for the analysis of damage cases for joints of a truss bridge. Input data comprised natural frequencies and mode

shapes of the structure. It was indicated that five modes were sufficient for this algorithm to function, and that the average errors for the testing data were 1%.

Gül and Catbas (2009) investigated application of statistical pattern recognition based methods for damage detection process of a simply supported steel beam and a steel grid laboratory structure. AR models were defined based on the obtained vibration data, and were used along with the Mahalanobis distance in order to retrieve damage indicators for this method. Methodology was successful for most of the damage cases. Importance of proper determination of threshold values for damage indicators was emphasized.

Gül and Catbas (2011) introduced a time series analysis based damage detection algorithm. This process was based on determining Auto-Regressive models with eXogenous input (ARX) from the free vibration response of the structure. Important feature of this methodology is that the sensor nodes were grouped in different clusters. ARX models were then defined by vibration data from neighbour sensors within one sensor cluster, in order to predict behaviour of the reference sensor in the cluster. Damage features used in this methodology were the fit ratios of the ARX model. This methodology was applied to a four DOF numerical model, and to the steel grid laboratory model. It successfully determined the existence, location and extent of the damage (levels 1, 2 & 3 by Rytter (1993)).

Shiradhonkar and Shrikhande (2011) employed a finite element model updating method for determination of damage location in a moment resistant frame structure. Vibration data from the structure, initialized by several strong earthquakes, was used to obtain modal parameters needed for the updating algorithm. Possible effects of the noise on the updating process were also discussed.

Samali et al. (2012) investigated combination of artificial neural networks (ANN), frequency response functions (FRF) & principal component analysis (PCA) as a vibration based damage detection process. PCA was utilized to determine principal components of the difference between FRF components in damaged and undamaged state. PCA was also employed to compensate the noise effects of 10% applied in this study. ANN was finally used for damage detection, where FRFs from different locations in the baseline model were used for training of the network, and then for the simulation process. Similar

algorithms were employed by Li et al. (2011), Dackermann and Samali (2013) and Bandara et al. (2014).

Shu et al. (2013) analyzed a finite element model of a simply supported railway bridge. Acceleration and displacement data from the bridge were used for determination of the changes of variances and covariances between baseline and damaged condition of the structure. A backpropagation neural network was then trained with the data from pre-defined damage cases in order to successfully determine location and extent of the damage. Influence of noise and train properties is indicated. The methodology could successfully detect damage cases with reduction of element stiffness above 10%.

Fassois and Kopsaftopoulos (2013) discussed different statistical time series methods based on the vibration data, and applied them to a laboratory truss structure for damage detection. Time series methods were classified as non-parametric and parametric based methods, and properties of both groups were analyzed. It was indicated that although parametric based methods were more effective with damage detection, they required parameter estimation to be conducted more accurately and elaborately. It was also concluded that adequate damage threshold should be determined in order to properly conduct the damage detection process. Finally, importance of using random excitation/vibration based data was emphasized.

Liu et al. (2015) employed guided ultrasonic waves along with the singular value decomposition (SVD) method for damage detection in a pipeline structure. Field experimental data of a hot water piping system had been collected for a period of seven months. Damage detection process was based on the orthogonality between singular vectors from damage and environmental effects. Method was able to detect the damage from the mass scatterer.

As indicated in this chapter, a variety of damage detection methods can be employed in SHM process. Every type of methodology experiences some limitations. Some of the localized methods (such as non-destructive evaluation NDE methods) need to know the location of the damage in advance. Other global methods, e.g. based on the modal parameters of the structure, do not have this issue. However, methods that are based on modal parameters can be conducted at only several points in the structure. Challenge with

the global methods is that damage usually occurs locally, which means that lower frequency response of the structure, usually measured during ambient excitation, may not be significantly affected with this damage.

2.2 Literature Review of Environmental Effects on the Behaviour of Bridges and Damage Detection Process

As already emphasized, environmental effects can have detrimental effects on damage detection methodologies. Here, different studies are listed, where effects of the environmental variability in bridges and damage detection of structures are indicated.

Moorty and Roeder (1992) examined temperature dependent bridge movements. It was concluded that increase in bridge temperature causes uniform expansion in all directions of the bridge. Considering that some bearings allow movement only in one direction, large thermal forces can be introduced to the structure from temperature variation. Also, condition of the bearing is an important factor, considering that the deterioration of the supports can increase stiffness of the bearings and resistance to movement, which can cause increase of the thermal forces in the bridge.

Wahab and De Roeck (1997) concluded that the temperature variation mostly influences the elasticity modulus in the bridge structure. Also, frequency variation of 4-5% was indicated due to 15°C temperature variation. Alampalli (1998) investigated support freezing effect at the bridge structure, and concluded that this condition can have bigger effects on the change of modal frequencies than the damage cases.

Modal frequencies of the Alamosa Canyon Bridge (Doebling et al. 2000; Cornwell et al. 1999) varied approximately 6% during a 24 hour test period. Modal frequencies varied mostly because of the material changes due to the temperature change, and due to the changes in the boundary conditions, considering that debris in the support location obstructed free expansion of the joints.

Fujino et al. (2000) analyzed wind effects on a 720m suspension bridge, and compared it to the wind tunnel experiments. Natural frequency variation was not confirmed from the field measurements, considering that the natural frequency decreased with the increase of the wind speed up to 14.9m/s. However, it was expected that natural frequency would

increase after some level of the wind speed. Damping ratio significantly decreased up to a wind speed of 8m/s, and then it behaved in increasing manner, as in the wind tunnel experiment.

Fu and DeWolf (2001) analyzed a two span steel girder bridge with temperature variation. FE modeling was used to verify the field measurements, where vibration data was used for the model calibration. Increase of the natural frequencies occurred with the drop of the temperature. It was also concluded that increased friction in the bearings for the lower temperatures partly restrained rotation of the supports, causing axial tensions forces in the structure. With the temperature increase from -17.8°C to 15.6°C, first three natural frequencies decreased by 12.3%, 16.8%, and 8.96%.

Simonsen et al. (2002) investigated change of resilient modulus of coarse and fine grained subgrade soils due to temperature change. It was concluded that all soils experience reduction of the modulus due to the freeze-thaw process, therefore affecting the support conditions of structures.

Breccolotti et al. (2004) analyzed a simply supported internal span of the reinforced concrete bridge over the Tiber River. They concluded that level of frequency change due to the damage and temperature variation is comparable, which means that temperature effects can mask the effects of the damage. They also indicated that methods based on pattern recognition, statistical analysis and neural networks may be more efficient for damage detection, compared to the frequency based methods.

Catbas et al. (2008) analyzed reliability of cantilever truss bridge, with one year of temperature monitoring data. During that year temperature values varied between 15°F and 90°F. It was determined that annual peak-to-peak strain differential is ten times higher than strains caused by the traffic, which demonstrates the importance of temperature influence regarding the system reliability. It was also concluded that monitoring of the structure should be performed at bigger number of locations for better determination of temperature.

Zhou et al. (2008) performed damage detection on cable-stayed Ting Kau Bridge with relative flexibility change (RFC) index, which was formulated from modal frequencies

and mode shape vectors of the structure. Seventeen damage cases were analyzed, incorporating measurement noise, traffic and temperature effects. While RFC index identified damage location successfully with no ambient effects, it encountered difficulties when these effects were added. Finally, it was concluded that data should be retrieved from a range of ambient conditions for successful elimination of ambient effects.

Xu and Wu (2007) investigated a long-span cable stayed bridge and its mode shapes, as well as frequency variability due to the temperature changes. It was indicated that uniform temperature variation in a structure can be caused by seasonal weather changes, and non-uniform temperature distribution by radiation of sunshine during the day. Frequency change due to temperature variation from 40°C to -20°C was around 2%. It is also mentioned that asymmetric temperature distribution causes similar variation behaviour of frequency and mode shape variation as with the symmetric temperature distribution. Finally, it was determined that temperature variation causes bigger frequency changes than damage of cables and girders in the structure.

Pham (2009) analyzed the Attridge Drive Overpass in Saskatoon, Saskatchewan. Due to the temperature change from -12°C to 40°C, first three natural frequencies decreased by 8.3 %, 12.3 %, and 12 %. It was indicated that the major factor for frequency change was the reduction of the modulus of elasticity of bridge materials. Considering that the asphalt layer was present, relationship between the temperature variability and frequency change was bilinear.

Shoukry et al. (2009) analyzed the environmental effects on Star City Bridge in West Virginia. Temperature varied between -8°C and +38°C. It was concluded that non-uniform temperature gradient across the bridge was around 6.5°C.

Li et al. (2010) used a combination of NLPCA (non-linear principal component analysis) and ANN (artificial neural network) for analysis of Tianjin Yonghe cable-stayed bridge in order to analyze the effects of temperature and wind on modal parameters. NLPCA was first used to separate effects of temperature and wind on vibration behaviour of the bridge, and to determine pre-processed modal parameters. In the next step, environmental factors were used as an input data for ANN regression model, where relationship between

these factors and modal parameters from the first step was analyzed. They concluded that temperature variation can affect material properties and boundary conditions.

A simple RC slab was analyzed by Xia et al. (2011), where temperature distribution of the slab was confirmed using thermal analysis in the FE model. Also, natural frequencies were obtained from the vibration data, and were then verified with the FE model. Linear regression models between the structural temperature and modal frequencies were also determined. No clear relation between the temperature and the damping change was determined. Finally, it was concluded that modal analysis could be improved with analyzing temperature distribution of the entire structure. Xia et al. (2006) also concluded that natural frequencies decreased with the temperature increase in the RC slab. The same pattern of natural frequencies reduction occurred with the increase of humidity environment, considering that the mass of the RC slab increased. With the increase of temperature and humidity, damping also increased, but no clear relationship was determined. Finally, it was indicated that temperature of the structure lags to the air temperature because of thermal inertia effects. Considering that ARX models define the relationship between present outputs and previous output and input data (Ljung 1999), AR models or dynamic regression models were recommended as more suitable to capture this lag effect than the linear regression models.

Operational and environmental factors of Tamar Suspension Bridge were analyzed by Koo et al (2013) with long-term monitoring data. Ambient vibration testing was also conducted as a part of this study. It was concluded that compared to the minor effects from wind, thermal effects were the major contributor to the deformation of the bridge. Modal frequencies also experienced large variations during the monitoring. The same structure was investigated by Cross et al. (2013), where acceleration data was used to observe changes in the modal frequencies of the deck. It was determined that daily frequency change was caused mainly by the traffic loading, and that seasonal frequency change was mostly affected by the temperature changes.

Zhou and Yi (2014) analyzed the difficulties of defining the relationship between varying temperatures and vibration properties of long-span bridges. Firstly, it was presented that temperature effects cause change of several percent of bridge's modal properties, which

indicates that modal properties should be defined with improved precision. Also, introduction of new materials to bridge structures was mentioned as another difficulty in regards to variability of vibration characteristics. Numerical and thermodynamic analysis was indicated as reliable part of any temperature compensation process, especially if field data is unavailable.

Baptista et al. (2014) analyzed temperature effects on an electrical impedance damage detection algorithm. It was concluded that temperature effects cause the change of the amplitude and frequency shift of the resonance peaks, which demonstrated the detrimental effect of temperature on impedance signatures. It was determined that narrow range of frequency should be used for damage detection algorithm.

As indicated in the mentioned studies, the governing factor in environmental variability of bridge structures is the temperature change. Thus, in order to achieve a successful continuous damage monitoring system, the effect of the temperature should be compensated.

2.3 Literature Review of Methods for Compensation of Temperature Effects

Relevant and recent studies where compensation of temperature effects is applied in different methodologies are presented in this section.

Peeters and De Roeck (2001) investigated the Z24 Bridge in Switzerland during a period of one year. They observed bilinear behaviour of natural frequencies versus the temperature, due to the increased stiffness of the asphalt layer for temperature below 0°C. Besides the temperature - wind, rainfall and humidity were also monitored, but no clear relation was found between natural frequencies of the bridge and these parameters. It was recommended that data collecting should be performed after initial significant increase of concrete Young's modulus in newly built concrete bridges. Only one temperature location was employed for collecting temperature input data used for determining ARX models, which were used for simulation of natural frequencies. Damage was confirmed if simulated natural frequencies from ARX models were outside of the confidence intervals. It was also concluded that ARX models were more suitable to static regression models when considering thermal effects in the dynamic behaviour of the structure.

Sohn et al. (2002) utilized a non-linear principal component analysis with auto-associative neural network (AANN) in the data normalization process under variable environmental effects. AANN used parameters of the ARX model as input and output training data. Damage index was formulated based on the standard deviation of the residual error. The damage index used in this study was able to indicate the existence of the damage only (level 1).

Sohn et al. (2003) performed damage detection of delamination on composite structures using lamb-waves, where input waveforms were designed to be damage sensitive. Damage detection included the effect of temperature and boundary support variability, and was conducted on laboratory models. The method was able to detect damage in the form of delamination. It was indicated that the methodology depends on the spacing of sensors, actuating frequency, and the wavelength of the waves.

Principal component analysis (PCA) was applied by Yan et al. (2005a) for temperature effect compensation of simulated and experiment bridge models. This method was based on the fact that environmental effects and damage effects act as separate components in the damage process. Important feature of this method is that temperature measurements were not required. PCA was conducted on vibration data of the structures in the baseline state with the environmental effects. Next step was to conduct PCA analysis on models with variable environmental effects, and with the damage cases. Novelty index used for this method was a residual error of the prediction, which successfully detected different levels of damage. Method was later improved with non-linear models (Yan et al. 2005b).

Ko and Ni (2005) indicated that modal frequency change due to the temperature effect can reach 5% to 10% for highway bridges. Ko et al. (2003) and Ni et al. (2008) monitored cable stayed Ting Kau Bridge continuously for one year. They determined that different frequencies were affected with different levels by temperature variation. Feed-forward neural networks with backpropagation training algorithm were utilized for prediction of natural frequencies from 20 temperature measurements, with separate neural networks for each natural frequency. Finally, neural networks successfully performed the mapping between the measured temperatures and natural frequencies of the bridge.

Kullaa proposed a damage detection algorithm based on the missing data analysis (2004, 2005, 2009) and the data analysis (2002). An experimental bridge structure and numerical model of a vehicle crane were analyzed with algorithm based on the missing data analysis (Kullaa 2009). Significant feature of this method is that there is no need of measuring environmental parameters, and the only data needed for the training process is from the baseline state of the structure. Missing data analysis considers estimation of features by utilizing other available features, based on the assumption that the features are cross correlated. Considering that with estimation of each feature matrix inversion process is applied, this algorithm performs slower than the methods based on data analysis. Damage features from this algorithm are based on the maximum principal components of the residual. This method performed successfully with identification of the damage levels in two structures.

Sohn (2007) summarized data normalization methods regarding the temperature variability effects. Methods were divided in groups, depending on whether the temperature data is available for analysis, or not. When temperature measurements are feasible, usually regression or interpolation analysis methods are conducted in order to conduct damage detection (Peeters and De Roeck 2001). Second group includes methods which do not use temperature for determination of damage features (Yan et al. 2005).

Kim et al. (2007) analyzed a model of a plate-girder bridge for damage detection under variable temperature conditions. Vibration data of the bridge was used for determining existence, location and extent of the damage (levels 1, 2 & 3 by Rytter (1993)). Temperatures between 0°C and 30°C were considered, and the damage was introduced at 23°C. Damage detection process employed frequency based & modal strain energy based methods, as well as temperature-frequency control charts. Eventually, empirical formulas for frequency correction were determined as a part of data normalization process. The method was less effective as the temperature gap between the baseline and damage case increased.

He (2008) analyzed the Voigt bridge structure over a period of 50 days, under different environmental conditions, and used ARX models for simulation of natural frequencies of the structure. Air and element temperatures, as well as the wind speed were the inputs to

the ARX model. Output data were the natural frequencies. Damage detection was based on the comparison between the measured natural frequencies and ARX simulated frequencies – if identified frequencies were lower than simulated ones, and outside of the confidence interval, damage was indicated.

Balmès et al. (2008) proposed an extension of parametric subspace identification method based on a residual of a covariance matrix. A non-parametric algorithm was proposed for compensation of temperature effects on modal parameters of the structure. This methodology was based on the fact that any non-stationarities present in the signal can be distinguished from the rest of the signal. This algorithm was applied to the simulation of bridge deck model and laboratory clamped beam structure.

Deraemaeker et al. (2008) employed factor analysis in order to compensate environmental effects on the modal parameters of a bridge structure. Output-only vibration measurements were used. Modal features of the structure were ranked in terms of sensitivity, with or without the effect of the noise. It was indicated that the mode shapes seem to be the most optimal parameter for output-only damage detection methodology under average levels of noise and variable environmental conditions.

Hu et al. (2009) used PCA in order to compensate the effects of the environmental factors on modal frequencies of the Coimbra footbridge. It was determined that temperature effects cause modal frequency variation of 1.7%. Hu et al. (2015) also utilized PCA method for compensation of temperature effects on damage detection algorithm for wind turbine system. PCA algorithm considers temperature effects as embedded variables in the system. The novelty index used for damage detection is then expected to be sensitive only to the damage.

Oh and Sohn (2009) analyzed an eight degree of freedom mass-spring model with application of principal component analysis based damage detection algorithm. Firstly, AR-ARX models were defined based on the baseline vibration data from random excitation sources. Coefficients of these models were then used as an input data to the non-linear principal component analysis, where the correlation between these coefficients and the environmental parameters was analyzed. After the introduction of the damage, entire process was repeated, and AR-ARX parameters that are the closest to the new case,

were selected from the previous baseline data. Prediction errors from this algorithm were then used for determination of damage features.

Zhou et al. (2009, 2010, 2012) investigated Ting Kau Bridge along with its FE model. This model was used for determination of corresponding modal properties at different temperature conditions. A combination of backpropagation neural network (BPNN) and auto-associative neural network algorithms was then used for damage detection process. BPNN was employed to normalize modal features of the structure from different temperature levels. A BPNN was determined for each modal frequency separately in order to compensate for the temperature effects. An AANN was then utilized for damage detection, where normalized modal properties were used for training and simulation, and novelty index was in the form of Euclidean norm of the reconstruction error. The maximum change of natural frequencies was 6.7%, and the methodology was successful at detecting the damage for frequency change of more than 1%. It was indicated that the method should be verified on another structure in order to confirm robustness of the method. It was also concluded that the relationship between the modal frequencies and the temperature can be improved if principal components of the temperature are used as input to the BPNN.

Hsu and Loh (2010) analyzed a bridge model for the compensation of the effects of temperature, temperature gradient, frozen supports and humidity. Non-linear principal component analysis was utilized with auto associative neural networks, where residual error of the simulation algorithm was used for damage identification. It was mentioned that data should be collected for variety of different environmental conditions, in order to successfully train the neural network. Also, it was indicated that temperature, as an important environmental factor, is experiencing periodic behaviour annually.

Basseville et al. (2010) conducted damage detection of a laboratory test beam with a climatic chamber using two subspace-based damage detection methods. In the first case null space is modified to temperature effects, where in the second case temperature effects are considered as nuisance effect. Model considered only axial thermal prestress forces, and it was indicated that three-dimensional temperature effects should be analyzed in the future research.

Figueiredo et al. (2011) analyzed a laboratory three-story frame structure with comparison of four methods for damage detection process under variable environmental conditions: auto-associative neural network, factor analysis, Mahalanobis squared distance (MSD), and singular value decomposition. Environmental variability was applied as a mass and stiffness change in the structure, assuming that the same effect would be produced from environmental variability effect in the real structure. Damage was introduced by a bumper mechanism simulating cracks and loose connections, and introducing non-linear effects in the structure. Parameters of AR time series model were used as damage features. An important feature of these procedures was that direct measurement of the environmental parameters was not needed. All of the algorithms performed satisfactorily, where the MSD algorithm was most successful considering the classification performance. It was indicated that the training process should be performed properly with adequately representative set of operational and environmental data. Also, adequateness of AR models for feature extraction was indicated considering that they could be used for cases when there was only output set of data, and that they responded well to non-linear damages.

Sepehry et al. (2011) investigated effect of temperature on impedance-based structural health monitoring process. Piezoelectric wafer active sensors (PWAS) were used for this algorithm, where damage detection was based on the electrical coupling effect of these sensors. If there was any damage introduced in the structure, mechanical impedance would change, and electrical impedance of these sensors could detect this by the coupling effect. The study was based on the theoretical model of the Euler Bernoulli beam, which included coupling of the sensors and the structure by using corresponding kinetic and strain. The beam was tested under different conditions, and modal properties detected with PWAS sensors were in accordance with the properties from the theoretical model.

Moser and Moaveni (2011) analyzed the relationship between modal frequencies and temperature changes for Dowling Hall footbridge, using ambient vibration data. Temperature range was from -14°C to 39°C, and modal frequency relationship to temperature was determined to be bi-linear, with no clear relationship between temperature and damping, or mode shapes. A static linear model, ARX model, bi-linear

model, and polynomial models were used for the analysis. Moaveni and Behnamesh (2012) also analyzed effect of the temperature on finite element model updating process. They concluded that damage detection process can be improved if temperature effects are considered in the FE model updating process.

Hong et al. (2012) performed damage detection on laboratory steel girder model with bolted connections. Damage detection algorithm employs vibration and electromechanical impedance signatures from the sensor nodes. Global damage detection was based on vibration data, where correlation coefficient of power spectral density was used as a damage feature. Local damage was then based on the change in electromechanical impedance, where cross coefficient of impedance was used as a damage feature. Temperature compensation was performed with linear regression between the temperature values and corresponding cross coefficients. Damage detection and localization were performed successfully, with less successful results for determination of damage extent level.

Meruane and Heylen (2012) investigated a model-based damage detection methodology based on the parallel genetic algorithm. This algorithm employed an objective function of the relationship between natural frequencies and mode shapes of the structure. The methodology was validated with simulated three-span bridge and experimental I-40 bridge. Three-span bridge was analyzed for 30% of stiffness reduction in the middle span region, under temperature variation between 0°C and 30°C. I-40 bridge was tested for 4 damage cases, where the smallest damage detected with this methodology was 10% stiffness reduction of the plate girder. Damage detection was performed for temperature above 0°C. It was indicated that in the future study gradient of temperature throughout the height and width of the bridge should be included, and that the change of boundary conditions and non-linear behaviour of the materials due to the temperature effect should be considered.

Mosavi et al. (2012) analyzed damage cases in a steel bridge girder using random vibration data simulated by a hydraulic actuator, where white noise signal sets were used as the input to the actuator. Vibration data was used to define multivariate vector autoregressive models, and Mahalanobis distance was applied to coefficients of these

vectors in order to determine damage features. It was indicated that optimum distance of vibration sensors should be determined for successful damage detection process.

Fritzen et al. (2013) analyzed compensation of environmental effects for a wind turbine structure. Acceleration data was used for the analysis. Damage detection was performed with the space based fault detection method along with the fuzzy-classification algorithm. The need for future studies on the effect of the noise was indicated.

Reynders et al. (2014) applied a damage detection methodology under environmental and operational effects for the Z24 Bridge in Switzerland. This methodology employed non-linear principal component analysis, and it did not require measurement of environmental parameters. Prediction error of the model between baseline and damaged cases was used as a damage indicator.

Kullaa (2014) analyzed Z24 bridge damage detection process under variable environmental effects. Firstly, non-linear effects from the environmental factors were compensated with a data based Gaussian mixture model (GMM), where the measurement of environmental variables was not needed. After defining GMMs, minimum mean square error was applied to all components of the model, where control charts were then used for detection of any novelties. It was indicated that this method depended on the signal to noise ratio (SNR), and that the method could work even for relatively lower SNR.

Laory et al. (2014) analyzed Tamar Suspension Bridge natural frequency relationship to variable environmental parameters, utilizing five methods: regression tree, random forest, artificial neural networks, support vector regression and multiple linear regression. Data from three years of monitoring was used, and it was determined that support vector regression and random forest were the most optimal methods for modal frequency prediction, probably because of the non-linear behaviour.

Kromanis et al. (2014) used several regression models for determining a relationship between temperature and thermal response of a concrete footbridge - multiple linear regression (MLR), robust regression (RR), artificial neural networks (ANN) and support vector regression (SVR). With the use of this methodology, thermal response of the bridges due to the variable environmental influences was predicted successfully. Thermal

inertia effects were also considered by providing current and past temperature measurement values to the models.

Hios and Fassois (2014) analyzed a composite beam structure using a vibration based stochastic global model in order to define damage detection algorithm under variable environmental effects. Functionally Pooled Vector AutoRegressive models used in this study were based either on modal parameters or discrete-time model parameter estimates, along with the principal component analysis data compression step. Finally, method proved to be effective in damage detection.

Yarnold and Moon (2015) introduced a 3D baseline methodology for tracing any introduction of the damage to the bridge structure. It was determined that temperature changes and corresponding strains and displacements of the structure define unique baseline state, which in 3D space corresponds to near-flat surface. Sensitive to the damage effect and insensitive to the environmental effects are the bounds and orientation angles of these surfaces, which are used for damage detection.

Torres-Arredondo et al. (2015) used guided ultrasonic waves in order to compensate for the variable environmental effects in a pipeline structure. It was indicated that the variable temperature effects can affect wave-propagation damage detection methods. Optimal baseline selection (OBS) and optimal signal stretch temperature compensation techniques were applied in this method. OBS method uses waveform from the baseline set closest to the recorded signal, which was then stretched based on the baseline signal. This methodology was successful in compensating the temperature effects. It was also concluded that modes of the guided waves should be determined for the optimal damage detection algorithm.

Hu et al. (2015) analyzed effect of operational and environmental influences on modal properties of a wind turbine system, in order to successfully compensate these effects for the damage detection algorithm. Correlation analysis indicated that modal frequencies of the wind turbine are mostly influenced by the nacelle position, rotation speed, wind speed and the temperature. Two damage cases were simulated in a numerical model. Principal component analysis was applied for compensation of the temperature effects in the

damage detection process, where relation between temperatures and modal frequencies was determined.

As discussed above, there are variety of methods investigated for damage detection under variable temperature effects. Authors have demonstrated that these methodologies can compensate temperature effects up to a certain level, for specific type of structures. However, there are certain limitations which affect the robustness and effectiveness of these methods. Some of the methods are only able to detect the existence of the damage (level 1 by Rytter). Certain methodologies need to know the location of the damage in advance (local methods), or are used for only one type of damage cases. In some methods only positive temperatures were considered for the analysis.

The purpose of this thesis is to develop a new framework for effective damage detection under temperature effects. As demonstrated in later phases of this thesis, the methodology presented in this study is able to detect existence, location and extent of the damage (levels 1, 2 & 3 by Rytter). Temperature range used in this study incorporates the entire range that can occur for real type bridge structures. Damage location or type of the damage is not expected to affect the effectiveness of this methodology.

CHAPTER 3:PROPOSED METHODOLOGY FOR DAMAGE DETECTION UNDER TEMPERATURE EFFECTS

As already indicated in the previous chapters, the objective of this thesis is to develop a damage detection algorithm based on the vibration response of a structure, where temperature effects on damage detection process are successfully compensated. In order to assess the damage under temperature effects, a sensor clustering based time series analysis method is employed along with backpropagation algorithm based artificial neural networks.

Time series based damage detection algorithm described in Chapter 3.1 was originally proposed by Gül and Catbas (2011). It employs free vibration output-only data in order to define ARX models for different sensor locations. This methodology introduces a novelty approach where sensors are grouped in different sensor clusters, which are composed of one reference channel and other neighbour channels. Output data of the neighbour channels is used for predicting the behaviour of the reference channel. Changes in these models indicate the existence, location and severity of the damage in structure. Damage features are defined as the fit ratio of the ARX models (which will be referred as DF_{ARX}) and are sensitive to damage. However, they are also sensitive to the effects of temperature on the output vibration data of the structure. Therefore, effects of the temperature on vibrational properties of the structure must be compensated for efficient damage detection process.

This thesis uses backpropagation algorithm based artificial neural networks (ANN) to improve the method proposed by Gül and Catbas (2011) for compensating the temperature effects (Chapter 3.2). First step with the ANN application is to train the network with DF_{ARX} from different temperature scenarios in the structure without introducing any artificial damage. Input data for the training process are temperature values from specific parts of the structure, where the output data are the mentioned DF_{ARX} values. Output of the ANN will be referred as DF_{ANN}, which represents damage features

from the time series analysis based method under temperature effects only, without any damage being present.

Final damage features are presented in Chapter 3.3. They are determined as absolute value of the difference between the damage features from Chapter 3.1 and from Chapter 3.2. In order to prove its effectiveness, this methodology is applied to a footbridge FE model with five damage cases. Characteristics of the model are presented in Chapter 4, and the results are explained and discussed in Chapter 5.

3.1 Time Series Modeling for Structural Dynamics

Time series modeling enables creation of systems based on sequence of data points in time, measured at uniform time intervals. Time series models can be applied to various problems in SHM. In this research, they are utilized for defining dynamic behaviour of the structure. Time series models that are relevant to this research are Auto-Regressive Moving Average model with eXogenous input (ARMAX model) and the Auto-Regressive model with eXogenous input (ARX model). A more detailed description of these models is given in (Ljung 1999; Box et al. 2013).

Linear time series difference equation is shown in Eq. 3.1 (Ljung 1999), which represents the relationship of the input, output and the error terms:

$$y(t)+a_1 y(t\text{-}1)+\ldots+a_{n_a} y(t\text{-}n_a)= b_1 u(t\text{-}1)+\ldots+b_{n_b} u(t\text{-}n_b)+e(t)+c_1 e(t\text{-}1)+\ldots+c_{n_c} e(t\text{-}n_c) \quad (3.1)$$

Where $y(t)$ is the output of the model, $u(t)$ is the input to the model, and $e(t)$ is the error term. The unknown parameters of the model are a_i, b_i, and c_i, and the model orders are n_a, n_b, and n_c. A reduced form of this expression is given in Eq. 3.2, and it represents an ARMAX model:

$$A(q)y(t)=B(q)u(t)+C(q)e(t) \quad (3.2)$$

where $A(q)$, $B(q)$, and $C(q)$ are polynomials in the back shift operator q^{-1}, given in Eq. 3.3:

$$\begin{aligned} A(q)&=1+a_1 q^{-1}+a_2 q^{-2}+\ldots+a_{na} q^{-na} \\ B(q)&=b_1 q^{-1}+b_2 q^{-2}+\ldots+b_{nb} q^{-nb} \\ C(q)&=1+c_1 q^{-1}+c_2 q^{-2}+\ldots+c_{nc} q^{-nc} \end{aligned} \quad (3.3)$$

A(q)y(t) represents an AutoRegressive model, *B(q)u(t)* is an external input *and C(q)e(t)* is moving average of error.

AutoRegressive implies that the current values of the variables *y(t)* do not depend solely on the other variables, but also on their own past values. Back shift operator q^{-1} is used for determining previous values of variables. Moving average part relates current value of the output to the current and previous values of the error terms in the system. Assumption in this algorithm is that the error terms are not measurable, but added to the input and output signals.

The exogenous input *u(t)* is an observable quantity, and it is usually independent of other system variables. Linear time-invariance is one of the important assumptions of this system. As the final step of defining the time series models, parameters of the model are determined in order to provide the best fit for the data observed. In this study, time series models are fitted to the free vibration (acceleration) data from the structure.

Block diagram of ARMAX model is indicated in Figure 3.1:

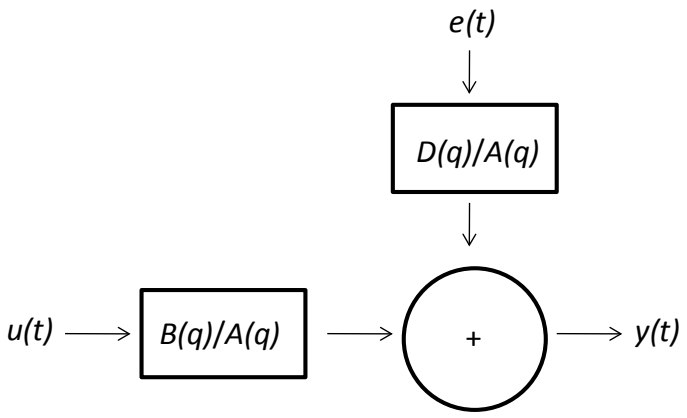

Figure 3.1. ARMAX model block diagram (adapted from Ljung 1999)

If the model orders for different components are adjusted, different time series models can be defined. If n_b and n_c are both zero, an AR model is formulated. Also, if n_a and n_b are zero, an MA model is defined. In this method, by setting n_c equal to zero, the ARX model, used in this study, is formulated:

$$y(t)+a_1 y(t\text{-}1)+\ldots+a_{n_a} y(t\text{-}n_a)=b_1 u(t\text{-}1)+\ldots+b_{n_b} u(t\text{-}n_b)+e(t) \quad (3.4)$$

which can be also written as:

$$A(q)y(t)=B(q)u(t)+e(t) \tag{3.5}$$

All the parameters defined in ARMAX follow the same definition in the ARX model. Block diagram of ARX model is indicated in Figure 3.2:

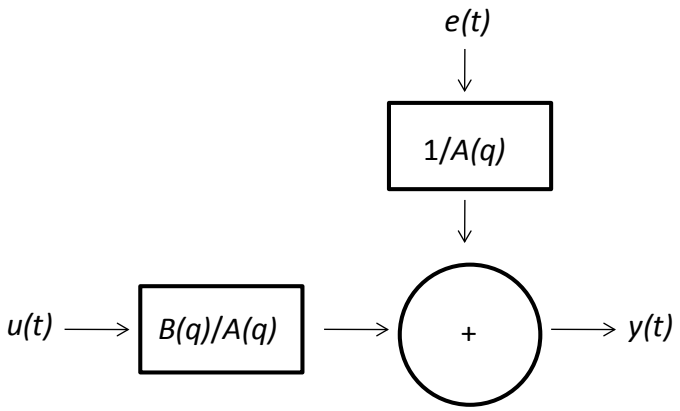

Figure 3.2. ARX model block diagram (adapted from Ljung 1999)

Gül and Catbas (2011) proposed a damage detection methodology, based on the ARX models. The basis of this methodology is the equation of motion of *N* degrees of freedom (DOF) for linear dynamic system:

$$[M]\,\ddot{x}(t)+[C]\,\dot{x}(t)+[K]x(t)=f(t) \tag{3.6}$$

where *[M]* is the mass matrix, *[C]* is the damping matrix, and *[K]* is the stiffness matrix. If only the first row of the Eq. 3.6 is considered, and rearranged for the free vibration case, the following equation for the acceleration output of the 1st DOF is obtained:

$$\ddot{x}_1 = -\frac{(m_{12}\ddot{x}_2 + \ldots + m_{1N}\ddot{x}_N) + (c_{11}\dot{x}_1 + \ldots + c_{1N}\dot{x}_N) + (k_{11}x_1 + \ldots + k_{1N}x_N)}{m_{11}} \tag{3.7}$$

Using this relation, output of a reference DOF can be obtained using the outputs of the neighbouring DOFs in one sensor cluster. Example of a sensor cluster scheme is given in Figure 3.3, where reference channel is channel L1, and neighbour channels are channels L2, R1 & R2. In the ARX model this means that a model for predicting the output of any DOF can be created, with employing the outputs of the neighbour channels as the input terms *u(t)* in Eq. 3.5. Acceleration of the reference channel in a sensor cluster is then defined as *y(t)* component, and *u(t)* is the acceleration of the neighbour channels in one cluster. Considering that this approach is using acceleration data only, one of the

assumptions is that the model is inherently considering velocity and displacement to be dependent on the acceleration response.

$$A(q)\ddot{x}_1(t) = B(q)[\ddot{x}_1(t) \quad \ddot{x}_2(t) \quad \cdots \quad \ddot{x}_k(t)]^T + e(t) \tag{3.8}$$

This is the ARX model for determination of output of the first DOF, utilizing other neighbour's DOF, in a cluster with k sensors. Different sensor clusters which contain a reference channel and its neighbour channels can be formed. Any change in these models is expected indicate property change of the particular part of the structure. Basically, these models are then used for indication of the existence, location and severity of the damage in the structure. Kostić and Gül (2014) further verified this methodology with an experimental four span bridge model.

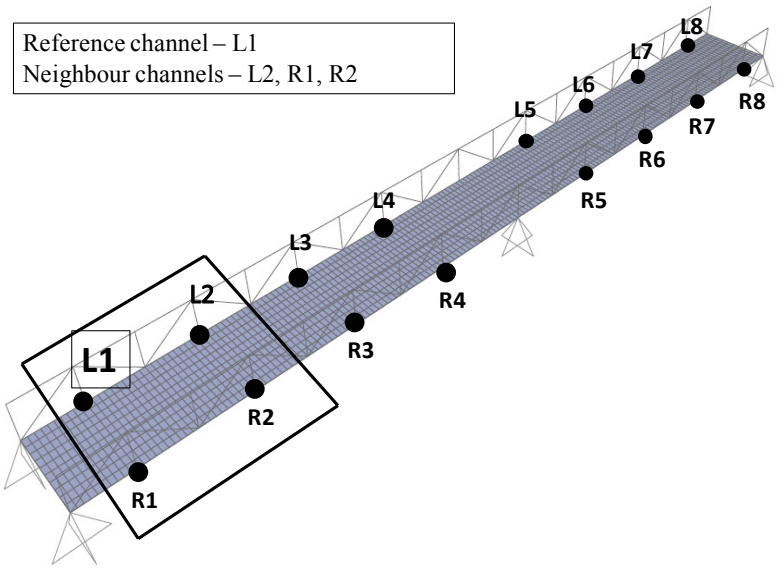

Figure 3.3. Scheme of sensor cluster 1

3.2 Artificial Neural Network – Backpropagation Algorithm

Rumerlhart et al. (1986) were among the first to introduce backpropagation algorithm for multilayer perceptrons, where they proposed adjustment of the weights from input to hidden layers. Backpropagation along with the Levenberg-Marquardt algorithm, which is the algorithm used in this thesis, are described in this chapter. A typical artificial multilayer neural network is depicted in Figure 3.4:

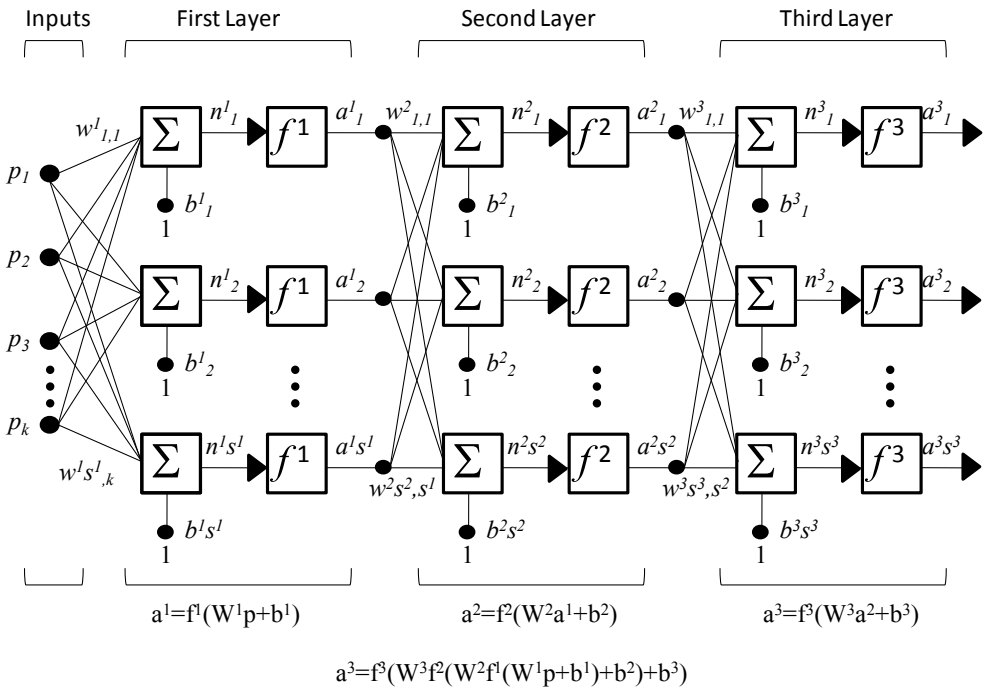

Figure 3.4. Multilayer network algorithm (adapted from Hagan et al. 1996)

The net input to unit *i* in layer *k+1* is defined as (Hagan et al. 1996):

$$n^{k+1}(i) = \sum_{j=1}^{Sk} w^{k+1}(i,j)a^{k}(j) + b^{k+1}(i) \tag{3.9}$$

The output of unit *i* will then be:

$$a^{k+1}(i) = f^{k+1}\left(n^{k+1}(i)\right) \tag{3.10}$$

If the network has *M* layers, equations in matrix form can be defined as:

$$a^{0} = p;\ a^{k+1} = f^{k+1}\left(W^{k+1}a^{k} + b^{k+1}\right);\ k = 0,1,...,M-1 \tag{3.11}$$

For the effective performance, network should be successfully trained with input and output data sets: $\{(p_1,t_1),(p_2,t_2),...,(p_Q,t_Q)\}$.

In the Levenberg-Marquardt method, performance index is used to minimize the sum of the squares of errors, with optimizing β parameter vector:

$$S(\beta) = \sum_{i=1}^{m}\left[y_i - f(x_i,\beta)\right]^2 \tag{3.12}$$

where y_i is measured vector, and $f(x_i)$ is estimated measurement vector.

This is an iterative procedure, and in each step β is replaced with $\beta+\delta$, with δ being the increment. In order to find optimal δ, LM algorithm uses linear approximation of f in the neighbourhood of x_i:

$$f(x_i, \beta + \delta) \approx f(x_i, \beta) + J_i \delta \tag{3.13}$$

where J_i is gradient of f with respect to β:

$$J_i = \frac{\partial f(x_i, \beta)}{\partial \beta} \tag{3.14}$$

As mentioned before, at each step parameter δ, that minimizes Eq. 3.15, should be determined (Lourakis 2005):

$$\|y_i - f(x_i, \beta + \delta)\| \approx \|y_i - f(x_i, \beta) - J_i \delta\| = \|e - J_i \delta\| \tag{3.15}$$

Minimum is reached when $J_i\delta - e$ is orthogonal to the column space of J, which leads to the following equation in vector notation:

$$J^T(J\delta - e) = 0 \tag{3.16}$$

This can be arranged as:

$$J^T J\delta = J^T e \tag{3.17}$$

J is the Jacobian matrix which contains first derivatives of the network errors with respect to weights and biases; $J^T J$ is the approximate Hessian matrix - approximation to the matrix of second order derivatives; $J^T e$ is the gradient, and e is a vector of network errors. LM algorithm practically solves a slight variation of previous equation, known as augmented normal equation (Lourakis 2005):

$$N\delta = J^T e \tag{3.18}$$

In this equation, off-diagonal elements of N are identical to the corresponding elements of the approximate Hessian matrix, and the diagonal elements are given as:

$$N_{ii} = \mu I + [J^T J]_{ii} \tag{3.19}$$

I is the identity matrix, and μ is the damping coefficient. Introduction of the damping coefficient μ was Levenberg's contribution to the method.

Previous equation can be arranged as:

$$\left(\mu I + J^T J\right)\delta = J^T e \tag{3.20}$$

$$\delta = \left[\mu I + J^T J\right]^{-1} J^T e \tag{3.21}$$

If the damping coefficient is too large, then instead of inverting matrix $J^T J + \mu I$, Marquardt proposed to replace the identity matrix I with the diagonal matrix consisting of the diagonal elements of $J^T J$, which gives us the Levenberg-Marquardt algorithm:

$$\delta = \left[\mu diag(J^T J) + J^T J\right]^{-1} J^T e \tag{3.22}$$

In this algorithm, values of the damping coefficient are modified throughout the steps. If the error is reduced with the new increment, update is accepted and the process continues with a decreased damping coefficient. If the error increases, then augmented normal equations are solved again and the process is repeated until error decreases. If μ is large, this algorithm is known as steepest descent method, and for small values of μ it is known as *Gauss-Newt*on method.

The final order for all the steps of this algorithm is:

- All inputs are presented to the network, and outputs are calculated with Eq. 3.11, along with the errors. Sum of squares of errors is then computed for all inputs.
- Jacobian matrix is then calculated, and δ is obtained with Eq. 3.22.
- Sum of squares of errors is computed again. If it is smaller than the value in the first step, μ is reduced by β, and algorithm goes to step 1. If not, then it is increased by β, and algorithm solves for δ again.
- Algorithm terminates when one of the stop training criteria conditions is achieved.

3.3 Methodology of the Damage Detection Analysis

Time series analysis and neural network method represent the basis of the methodology used for damage detection process in this study. The main goal of this research is to develop methodology for damage detection under temperature effects. Time series analysis method is utilized here as a non-parametric method, whose output values are defined as damage features (DF_{ARX}). In order to obtain these damage features, time series models are fitted to the free vibration acceleration data of the structure, using a procedure explained in Chapter 3.1. When these ARX models are defined, the predicted output acceleration values for all the reference channels can be determined. With this data, Fit ratio (FR) values can be obtained with the following equation:

$$FR = (1 - \frac{\|\{y\} - \{\hat{y}\}\|}{\|\{y\} - \{\bar{y}\}\|}) \times 100 \tag{3.23}$$

where $\{y\}$ is the measured output, $\{\hat{y}\}$ is the predicted output, $\{\bar{y}\}$ is the mean of $\{y\}$ and $\|\{y\} - \{\hat{y}\}\|$ is the norm of $\{y\} - \{\hat{y}\}$.

The difference between the fit ratios of the ARX models from the baseline healthy case and damage case is used as a damage indicating feature (DF_{ARX}), which can successfully indicate the location and severity of the damage if no detrimental temperature effects are present. DF_{ARX} values are calculated as described in Chapter 3.1 (Gül and Catbas 2011; Kostić and Gül 2014):

$$DF_{ARX} = \frac{FR_{Healthy} - FR_{Damaged}}{FR_{Healthy}} \times 100 \tag{3.24}$$

DF_{ARX} indicates the change in the stiffness of the structure at the damage location, in regards to the baseline case (assuming mass of the structure is time invariant). However, different changes in the system that act simultaneously, can produce opposite effect on the stiffness change in regards to the baseline case. Specifically, if temperature effects cause the increase of the stiffness, and the damage case decreases the stiffness, these two cases will have opposite effect on the damage features (Figure 3.5 – case 1). If both changes cause increase of the stiffness, then they will both have the same effect on the damage features (Figure 3.5– case 2). In order to formulate efficient damage detection

methodology, where different damage and temperature cases will produce the same stiffness change in regards to the baseline case, three baseline cases are used for the analysis. Two baseline cases are defined for environmental temperatures at maximum negative and positive values, and one at the time of construction. With this arrangement, for every combination of damage case and temperature distribution, there will be at least one baseline case for which damage and temperature effects will produce the same stiffness change in regards to that baseline case. For that particular combination of baseline, temperature and damage case, damage features will have maximum values, compared to combinations with other baseline cases. Therefore, envelope of the damage features is adopted for the damage detection. The reason for multiple baseline cases is due to the fact that the damage type cannot be anticipated in advance.

In Figure 3.5 two sets of damage features with environmental temperature load of -10°C are indicated. Considering that the environmental load is lower compared to the baseline case, it causes increase in stiffness of the structure. First set includes reduction of the steel modulus between channels L2 & L3 and R2 & R3, and the second set includes increase of the steel modulus in the same location. It is indicated that the damage features in the other span have almost the exact values for both cases, which means that they are indicating damage from the temperature only. However, in the span where the damage is occurring, it is indicated that damage features are much higher for the second case, where temperature and the damage act simultaneously, increasing the steel modulus. This confirms that if both damage cases have the same effect on the stiffness of the structure, they will have the same effect on the damage features.

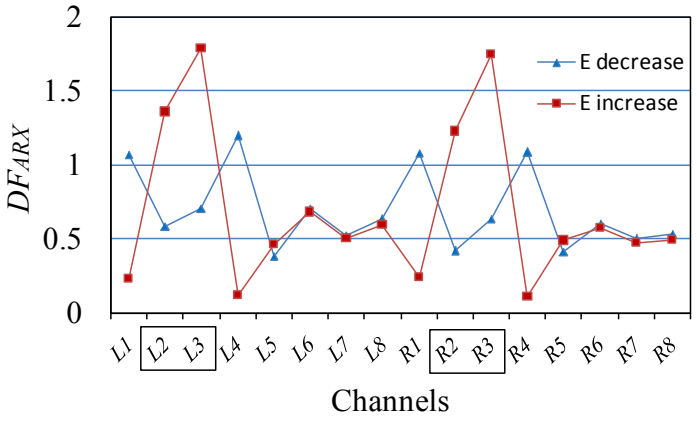

Figure 3.5. DF_{ARX} for damage case with 20% E_{decrease} (case 1) and 20% E_{increase} (case 2) with environmental temperature at -10°C

Damage detection algorithm is explained in detail in Figure 3.6, where all the steps are indicated. First step is to adopt three baseline cases, with environmental temperature loads at -10°C, +15°C and +30°C, and no damage applied. Second step is to define 500 finite element models with random environmental temperature load from -10°C to +30°C, and with no damage applied. However, temperature change in the model is treated as another damage case, considering that it alters the natural frequencies and vibration response of the structure. Therefore, these 500 models are used as damage case models, and the first three cases are used as the baseline cases. DF_{ARX} are determined for all 500 models, compared to each of the baseline cases. These damage features (DF_{ARX}) are the result of the temperature difference between the damage case and the baseline case.

Neural network training part is conducted with 500 input sets of data, with 3 different temperature values. These temperatures represent environmental temperature values for three groups of bridge elements: top steel beams, bottom steel beams and concrete deck. Temperatures of these groups of elements are all related to the environmental temperature, and they can obtain a random value between -25°C and 55°C. Randomness of the temperature values is improved with introducing random value of ±2.5°C for temperature of each group. Corresponding output data comprises 500 sets of damage features values (DF_{ARX}) from temperature load only.

Next step of damage detection analysis under temperature effects includes formation of 100 finite element models, with appropriate damage case, and with random

environmental temperature load from -10°C to +30°C. Damage Features (DF_{ARX}) are then computed for finite element models of the footbridge with temperature load and introduced damage cases. For damage cases with noise effect, average value of 5 simulations was used for final value of DF_{ARX}. With this approach, random effect of the noise on DF_{ARX} parameters is minimized. In order to compensate these temperature effects, artificial neural networks are then employed. Neural network is first trained with the DF_{ARX} parameters from the healthy state, with random temperature effects, where DF_{ARX} parameters are used as output data. Also, temperature values for three groups of elements are used as the input data. Simulation output data of the Neural Network are the DF_{ANN} parameters, which represent damage features from the time series analysis based method. These damage features are result of temperature acting in the damage case, but without the damage effect on the parameters. Finally, Damage Features (DF_{ANN}) are used for determination of final Damage Features (DF) which are then used for damage detection under temperature effects.

Final Damage features are defined as:

$$DF = abs(DF_{ARX} - DF_{ANN}) \tag{3.25}$$

Damage Features from all three baseline cases were analyzed, and the envelope of all the DFs was adopted at the end. This algorithm was performed for noise levels of 0%, 1%, 3% and 5%.

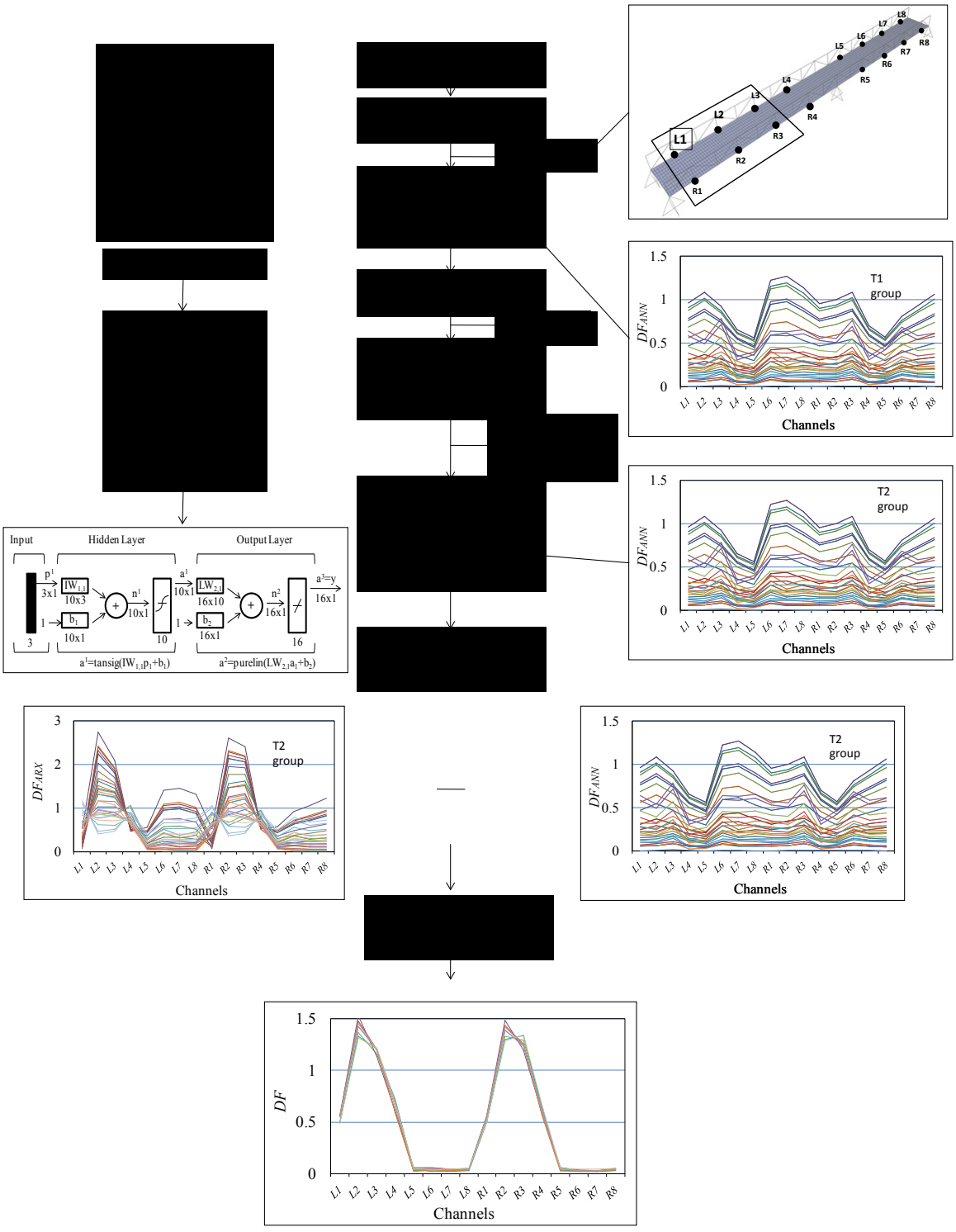

Figure 3.6. Proposed framework for damage detection under temperature effects

CHAPTER 4:CASE STUDY – FOOTBRIDGE FINITE ELEMENT MODEL

4.1 Introduction

The proposed method presented in Chapter 3 is applied to a finite element model of a 44.1m footbridge structure for verification. This model is inspired by the footbridge structure shown in Figure 4.1, analysed by Moser and Moaveni (2011). It should be noted that bridge geometry and properties are adopted as similar, but not the same, as in the paper from Moser and Moaveni (2011). Also, some details of the structural configuration in the model are different than that to the bridge presented in Moser and Moaveni (2011).

Figure 4.1. Dowling Hall Footbridge (from Moser and Moaveni 2011 with permission)

Footbridge structure is composed of two equal spans of 22.05m. It is 4.1m wide and 1.8m high. The 19cm thick concrete slab is supported by HS 152x102x6 transverse steel beams located beneath the slab at 2.45m grid intervals. Longitudinal, vertical and diagonal steel elements in the vertical plane are rigidly connected and have the same cross section - HS 152x102x6. Based on the geometry of this footbridge, temperature is expected to produce the biggest effects in the structure, compared to other environmental factors. Therefore, this model was adopted as adequate one for analysis of temperature effects.

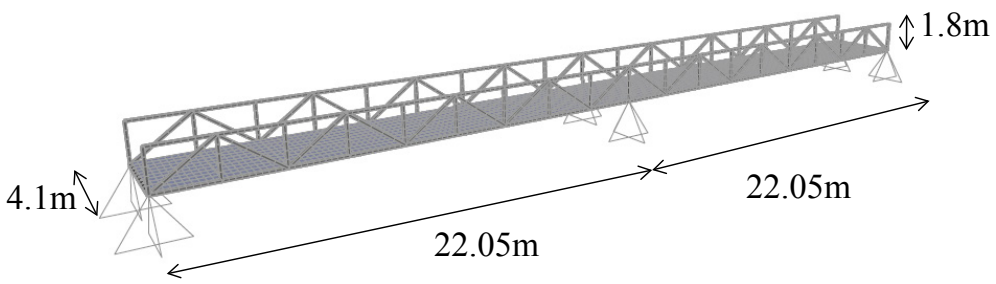

Figure 4.2. General overview of the finite element model of a footbridge structure modeled in SAP2000

The analysis was conducted in SAP2000 finite element software. Finite elements have the following dimensions: area elements size is adopted to be maximum 0.4m, and frame elements have maximum dimension of 0.6m. Orientation of frame elements is such that the larger dimension is in the horizontal direction (Figure 4.3)

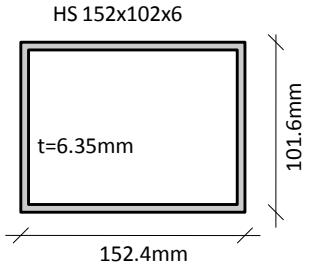

Figure 4.3. Cross section of steel elements in the footbridge structure

Footbridge structure is supported by six pinned supports, restrained in all three orthogonal directions (x, y, z). Fixity of supports in bridge structures can be affected by different factors – deterioration of supports (Moorty and Roeder 1992), increased friction due to low temperatures (Fu and De Wolf 2001), freezing of accumulated moisture (Alampalli 1998), presence of debris at support location (Cornwell et al. 1999). Also, increased fixity of supports is present at bridges with internal construction, where bridge structure is monolithically connected to substructure. If the bridge supports are not free to translate, additional thermal axial forces are caused by temperature effects. These axial forces affect the structural stiffness of the bridge, changing the vibration response of the bridge structure. In this study, pinned supports were adopted in order to maximize the effect from these additional thermal forces on stiffness of the footbridge structure.

Considering that the analysis method is based on vibrational behaviour of the structure, vertical acceleration data was simulated for 16 joints (channels) located at the ends of the transverse beams (Figure 4.4). Vibration of the supports was not analyzed considering that these nodes are fixed in the vertical direction, resulting in no vibration, which would cause instability in the ARX models.

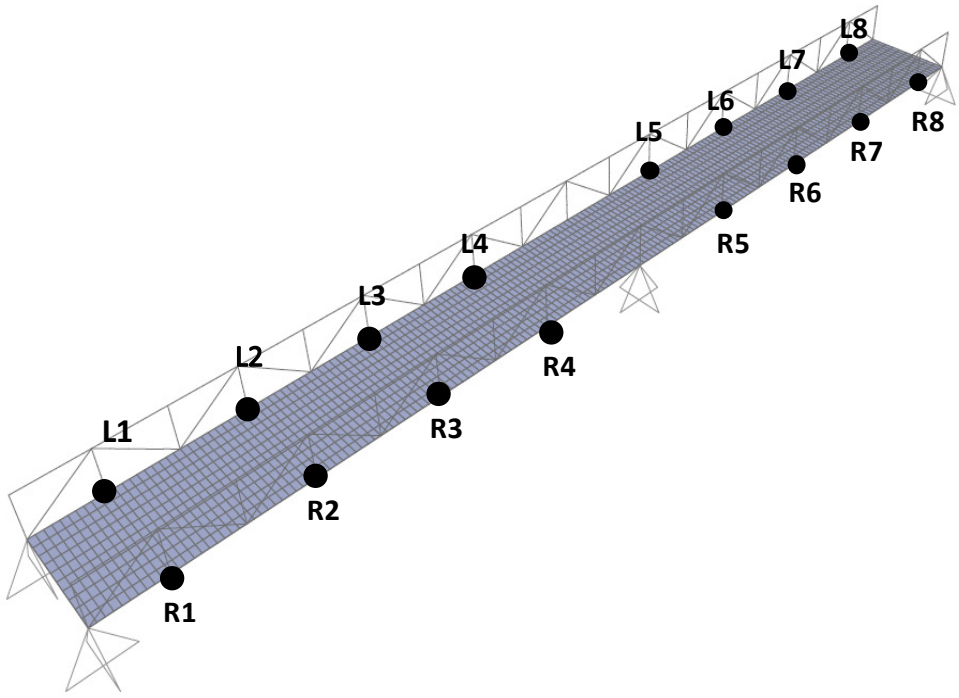

Figure 4.4. Arrangement of reference sensors (channels) in footbridge structure

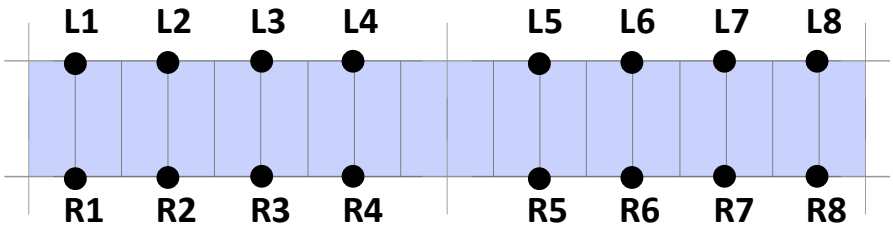

Figure 4.5. Plan arrangement of reference sensors (channels) in the footbridge structure

Table 4.1. Sensor cluster arrangement for the footbridge structure

Sensor Cluster	Reference Channel	Neighbour Channels
1	L1	L1, L2, R1, R2
2	L2	L1, L2, L3, R1, R2, R3
3	L3	L2, L3, L4, R2, R3, R4
4	L4	L3, L4, L5, R3, R4, R5
5	L5	L4, L5, L6, R4, R5, R6
6	L6	L5, L6, L7, R5, R6, R7
7	L7	L6, L7, L8, R6, R7, R8
8	L8	L7, L8, R7, R8
9	R1	L1, L2, R1, R2
10	R2	L1, L2, L3, R1, R2, R3
11	R3	L2, L3, L4, R2, R3, R4
12	R4	L3, L4, L5, R3, R4, R5
13	R5	L4, L5, L6, R4, R5, R6
14	R6	L5, L6, L7, R5, R6, R7
15	R7	L6, L7, L8, R6, R7, R8
16	R8	L7, L8, R7, R8

Channels were grouped in 16 sensor clusters, where each cluster is composed of the reference channel and neighbour channels (Table 4.1). As explained in the methodology of the ARX method, neighbour channels are used to predict vibration behaviour of the reference channel.

Vibration of the footbridge structure was initiated with a set of two vertical rectangular pulse forces, located at channel L7 and between channels R6 & R7 (Figure 4.6). Amplitude of these forces is defined with time history function in Figure 4.7:

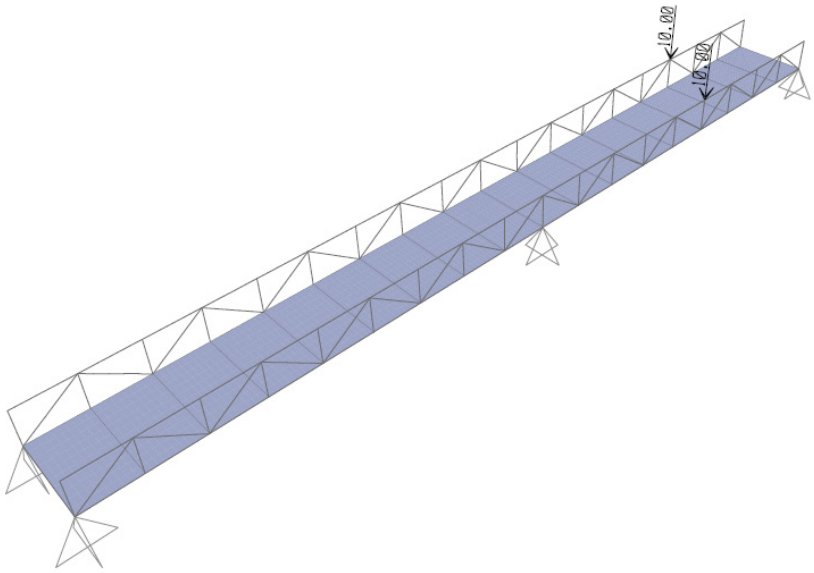

Figure 4.6. Triggering forces arrangement for the footbridge structure

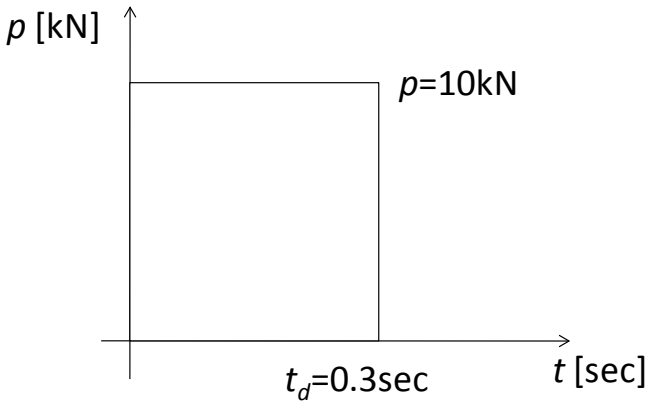

Figure 4.7. Time history function for triggering forces in the footbridge structure

Modal analysis of the footbridge model is performed considering the first 14 modes, with the modal participating mass ratio in vertical direction of 90%. This is considered to be adequate for the presented analysis method. First step of the modal analysis is to determine natural frequencies and modes for the model without any thermal effects on modal properties. Next step of the modal analysis includes calculation of the modal parameters with the stiffness properties of the structure that incorporates effects of axial forces from the temperature effect. Eigen vectors method are used for modal analysis in both steps. These modal parameters are then used for determination of acceleration response of the structure from the time history load case from the two rectangular pulse

forces. With this procedure, temperature effect is included in the vibration response of the structure.

Acceleration data of 16 channels indicated was used for the analysis (Figure 4.8). The sampling rate used in this analysis is 0.005, which corresponds to a sampling frequency of 200Hz. Modal analysis of the footbridge structure is conducted with first 14 natural modes, where the highest frequency is 17.7Hz.

A constant damping ratio of 1.2% was adopted for all modes of the structure. Starting point of the acceleration signal was shifted 6 seconds from the force impact moment, in order to capture free vibration data for the ARX model. Although it is not in the scope of this thesis, this methodology is also applicable to ambient vibration data where different techniques can be used a pseudo-free response data (Gül 2009). Based on the iterative process of determining the optimal value for the ARX model order (n_b in Eq. 3.4), a model order of n_b=8 was adopted as the optimal one.

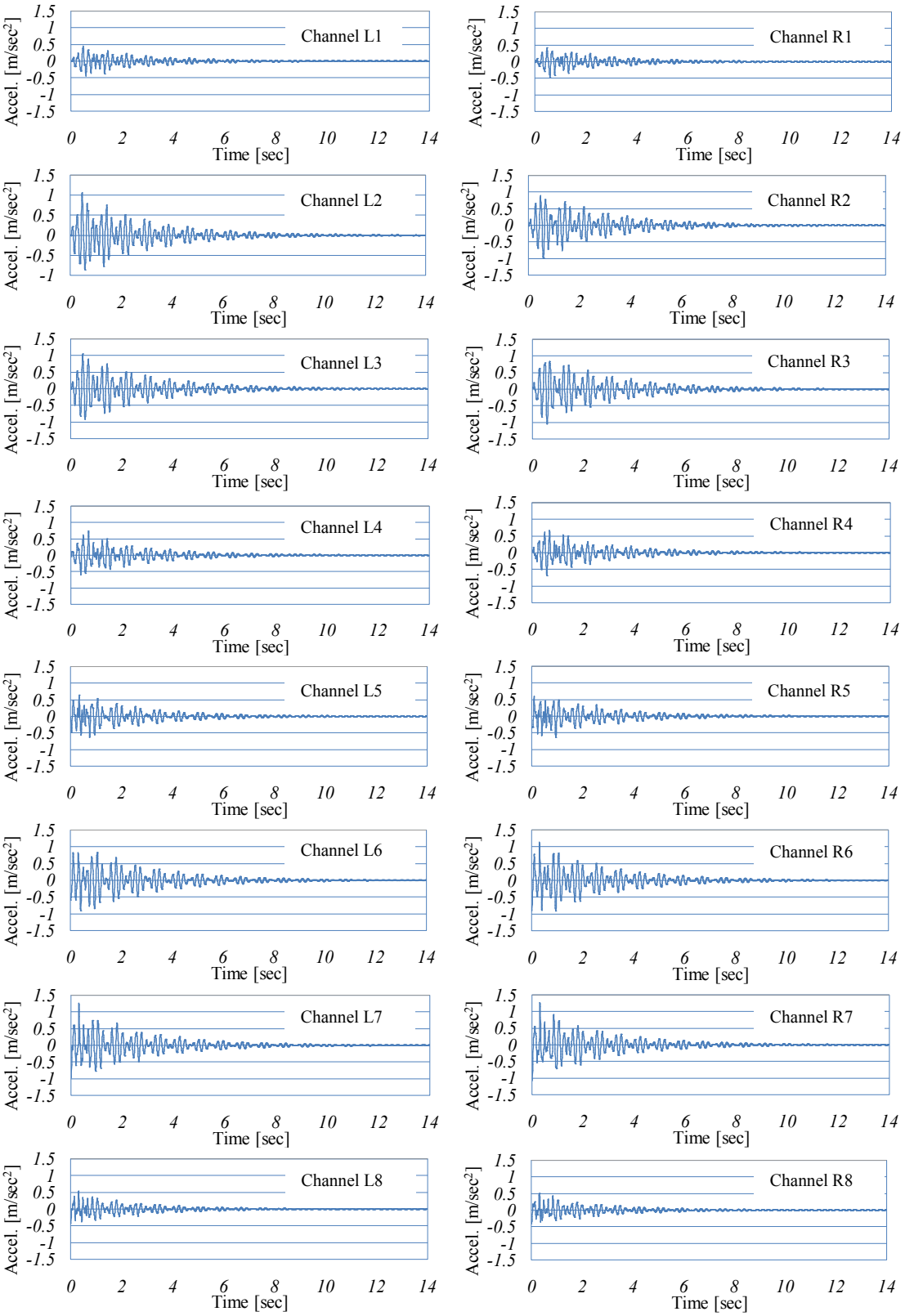

Figure 4.8. Acceleration data for channels L1-L8 & R1-R8

4.2 Temperature Variation

Temperature variation in the model was applied in two ways. Firstly, elastic modulus for steel and concrete was defined based on the temperature of these elements. Also, temperature load, acting uniformly across the cross section of the elements, was applied to the model, which is based on the temperature at the time of construction (default condition) and the current temperature. Temperature variation was defined for three groups of elements separately, where elements of each group had uniform temperature values:

- 1st group: concrete slab
- 2nd group: steel beams at concrete slab elevation
- 3rd group: vertical, diagonal and top steel beams.

Temperature arrangement that is used in this thesis represents one of the possible temperature distributions in bridge structures defined by different standards: BS 5400-2, AASHTO LRFD, German Bridge Code DIN 1072, Canadian Standard CAN/CSA-S6-06. A more detailed analysis of thermal effect distribution is not in scope of this thesis. Following summarises the temperature variations in bridges for different standards:

- BS 5400-2 states that the maximum bridge temperature is higher than maximum shade air temperature by maximum 20°C for bridges with steel decks, and by 11°C for bridges with concrete decks. Minimum effective bridge temperatures for steel elements is indicated to be -28°C, and for concrete elements -14°C. As for the maximum effective temperatures, for steel elements 47°C is defined, and for concrete elements 37°C is indicated. Temperature difference between top and bottom side of concrete slab is 10°C. This standard also mentions that temperature variation in a bridge is influenced by temperature fluctuations in shade, solar radiation, wind, convection, conduction and re-radiation of heat between the structure and surrounding environment.
- In AASHTO LRFD code, for a moderate climate, a range from -18°C to +49°C is given for temperature of bridge elements, and for a cold climate from -34°C to

+49°C. Maximum temperature difference between top and bottom side of the concrete slab is indicated to be 10°C. Temperature range for the steel elements specifically is indicated to vary from -35°C to +50°C, and for concrete elements from -18°C to +27°C.

- German code DIN 1072 indicates that a variation of ±35°C from the construction temperature should be considered, with differential temperature of 15°C between parts of the structure. Also, increase of 20°C for the top of the slab, and 35°C increase for the bottom edge of the steel girder is specified, compared to the construction temperature.
- Canadian Standard CAN/CSA-S6-06 mentions that steel has relatively high conductivity, which causes larger range of effective temperatures than in concrete structures (Emerson 1976a, 1976b). It is also suggested that an effective construction temperature of 15°C should be assumed, and that thermal gradient effects should be considered for continuous structures. Range of maximum effective temperatures varies from 10°C to 20°C above maximum daily mean temperature, and range of minimum effective temperatures varies from 5°C to 10°C below minimum daily mean temperature.

  Based on provisions of these standards, temperature variability in footbridge model was adopted as following:

  - Environmental temperature range is from -10°C to +30°C.
  - Temperature range for 1st group of elements (concrete slab) is from -10°C to +32.5°C.
  - Temperature range for 2nd group of elements (steel beams at concrete slab elevation) is from -15°C to +40°C.
  - Temperature range for 3rd group of elements (vertical, diagonal and top steel beams) is from -25°C to +55°C.

- Temperature in bridge elements depends on the environmental temperature (Figure 4.9). To provide more realistic distribution of temperature in bridge elements, randomness of ±2.5°C was adopted.
- Linear temperature distribution between left and right side of the concrete slab was adopted. Total temperature difference between these two sides is 5°C.
- Temperature load (Figure 4.10) in steel elements is based on the construction temperature (baseline case), which is adopted as 15°C. Temperature difference between the environmental temperature, and the construction temperature in the elements is then applied as the temperature load.
- Linear temperature gradient (Figure 4.11) between top and bottom side of the concrete side was adopted. For the minimum temperatures, this difference is 10°C, with the top side having smaller temperatures, while for the maximum temperatures this difference is 15°C, with higher temperatures for the top side.
- Elastic moduli of concrete (Figure 4.12) and steel (Figure 4.13) are assumed to have linear relation with temperature based on the references from Khanukhov et al. (1986) and Sabeur et al. (2007).

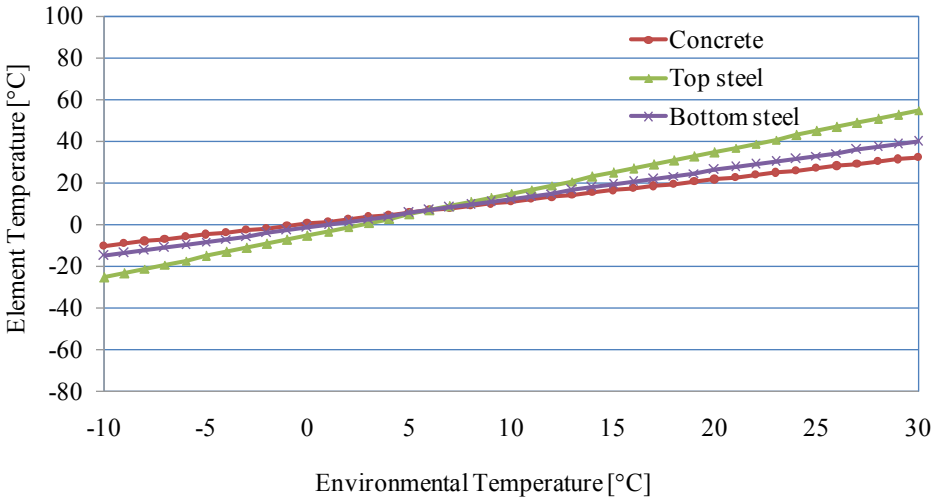

Figure 4.9. Relation between element temperature and environmental temperature

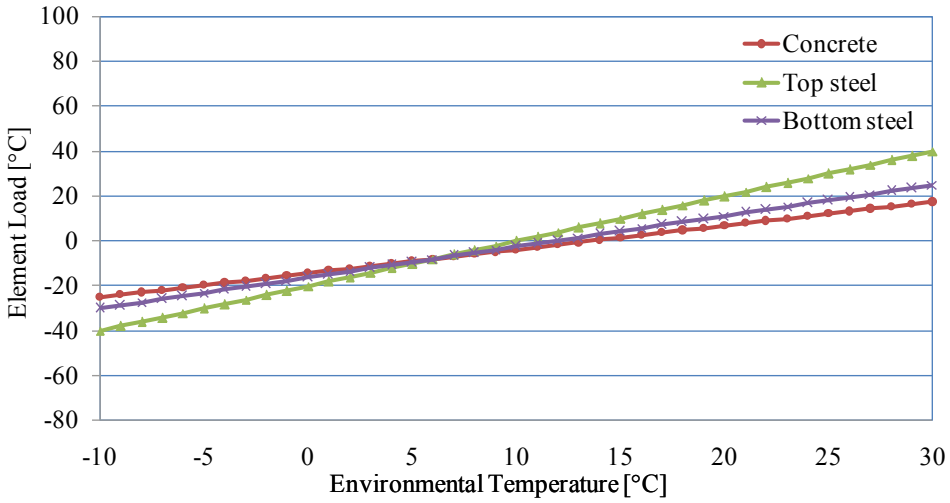

Figure 4.10. Relation between element temperature load and environmental temperature

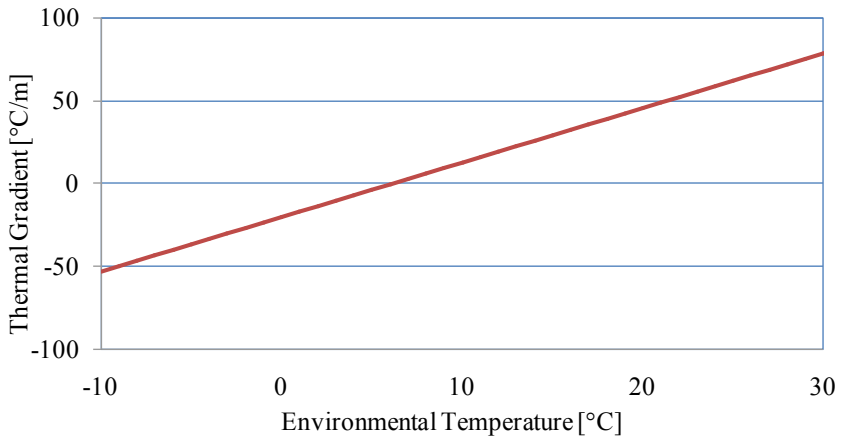

Figure 4.11. Relation between thermal gradient of slab and environmental temperature

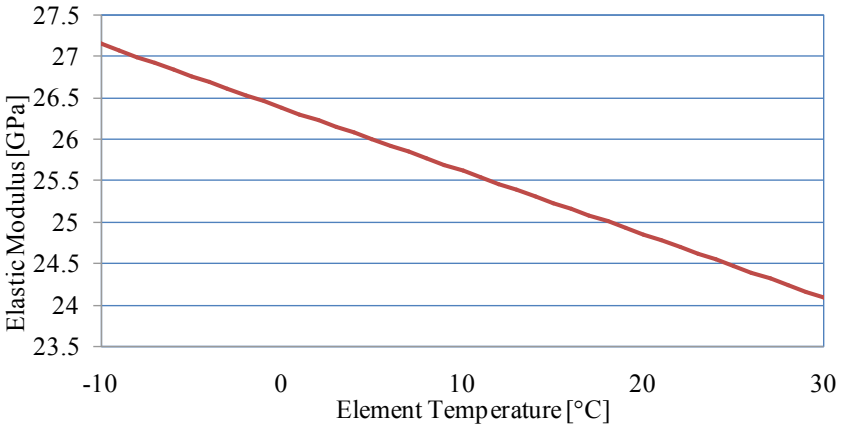

Figure 4.12. Relation between elastic modulus of concrete and element temperature

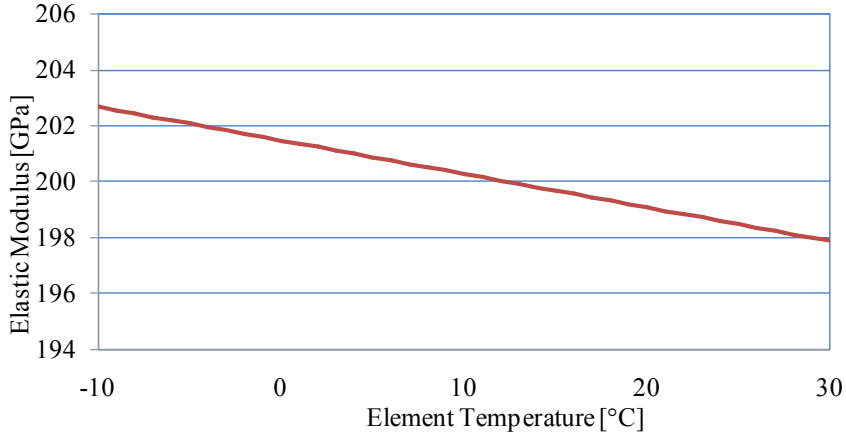

Figure 4.13. Relation between elastic modulus of steel and element temperature

4.3 Damage Cases

Damage cases applied in this research are:

- Damage case 1 (DC1): Reduction of steel elastic modulus of 20% for all steel beams between channels L2 & L3 and R2 & R3 (Figure 4.14)
- Damage case 2 (DC2): Reduction of steel elastic modulus of 10% for all steel beams between channels L2 & L3 and R2 & R3 (Figure 4.14)

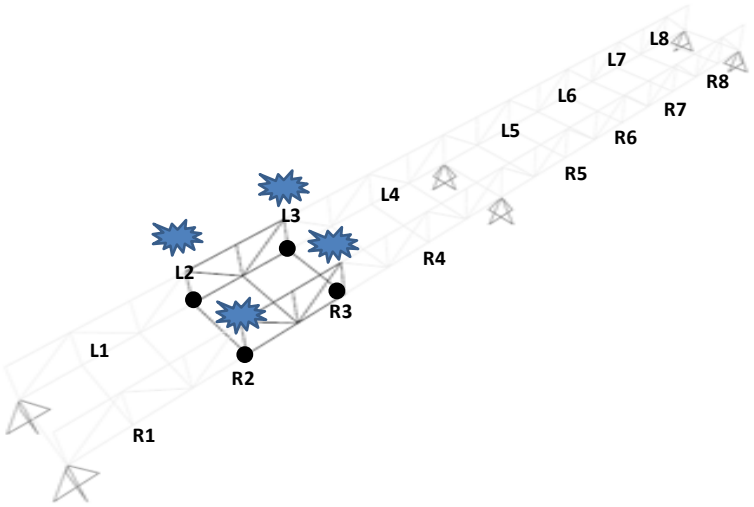

Figure 4.14. Damage cases 1 & 2 arrangement

- Damage case 3 (DC3): Assigning fixed support at channel R8 location, instead of the pinned support (Figure 4.15)

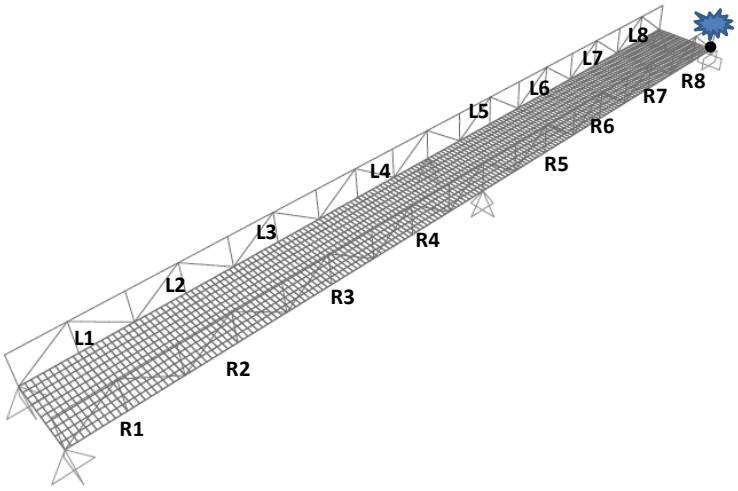

Figure 4.15. Damage case 3 arrangement

- Damage case 4 (DC4): Reduction of steel elastic modulus of 20% for all steel beams between channels L6 & L7 and R6 & R7 – symmetric case compared to DC1 (Figure 4.16)

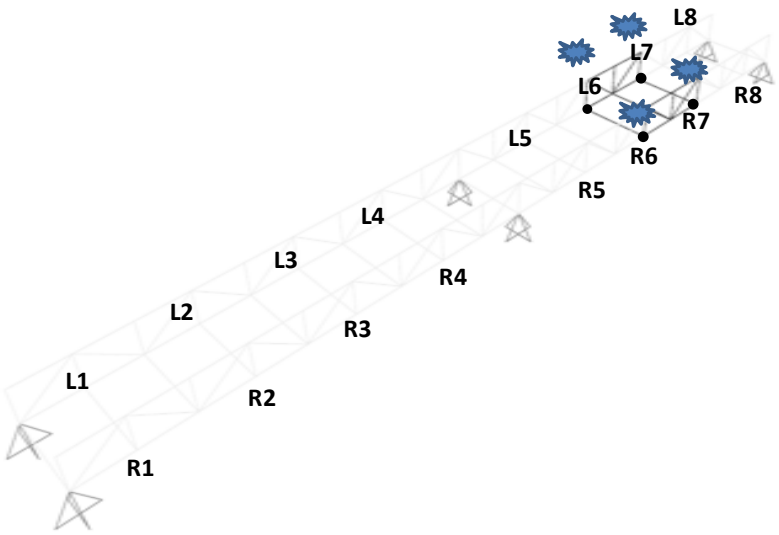

Figure 4.16. Damage case 4 arrangement

- Damage case 5 (DC5): Reduction of concrete elastic modulus of 25% for concrete deck between channels L2 & L3 and R2 & R3 (Figure 4.17)

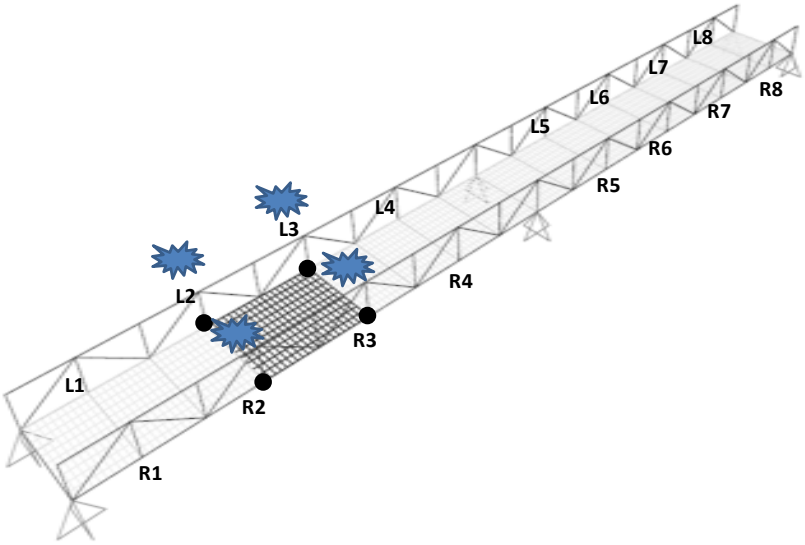

Figure 4.17. Damage case 5 arrangement

Damage cases analyzed in this research were chosen to represent some typical damage types that can occur at a footbridge structure. The way that the damage was simulated in the models is aligned with previous literature mentioned in Chapter 2. Giraldo et al. (2006) simulated damage as a loss of stiffness in a model. Wahab and De Roeck (1997) determined that elastic modulus is mostly influenced by the temperature variation. Doebling et al. (2000) and Cornwell et al. (1999) also concluded that temperature change influences modal frequencies mostly because of the material changes and the changes in the boundary conditions. Moorty and Roeder (1992) mentioned that stiffness of supports can be increased due to deterioration of the supports, considering that resistance to movement is also increased. Fu and De Wolf (2001) concluded that lower temperatures can increase friction in the bearings, and restrain rotation of the supports, causing axial tensions forces in the structure from the temperature effects.

Most of the damage cases in this study cause reduction of the stiffness in the footbridge structure, and they were applied as a reduction of the material's elastic modulus for the specific location in the structure. Several studies defined damage cases similarly (Meruane and Heylen 2012; Bakhary et al. 2007). In a real type structure this reduction can occur if there is a reduction in cross section of elements - due to corrosion of steel and reinforcement, chemical attack, wear, delamination, cracks, etc… Contrary to the reduction of stiffness in the structure, damage case 3 introduces fixed end support at channel R8, instead of the pinned support, which increases the stiffness of the structure (Moorty and Roeder 1992). Increased support fixity can occur at real type structures due to the effect of freezing, or obstruction of expansion by debris. This damage case is also more general in nature, considering that it affects support condition of the whole structure, and not just the elements in the specific location.

Damage case 2 (DC2) is adopted for comparing with damage case 1 (DC1), considering that damage type and location is the same as in DC1, with the smaller extent of the damage. Damage case 4 (DC4) is also adopted for comparison with the DC1, considering that DC4 has the same characteristics as DC1, only with the symmetric location compared to the middle supports. Finally, DC5 was adopted to investigate the damage effect on the slab element with concrete material.

4.4 Damage Detection Procedure

Damage detection procedure developed for this study comprises several sequential steps, indicated in Figure 3.6. For the purpose of this study damage detection procedure employed acceleration data of 16 channels, obtained from the SAP2000 software. Location of sensor channels, sampling rate, duration of the acceleration signal and location of the triggering forces were directly defined in SAP2000 software. VBA codes were employed in order to define SAP2000 input files, where variable temperature effects were applied to footbridge finite element models. Automatic analysis of SAP2000 models was performed using windows batch files.

Acceleration data obtained from the SAP2000 software was then utilized for time series analysis procedure, performed in the MATLAB software. MATLAB codes contained data about sampling rate, arrangement of the sensor clusters, duration of the acceleration signal used for the analysis, noise levels, delay values and time series analysis model orders. Time series analysis procedure employed acceleration data from baseline and damage cases of the footbridge model, where the output data of this procedure represented damage features (DF_{ARX}).

Final step of this methodology included neural network analysis with backpropagation algorithm. This analysis was performed using MATLAB Neural Network Toolbox, where number of input, hidden and output nodes was defined. Chapter 5.3 contains detailed description of the relevant parameters needed for the neural network analysis used in this thesis. Input data for the neural network analysis contained temperature values from the footbridge model. Output data used for the neural network training step contained DF_{ARX} features, obtained from the time series analysis step. Temperature values used as input data were automatically obtained from the SAP2000 input files using MATLAB codes. Output data of the neural network procedure represented damage features (DF_{ANN}) from the temperature effects only.

Final damage features (DF) were obtained using damage features from the time series analysis (DF_{ARX}) and neural network analysis (DF_{ANN}). All of the steps used in damage detection procedure were automated using MATLAB codes.

CHAPTER 5:ANALYSIS, RESULTS AND DISCUSSION

Damage detection analysis results and discussion for the introduced methodology are presented in this chapter. Five damage cases are introduced to the footbridge model as discussed in the previous chapter, along with addition of artificial noise of 0%, 1%, 3% and 5%. Also, frequency variation due to the temperature effects, threshold determination as well as influence of the location of the triggering forces on final damage features are discussed in this chapter.

5.1 Threshold Determination

In order to correctly identify damage in a structure, a threshold value of the damage features for the baseline structure for different tests should be determined. Threshold value was adopted based on the confidence level of 90% for damage features (DF_{ARX}) determined from the effect of noise on the structure. Three different threshold values have been determined – for the noise level of 1%, 3% and 5% (Figure 5.1, Figure 5.2 & Figure 5.3), where two baseline cases are compared with 100 simulations.

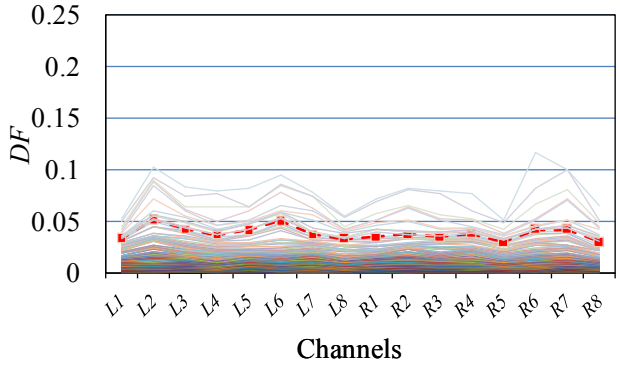

Figure 5.1. *DF* for 100 cases with 1% noise

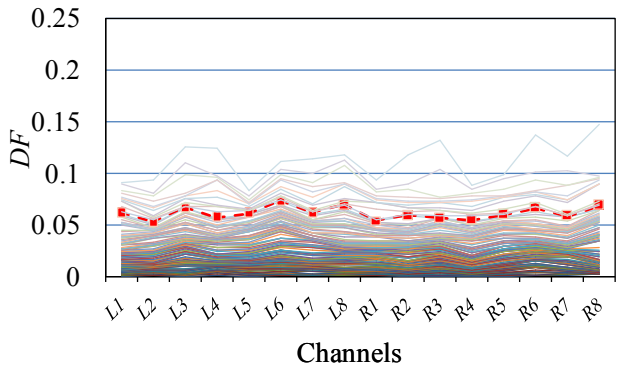

Figure 5.2. *DF* for 100 cases with 3% noise

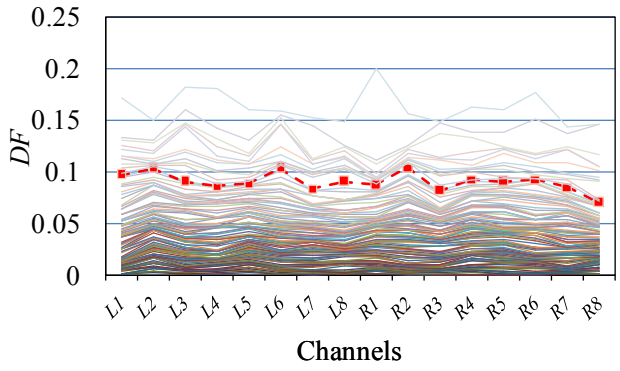

Figure 5.3. *DF* for 100 cases with 5% noise

5.2 Frequency Variation and Output Vibration Data

As already mentioned in the literature review chapter, modal frequencies of the structures change with the change in element temperatures. In Figure 5.4 the change of the first six natural frequencies, which depends on the environmental temperature load in the structure, is indicated. It can be concluded that the increase of the temperature causes decrease of the natural frequencies in the footbridge structure. Considering that element cross sections used in this model were not based on a specific reference, verification of the model was performed by comparison of natural frequencies and modal shapes with the results from Moser and Moaveni (2011). Figure 5.4 and Figure 5.5 display the relationship between natural frequencies and temperature change. In both cases natural frequencies decrease with the increase of the temperature. Considering that the asphalt layer was considered in the study performed by Moser and Moaveni (2011), frequency change has bilinear behaviour (Figure 5.5), while in Figure 5.4 frequency change is

mostly linear. Due to the fact that cross sectional properties are not identical between these two models, natural frequencies also do not have identical values. However, it can be concluded that frequency values and frequency change due to the temperature variation follow similar pattern in both cases, which indicates that both models are experiencing similar dynamic behaviour due to temperature effects. This is also verified in Figure 5.6 and Figure 5.7, where mode shapes of both models are displayed. Therefore, based on this model verification analysis, footbridge model adopted for this study can be considered as a representative model of a real type structure.

Based on the mode shapes indicated in Figure 5.6, it can be concluded that the governing direction affecting vibrational properties of the footbridge structure is the vertical direction. Therefore, vertical acceleration data obtained from 16 sensors at the footbridge structure can be considered to be representative enough for dynamic analysis of the structure needed for this study.

Sample output vibration data for the baseline case, used for determination of ARX models are shown in Figure 4.8. Finally, in Table 5.1 frequency variation due to the damage cases is also presented. Frequency variation is more pronounced for bigger reduction of the material modulus. It is also observed that the concrete slab is not contributing significantly in the structure's stiffness as the steel beams. Change in the value of the first natural frequency for DC5 is only 0.147%, compared to the DC2 where this change is 0.9%. It can also be concluded that if the concrete modulus reduces to 0%, change in first 4 modes is below 5%. Also, DC3 increases stiffness of the structures, which is indicated with opposite sign of the frequency change, whereas other damage cases introduce reduction of stiffness in the structure.

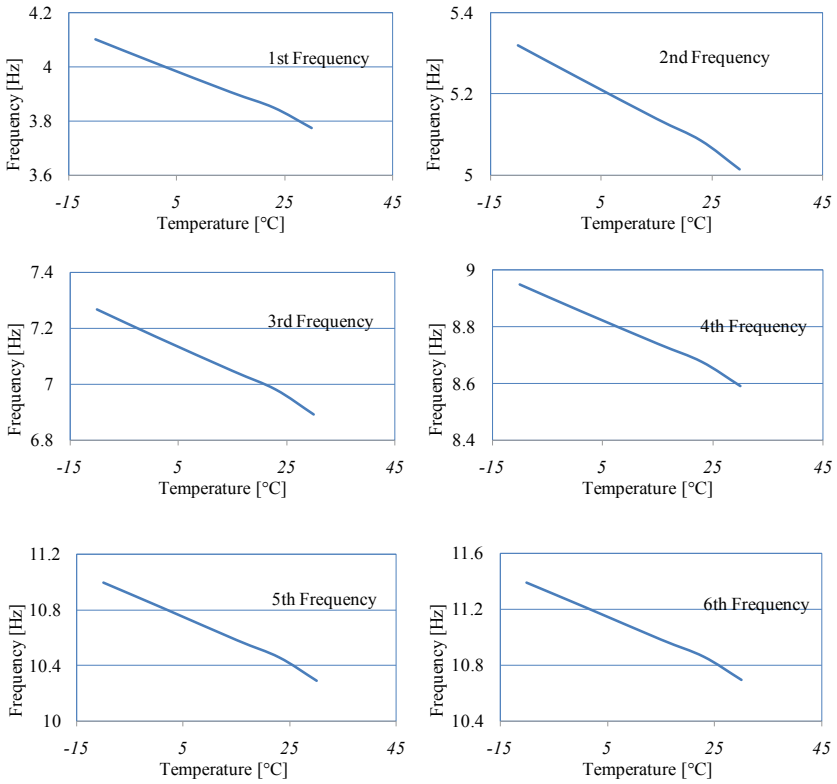

Figure 5.4. Relation between first 6 natural frequencies and the element temperature

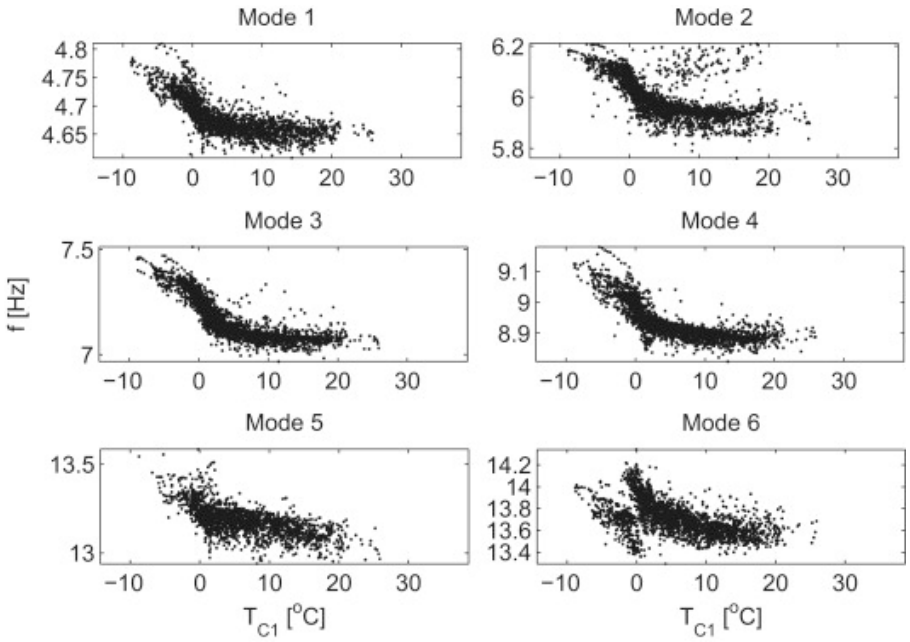

Figure 5.5. Identified natural frequencies versus western abutment temperature (from Moser and Moaveni 2011 with permission)

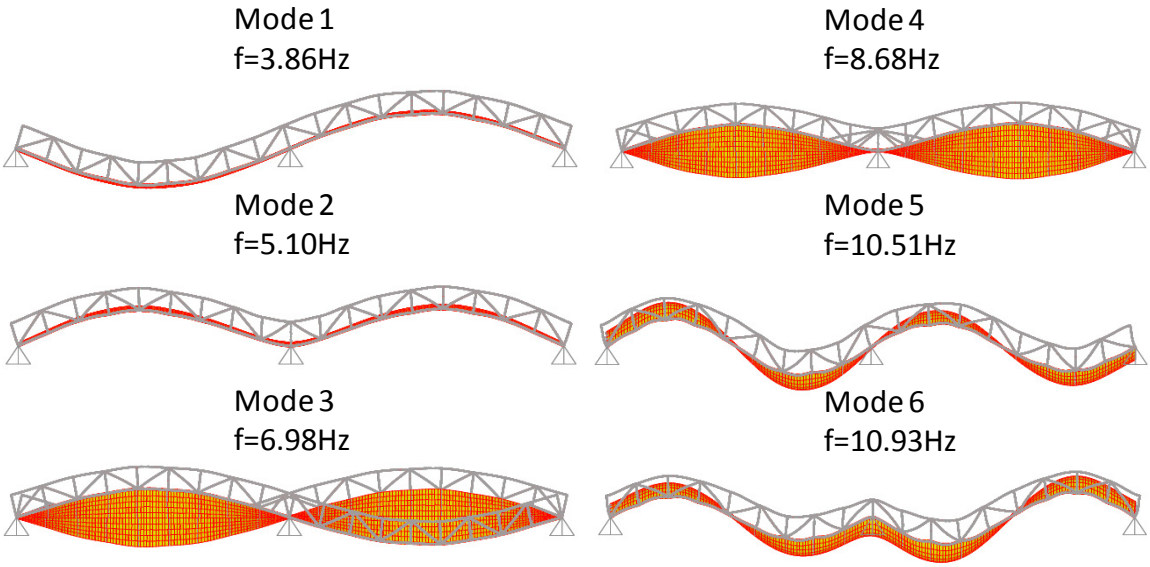

Figure 5.6. First 6 mode shapes of the footbridge structure

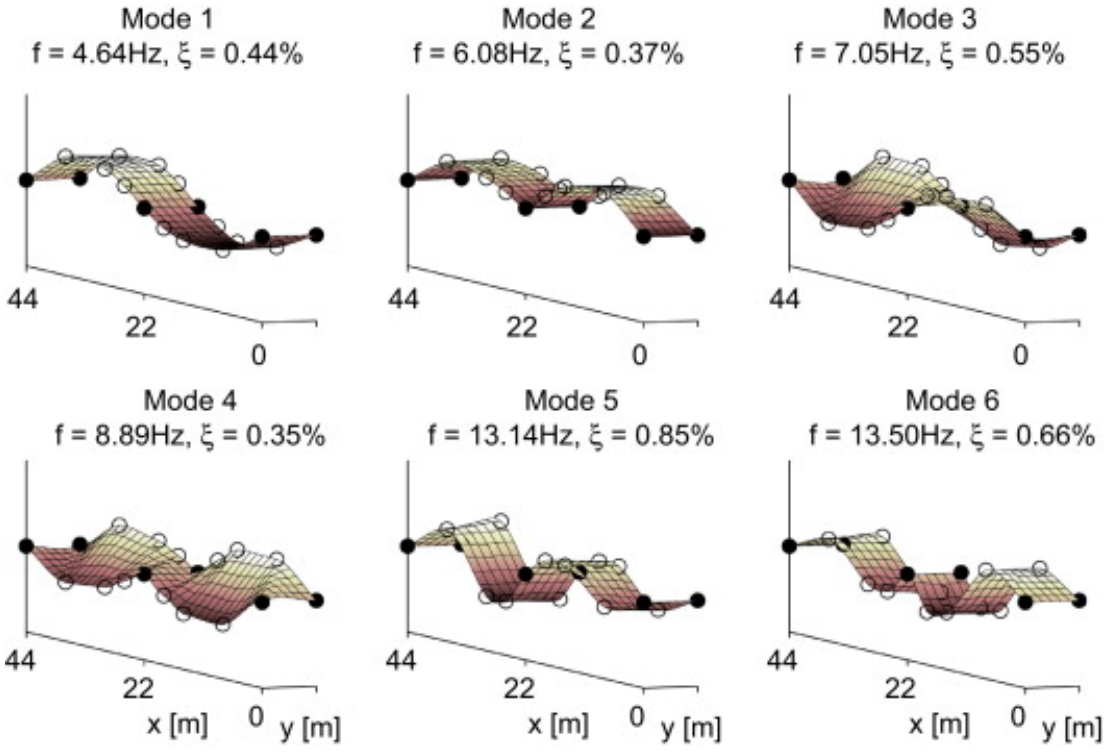

Figure 5.7. Mode shapes identified from a preliminary test on April 4, 2009 (from Moser and Moaveni 2011 with permission)

Table 5.1. Relation between first 14 natural frequencies and damage cases

Mode	DC1 – Esteel 80% (%)	DC2 – Esteel 90% (%)	DC 3 - Support fixed (%)	DC4 - Symmetric case Esteel 80% (%)	DC5 – Econc 75% (%)	Econc 0% (%)
1	-2.005	-0.900	0.432	-2.005	-0.147	-3.257
2	-1.212	-0.578	0.345	-1.212	-0.203	-4.617
3	-1.453	-0.656	0.299	-1.453	-0.112	-1.546
4	-0.989	-0.471	0.243	-0.989	-0.134	-2.155
5	-0.919	-0.389	0.360	-0.919	-0.209	-19.020
6	-0.502	-0.256	0.411	-0.502	-0.155	-18.796
7	-0.373	-0.162	0.733	-0.373	-0.204	-24.364
8	-0.381	-0.184	2.407	-0.381	-0.272	-23.861
9	-1.792	-0.290	1.730	-1.792	-0.111	-12.020
10	-2.297	-1.390	0.562	-2.297	-1.021	-11.368
11	-0.425	-0.353	0.060	-0.425	-0.323	-11.624
12	-1.910	-0.404	0.058	-1.910	-0.092	-10.964
13	-2.167	-0.827	0.125	-2.167	-0.143	-10.006
14	-0.962	-0.475	0.617	-0.962	-0.141	-8.114

5.3 Neural Network Model Development & Results

Artificial Neural Networks (ANNs) can generally be employed for problems for classification of data or prediction of data. Neural network in this thesis was used for prediction of data, and it belongs to the supervised network type, considering that the input and the output data are used for training.

Considering that the purpose of this research is to compensate temperature effects from damage effects using vibration monitoring data, input data set used for training consists of 500 sets of 3 different temperature values, ranging from -25°C to 55°C. These temperatures represent environmental temperature values of three groups of bridge elements: top steel beams, bottom steel beams and concrete deck. Corresponding output data comprises 500 sets of damage features (DF_{ARX}) for the 16 channels shown in the previous chapters. These damage features are the result of damage detection of bridge model under the environmental temperature load only (i.e. no damage cases are introduced to the model at this point).

The ANN is trained to predict damage features in regards to the environmental temperature data of three groups of bridge elements. When the damage is introduced to

the model, simulation of the ANN is performed with input data consisting of 3 sets of temperatures, applied within the damage cases. Outputs of the Neural Network (DF_{ANN}) are the damage features from the temperature effect only. These damage features (DF_{ANN}) are then used for temperature compensation process, along with the damage features calculated from the damage cases (Chapter 3.3).

The ANN used for this process consists of one hidden layer with 10 nodes, and of one output layer with 16 nodes, which corresponds to the number of channels on the bridge. After conducting the analysis with different configurations of nodes, ten hidden neurons were finally adopted considering that the network performed satisfactorily. Determining the number of units for the hidden layer is usually not straightforward procedure as for the input and output layers (Freeman and Skapura 1991). With too few nodes, network may not be powerful enough for a given task. With a large number of nodes, computation is too expensive, and the ANN can memorize input training samples – become over-fitted (Mehrotra et al. 1997). Number of hidden nodes should usually be between the number of input and output nodes (Heaton 2008). Number of input nodes is equal to number of input data sets, and the number of output nodes is equal to number of output data sets.

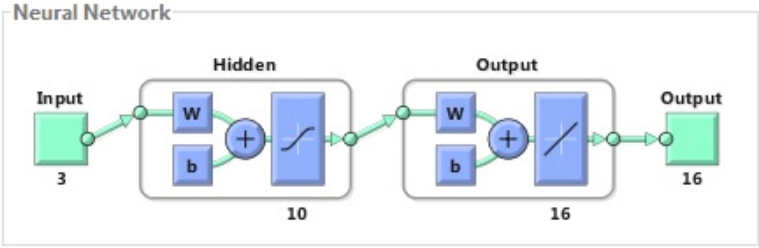

Figure 5.8. Neural network topology (MATLAB output)

The total input data is then divided into three groups - training, validation and testing group. Data division method used in this network is a random method (*dividerand* comment in MATLAB), which divides the data randomly into sets for training (70%), validation (15%) and testing (15%). During the training phase, gradient is computed, and weights and biases are updated. As mentioned earlier, backpropagation training method adopted for this network is the Levenberg-Marquardt method (*trainlm* comment in MATLAB).

Training can also be classified as incremental training or as batch training. Batch training was used for this network, considering that training occurred after all the input and output data was presented to the network. Weights are updated only after all samples are presented to the network (Mehrotra et al. 1997). After the whole data is presented to the network, cumulative error is computed (Jagannathan 2006). In the incremental training, training occurs after each input is applied to the network. Batch training usually produces smaller errors during the training, making the process faster (Demuth and Beale 2002).

Network should be trained with the sufficient number of input sets, and with proper set of data, which means that the training data should be fully representative of the environmental data. Training process can be controlled with the error rates. However, small learning error does not mean that the network is properly trained (Figure 5.9). Also, adding too many hidden layer units always decreases error in learning set, but it increases error in the test set after a point due to over-fitting (Kröse & van der Smagt 1994).

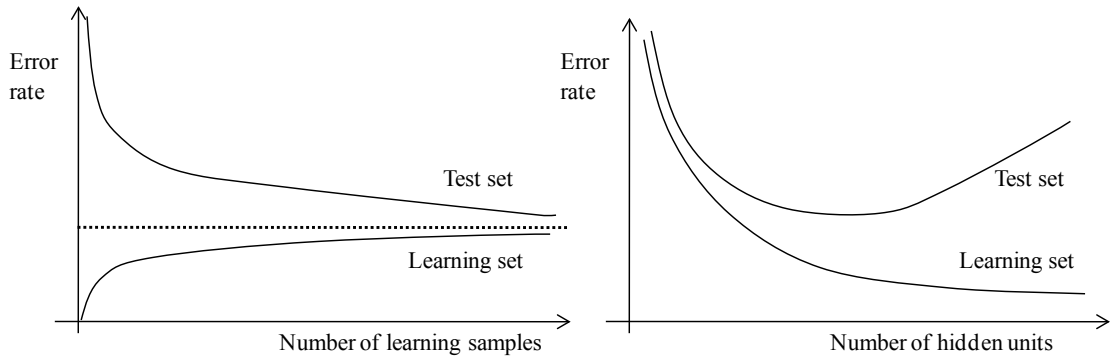

Figure 5.9. Error rate for test & learning set compared to number of learning samples (left) & number of hidden units (right) (adapted from Kröse & van der Smagt 1994)

During the training, back propagation method is used for determination of the optimal weights in the neuron connections. Back propagation (or generalized delta rule) indicates that error of the prediction is returned to the network, which then employs this error to modify connection weights between the nodes (Figure 5.10 & Figure 5.11). Firstly, initialization function initializes weights of layers and its bias values. For the ANN used in this thesis, this is performed with the *Nguyen-Widrow* initialization algorithm. The

goal of algorithm is to distribute active region of neurons evenly over the input space (Demuth and Beale 2002). This algorithm requires that the appropriate transfer function has a finite input range. Based on this criterion, *Tansig* function was selected. Advantages of this algorithm are that less neurons are wasted than in ordinary random weight methods, and that the training is faster (Demuth and Beale 2002). Considering that these values are random, each the network is run, results will be slightly different. After assigning initial values of weight and bias, input function in the layers defines how the input data is processed in the layer. It defines input of the layer based on the weights and bias values, and it combines input data by summation.

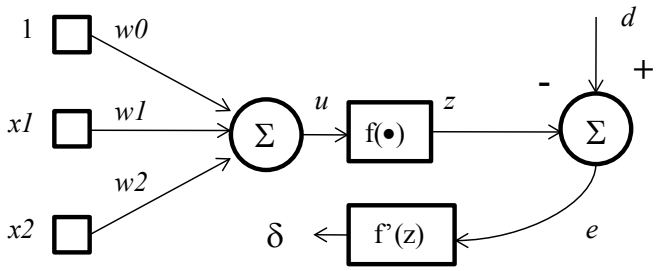

Figure 5.10. Backpropagation algorithm for single neuron (adapted from Hu and Hwang 2000)

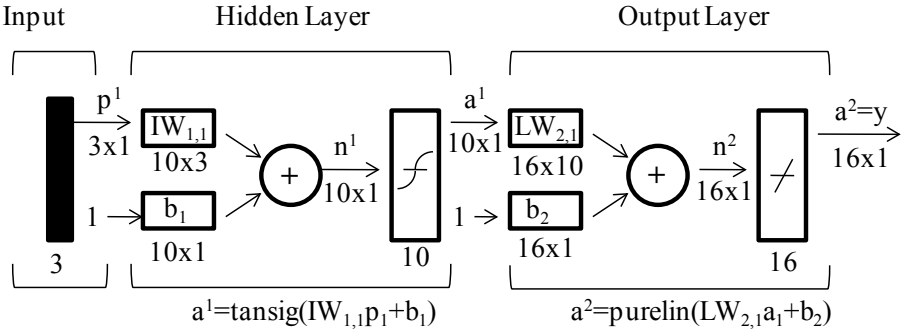

Figure 5.11. Backpropagation algorithm used in this thesis (adapted from Demuth and Beale 2002)

After the input layer receives the initial data and performs weighted summation in the nodes, information is then transferred to the next layer (hidden layer). The process of weighted summation is performed again in this layer, which produces its own output values to the next layer (output layer in this thesis). Function that defines output of the layer is a transfer function. In this thesis, *Tan-Sigmoid* Transfer function is used for

hidden layer, which is a MATLAB equivalent of *tanh* function (Figure 5.12). Certain transfer functions constrain output data values between some maximum and minimum limit values, which means that they rescale the summation data. This is the case with the *tansig* function, which limits output data values between -1 & 1. Some transfer functions introduce limits between 0 & 1, but considering that the input data of this network is the temperature of the bridge elements, which can have negative values, choosing transfer function with negative limits is more appropriate. This data is then transferred to the output layer.

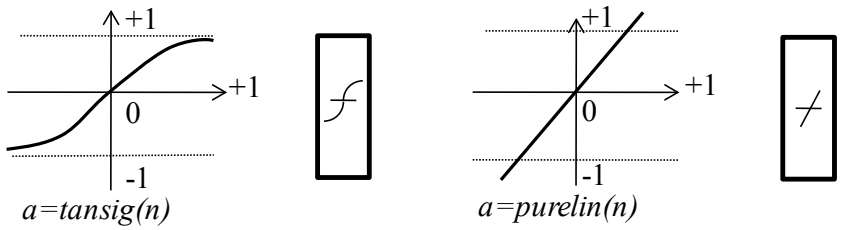

Figure 5.12. Activation functions of hidden and output layer with *n* input vectors (adapted from Demuth and Beale 2002)

With this data, the output layer produces the output values, which are basically prediction values based on the input data. Transfer function of the output layer is the *purelin* function (Figure 5.12). It does not have limit values, but returns the values passed to it. This is important, considering that network output can have any range of values. When these values are compared to the desired output values, error is calculated and "back propagated" to the hidden layer. However, every node receives a portion of the error, because of the corresponding weight. Process is repeated until each node in the network has received an error signal that describes its relative contribution to the total error. Based on this signal, connection weights are updated (Freeman and Skapura 1991). Weights on the output layer are updated first. Network tries to minimize the network performance function (calibration process), which is the mean square error (*mse*) function in our network. If the new introduced data comprises similar patterns as in the training data, hidden layers will be activated with the corresponding output data. One step of modifying the connection weights is defined as an epoch (all the weights are modified once).

One of the standard backpropagation algorithms is the gradient descent algorithm. With this algorithm, the network is updated in the direction of negative gradient of the performance function. With this type of training, learning rate, which refers to the rate of how the network learns and retains patterns from the data, is constant during the process. This can cause the algorithm to converge slowly. In conjugate gradient method, algorithms are being updated along conjugate directions, which makes the process faster than with gradient descent algorithm. Speed of training can also be improved with adaptive learning rate, learning with momentum, or with the application of better initial conditions - weights and activation functions (Jagannathan 2006). Newton's method is one of the alternatives to these conjugate gradient methods. However, it includes the calculation of the Hessian matrix, which can be a complex step for feed-forward neural networks. The Levenberg-Marquardt (LM) method (Chapter 3.2) is the method used for this network, and it does not involve calculation of the Hessian matrix, as in the Newton's method. It computes the approximate Hessian matrix. This method belongs to category of fast algorithms, which use standard numerical optimization techniques. It is also considered to be the fastest for moderate-sized feed-forward networks (Demuth and Beale 2002). It has characteristics of the Newton's method - speed, and of steepest descent method - convergence (Hagan and Demuth 1996).

In the backpropagation procedure, some steps include calculation of the derivatives of the transfer functions. For a static network, as in this thesis, static derivative algorithm is employed. It uses chain rule to determine derivatives from the networks performance (Demuth and Beale 2002). During the training, several indicators of neural network performance are displayed in output window of MATLAB: performance, magnitude of the gradient of performance, and validation check number.

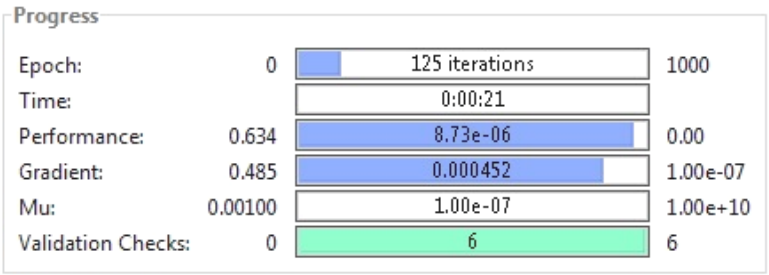

Figure 5.13. Neural network training progress

Output data of the neural network part of the methodology are also presented in this chapter. First, several plots are presented for comparison of how well the network fit the data: Error Histogram, Performance Plot, Regression Plot. In Figure 5.14 it is indicated that as the noise level increases from 0% to 5%, range of errors also increases. In Figure 5.15 graphs indicate that all three error curves are with similar shape, which is a good indicator of the network behaviour.

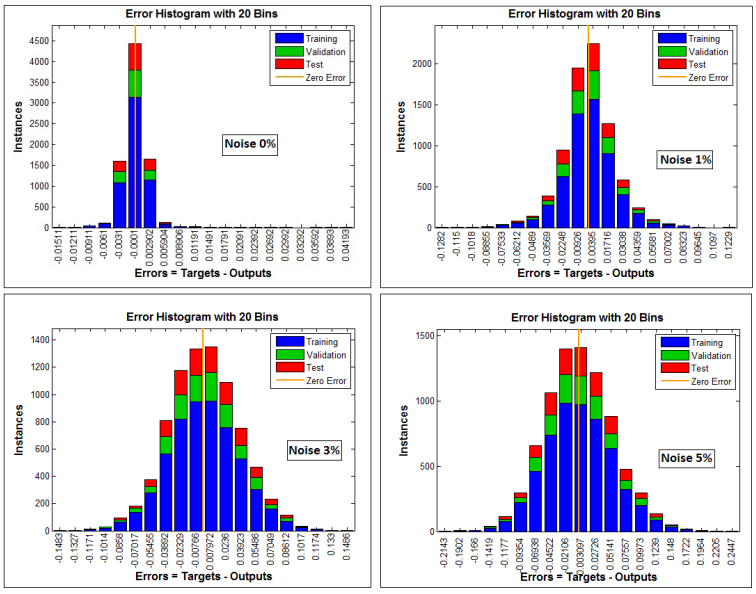

Figure 5.14. Neural network histograms for different levels of noise

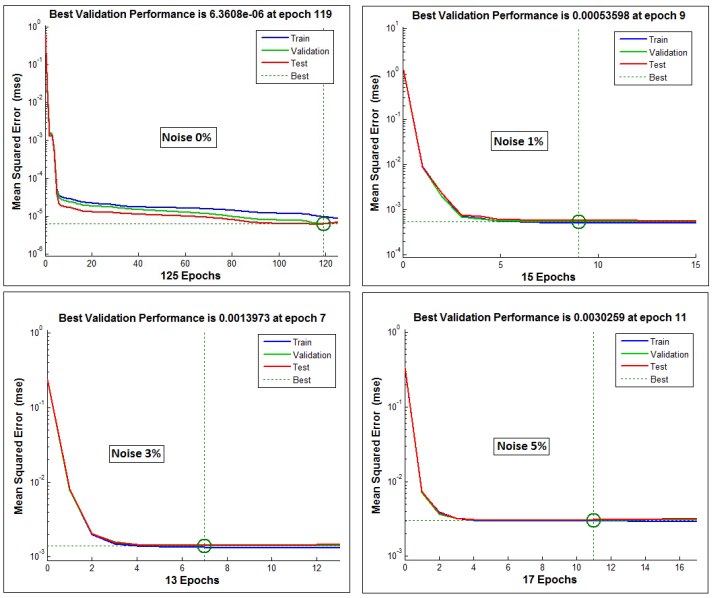

Figure 5.15. ANN validation performance diagrams for different levels of noise

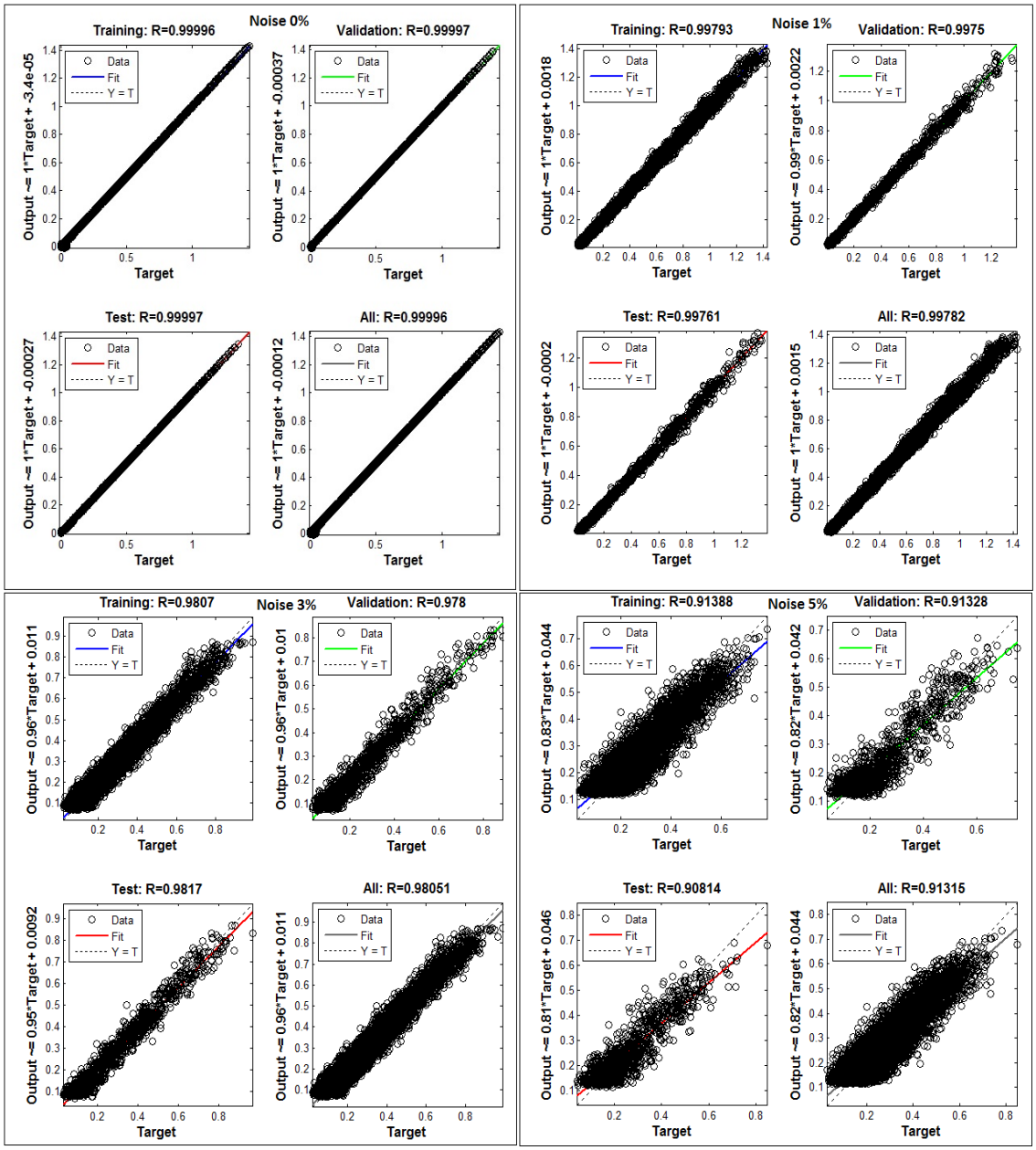

Figure 5.16. Neural network R values for different values of noise

This arrangement (topology) of the neural network performed satisfactory, which is proven by the correlation coefficient (R) value of 0.908 for noise of 5%, 0.981 for noise of 3%, 0.997 for noise of 1%, and 0.999 for the training case with no noise as shown in Figure 5.16. Perfect correlation in the regression analysis of the network, gives value of R=1 - exact linear relationship between target values and actual outputs.

It is also observed that the R value decreases as the level of the noise is increased. Noise in the data set of the real structure can occur due to instrumentation and operational issues. Considering that this is a numerical analysis, noise of 1%, 3% & 5% is introduced artificially. Adding noise to training sometimes helps the network to converge even if no noise is expected on the inputs (Freeman and Skapura 1991). This is especially the case when the size of the training set is small (Merhotra et al. 1997).

Criteria for stopping the procedure are usually when the number of these epochs reaches certain value, or when the error reaches some minimum value (convergence). These criteria are called "Stop Training Criteria". For this network, maximum number of epochs was 1000, minimum gradient value was 1e-07, and maximum number of validation checks was 6, which means that validation error fails to decrease for 6 iterations.

All the parameters from the MATLAB NN Toolbox indicated that the Neural Network successfully fitted the data needed for compensation of temperature effects on vibration monitoring data. In the following sections, results for the damage cases are presented.

5.4 Damage case 1 (DC1): Reduction of steel elastic modulus of 20% for all steel beams between channels L2 & L3 and R2 & R3

5.4.1 DC1 with 0% noise

Damage Features (DF_{ARX}) for DC1, indicated in Figure 5.17a, are damage features determined without any detrimental effect from the temperature. They clearly show the exact location of the damage, with the appropriate damage feature values. Channels L2 & L3 and R2 & R3 have the highest damage features as expected. Considering that this is a continuous structure, channels that are the closest to the mentioned channels have also high damage features, compared to the channels in the opposite span. This demonstrates that the location and the extent of the damage are clearly identified when there is no temperature effect in the structure. However, Figure 5.17b indicates that when there is temperature effect included in the response of the structure, DF_{ARX} for the most of the random temperatures cannot clearly indicate the location and severity of the damage. For clarity purposes only first 10 out of 100 cases with random temperature are indicated in Figure 5.17b and Figure 5.17c.

In the Figure 5.17c DF_{ANN} for the first 10 random temperatures are presented, which are the outputs of the Neural Network. They represent damage features for the temperature effect only, with no damage in the structure. These damage features are then employed for determination of final *DFs*, which are presented in Figure 5.17d. It can be concluded that these *DFs* can clearly indicate the existence, location and severity of the damage even when the damage and temperature changes are applied simultaneously. Moreover, the DF values in this graph are very similar to the reference DF values in Figure 5.17a.

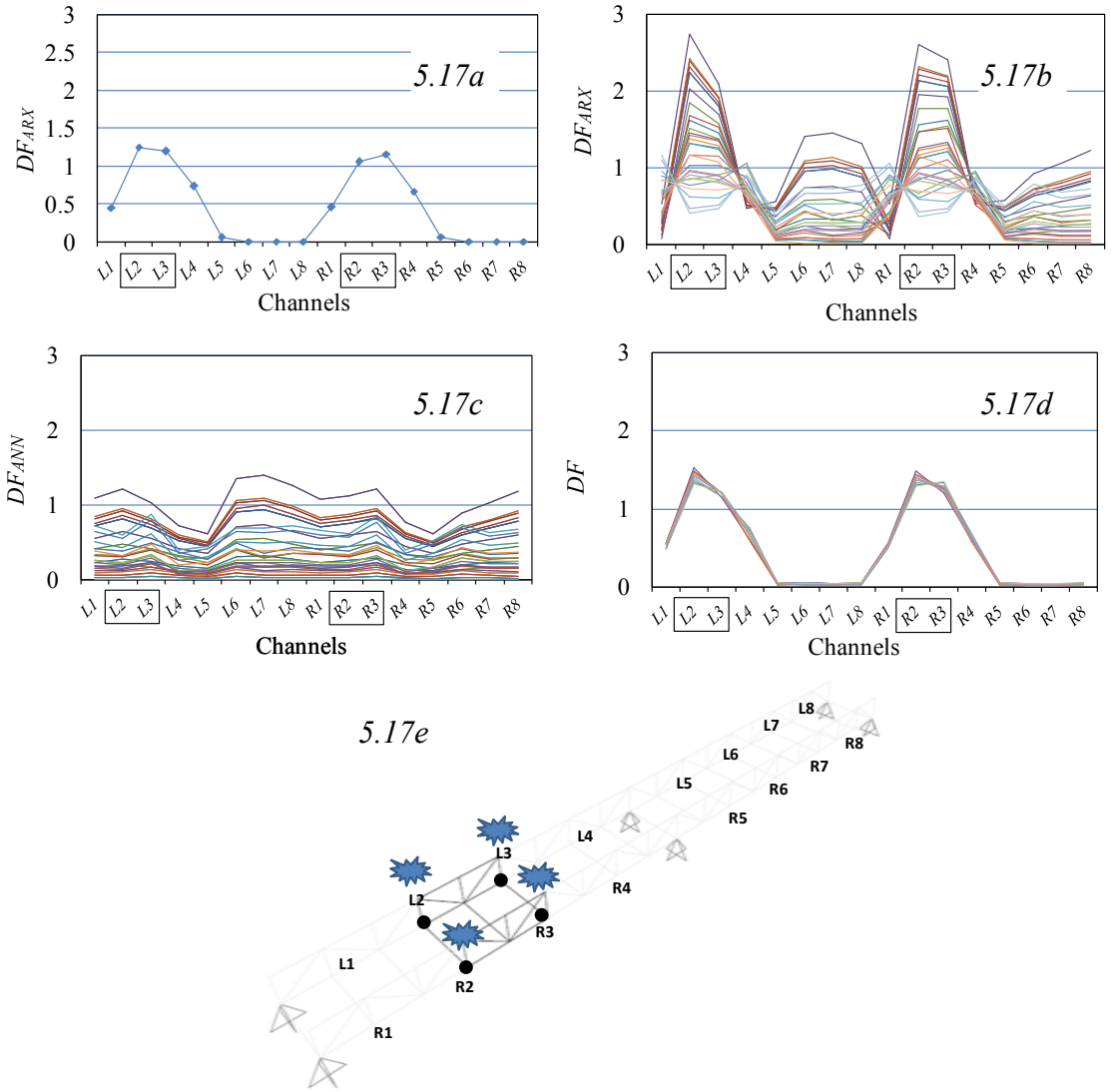

Figure 5.17. DC1 with 0% noise diagrams – (a) DF_{ARX} with damage only; (b) DF_{ARX} with damage and temperature effects; (c) Neural network output (DF_{ANN}); (d) Final values of *DF*s after correction using DF_{ANN}; (e) Damage location

5.4.2 DC1 with 1%, 3% & 5% Noise effect

In Figure 5.18a, Figure 5.19a & Figure 5.20a DF_{ARX} values are indicated for the structure with temperature effect, noise effect and damage. In Figure 5.18b, Figure 5.19b & Figure 5.20b final *DF* values are presented, where damage is still clearly indicated, but not uniformly as for the case with 0% noise. It can be concluded that as the level of noise increases, final *DFs* have less uniform pattern. This is due to the nature of the noise effect on the damage features. Noise introduces irregularity in the vibration signals, and mainly decreases the values of the damage features. Higher levels of noise will decrease damage features to a greater extent. Moreover, same levels of the noise will have different effects on the different levels of damage features. This means that specific noise will have smaller effect on the higher damage features, than on the lower damage features. This is why there is a bigger gap between the extreme values of the damage features for the higher levels of the noise. Nevertheless, even with the biggest level of noise, *DFs* in Figure 5.20b can still detect, locate and indicate severity of the damage in the structure. It is indicated that for the adjacent span, all the damage features have smaller values than the threshold, which confirms that there is no damage present in the mentioned span.

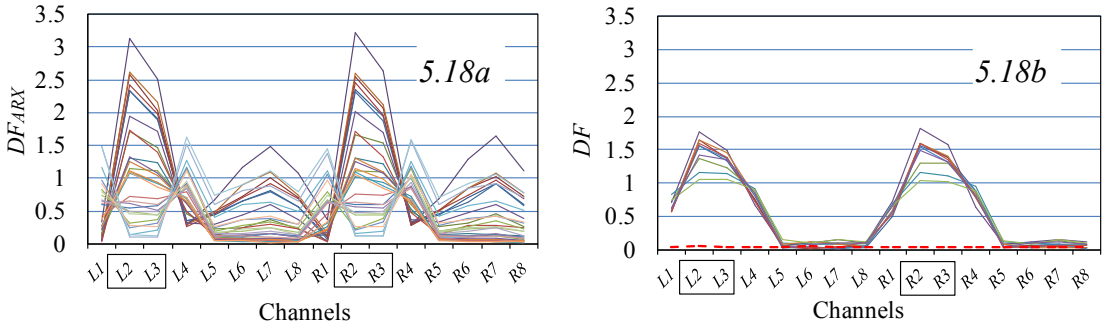

Figure 5.18. DC1 with 1% noise diagrams – (a) DF_{ARX} with damage and temperature effects; (b) Final values of *DFs* after correction using DF_{ANN}

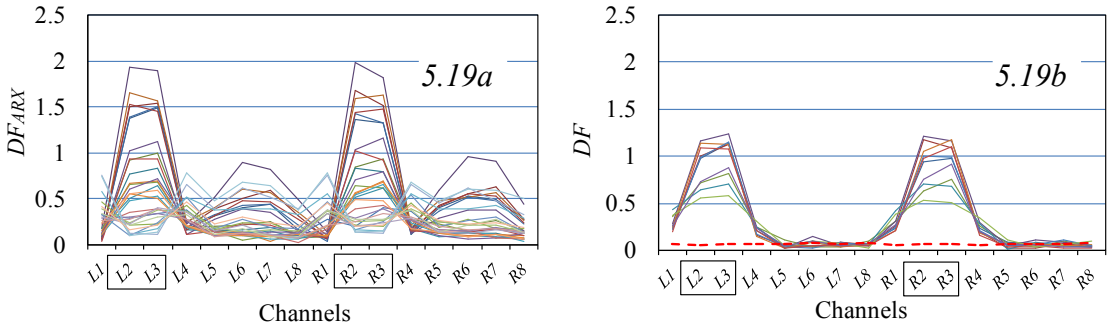

Figure 5.19. DC1 with 3% noise diagrams – (a) DF_{ARX} with damage and temperature effects; (b) Final values of *DFs* after correction using DF_{ANN}

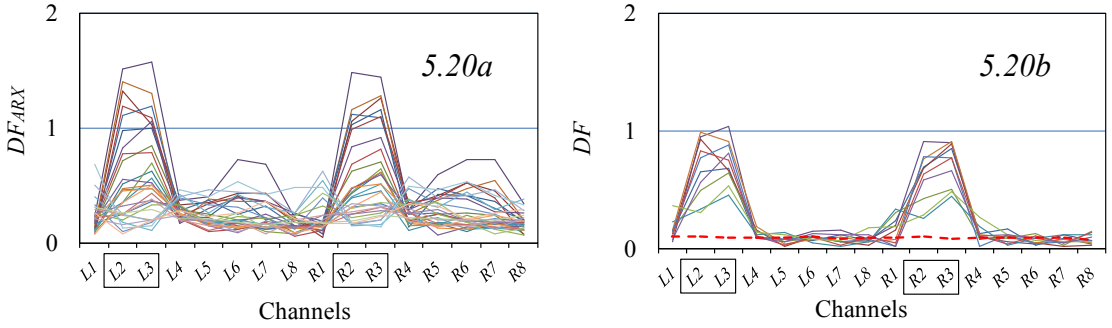

Figure 5.20. DC1 with 5% noise diagrams – (a) DF_{ARX} with damage and temperature effects; (b) Final values of *DFs* after correction using DF_{ANN}

5.5 Damage case 2 (DC2): Reduction of steel elastic modulus of 10% for all steel beams between channels L2 & L3 and R2 & R3

5.5.1 DC2 with 0% noise

This damage case is identical to DC1, except that the elastic modulus of the steel is reduced for 10%, instead of 20% as in DC1. Therefore, it is expected that the highest damage features will be at the same channel locations, but with reduced values of damage features. This is confirmed in the Figure 5.21a, where the highest damage features are observed for channels L2 & L3 and R2 & R3, with values around 0.6. If compared to the values in DC1 where the highest damage features had maximum values of around 1.2, it can be concluded that ratio of damage features is same as ratio of decrease of steel modulus – 10% vs. 20%. This relation confirms that the method can indicate the extent of the damage consistently. Figures 5.21b & 5.21c follow the same pattern as for DC1. In Fig. 5.21d it is shown that the final *DFs* match DF_{ARX} from 5.21a.

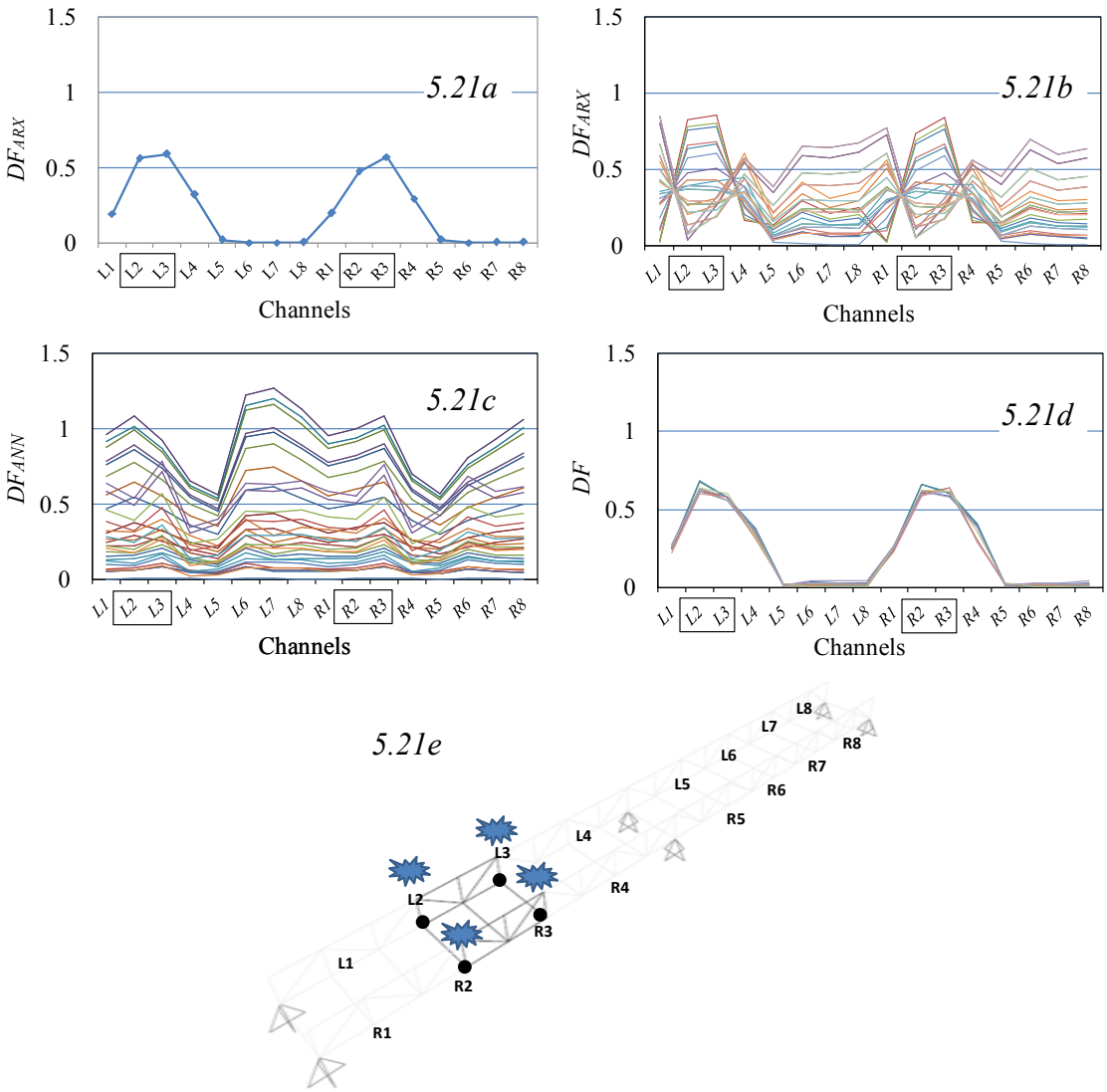

Figure 5.21. DC2 with 0% noise diagrams – (a) DF_{ARX} with damage only; (b) DF_{ARX} with damage and temperature effects; (c) Neural network output (DF_{ANN}); (d) Final values of *DFs* after correction using DF_{ANN}; (e) Damage location

5.5.2 DC2 with 1%, 3% & 5% noise

In Figure 5.22, Figure 5.23 & Figure 5.24 it is indicated that the noise affects final values of *DFs* in the same way as in DC1, and that the final values of *DFs* are approximately equal to 50% of the values in DC1. This is in accordance with the amount of the reduction of steel modulus, which was reduced for 10% in DC2, compared to the 20% in DC1. This confirms that although noise affects the final shape of the damage features, relative severity of the damage is still consistently indicated. Finally, although the amount of the damage in this damage case is 50% smaller than in DC1, location, existence and the severity of the damage is still indicated for majority of the random temperature cases. It is also presented that for the adjacent span, all the damage features have smaller values than the threshold, which confirms that there is no damage present in the mentioned span.

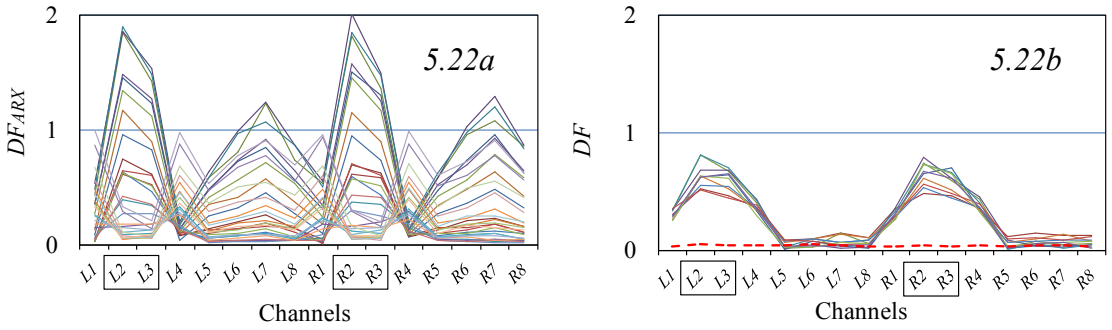

Figure 5.22. DC2 with 1% noise diagrams – (a) DF_{ARX} with damage and temperature effects; (b) Final values of *DFs* after correction using DF_{ANN}

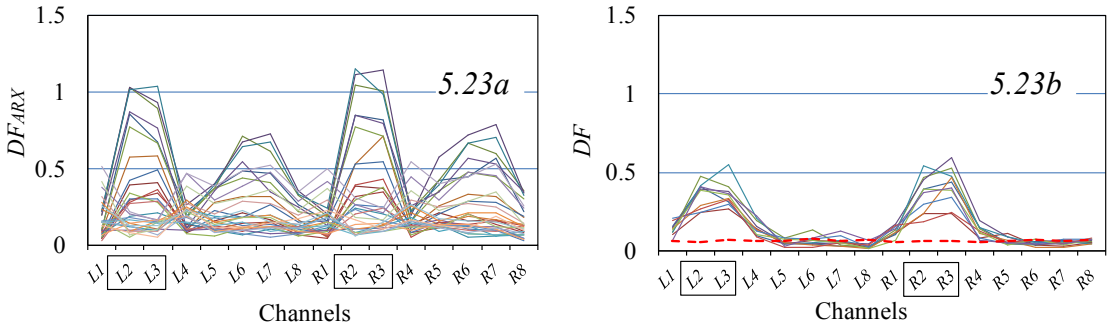

Figure 5.23. DC2 with 3% noise diagrams – (a) DF_{ARX} with damage and temperature effects; (b) Final values of *DFs* after correction using DF_{ANN}

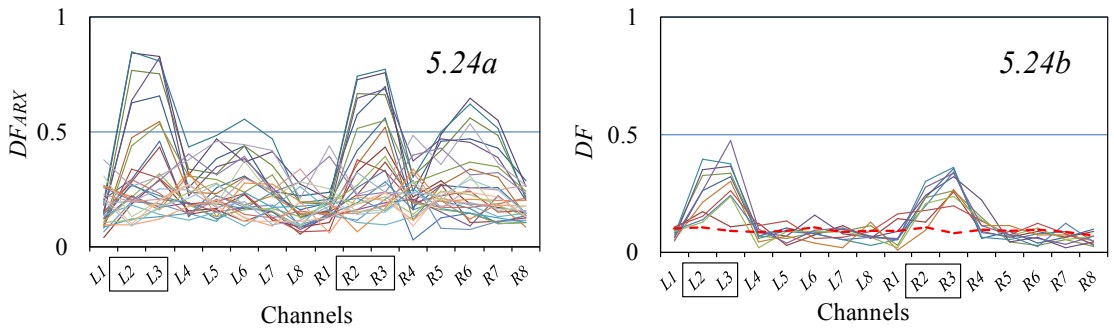

Figure 5.24. DC2 with 5% noise diagrams – (a) DF_{ARX} with damage and temperature effects; (b) Final values of *DFs* after correction using DF_{ANN}

5.6 Damage case 3 (DC3): Fixed support at channel R8 location, instead of the pinned support

5.6.1 DC3 with 0% noise

Damage case 3 is the only damage case in this study with the damage causing increase of the stiffness in the structure. The other four damage cases are applying decrease of the material modulus. Also, this damage case can be considered to be more global in nature than the other damage features, considering that it alters the boundary conditions of the structure. Considering that this damage case is more general in nature, the values of the damage features are higher than for the other damage cases. In Figure 5.25a it is indicated that the highest damage features are at the channel R8, which is the exact location of the damage. Moreover, channels L7, L8 and R7, which are the closest to the channel R8, also have higher damage features compared to the rest of the channels. With this graph, the exact path of the stiffness change due to the damage in the structure is indicated. Elements that are the closest to the damage location therefore experience the biggest change in the stiffness - damage.

In Figure 5.25b, it is shown that the detrimental effect of the temperature on damage detection process is not so pronounced as for the previous damage cases. This is due to the type of the damage, which is more global in nature, and the fact that the temperature has smaller effects on damage features with higher values. Nevertheless, it is indicated that temperature still has considerable effect on the shape of the damage features, compared to the Figure 5.25a. Finally, diagram of the final *DFs* in Figure 5.25d indicates

that this algorithm successfully determined damage features for all random temperature cases.

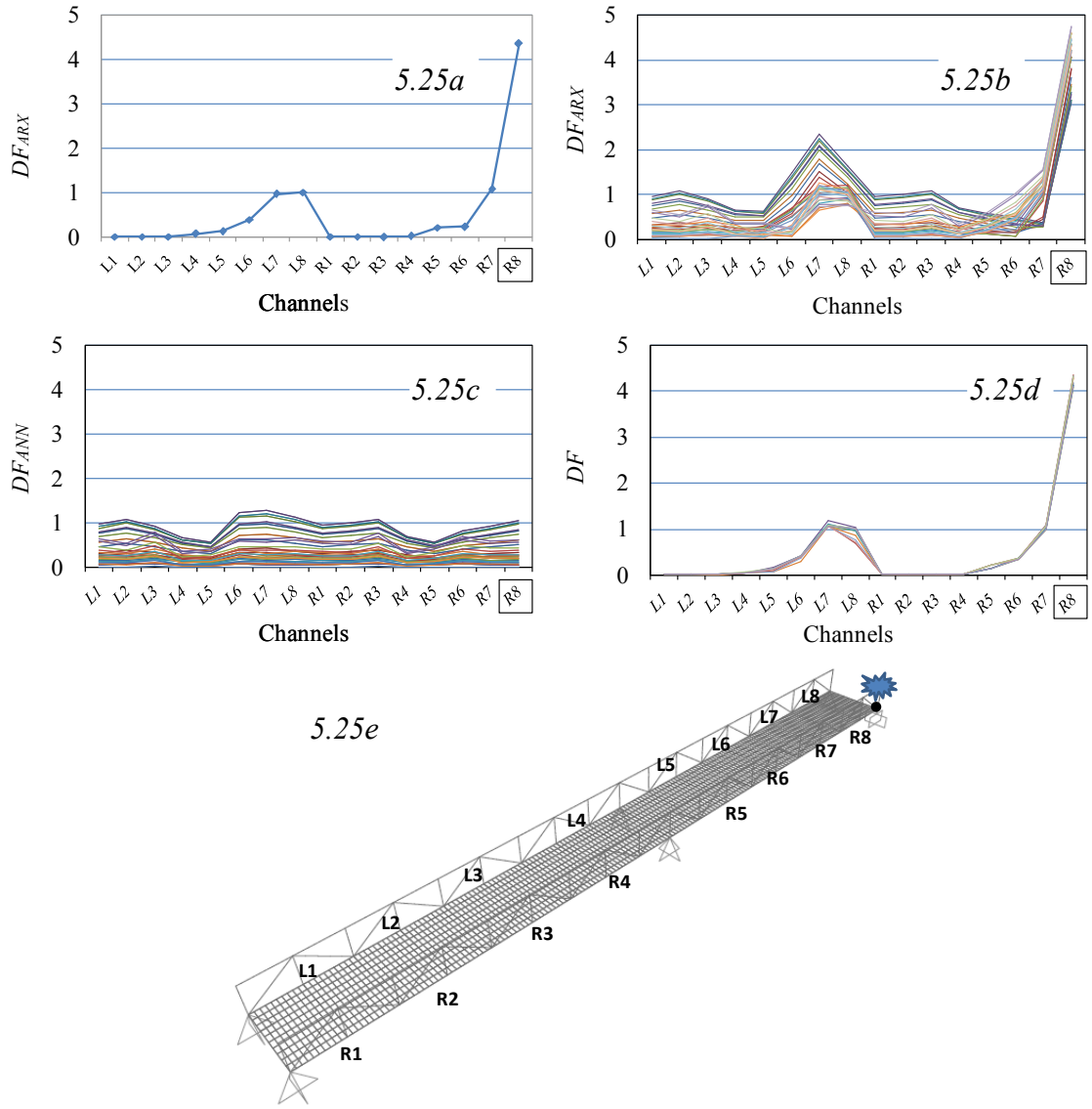

Figure 5.25. DC3 with 0% noise diagrams – (a) DF_{ARX} with damage only; (b) DF_{ARX} with damage and temperature effects; (c) Neural network output (DF_{ANN}); (d) Final values of *DFs* after correction using DF_{ANN}; (e) Damage location

5.6.2 DC3 with 1%, 3% & 5% noise

Figure 5.26a, Figure 5.27a & Figure 5.28a indicate that noise effect is not so pronounced as for the previous damage cases. Reasons for this are exactly the same as for the temperature effect – damage features have higher values than in previous damage cases, and the damage itself is more global in nature. However, noise effect is still considerable, especially considering that damage features at channel locations L7 and L8 are not so pronounced as for cases with 0% noise. As mentioned above, specific noise has smaller effect on the higher damage features, than on the lower damage features. That is why damage features at channels L7 & L8 are more influenced by the noise effect than damage features at channel R8. Damage features for channel R8 are clearly indicated with more uniform values compared to Figures 5.26a, Figure 5.27a & Figure 5.28a. These diagrams confirm that this algorithm can successfully solve damage detection problems with global damages, and with damages that cause the increase of the stiffness in the structure.

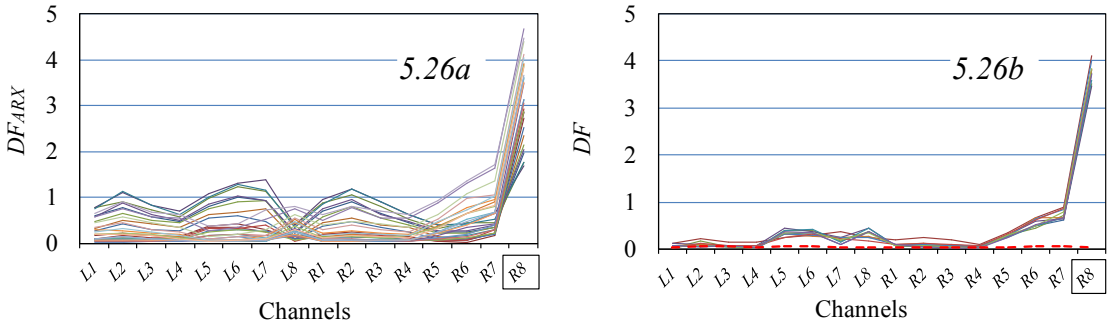

Figure 5.26. DC3 with 1% noise diagrams – (a) DF_{ARX} with damage and temperature effects; (b) Final values of *DFs* after correction using DF_{ANN}

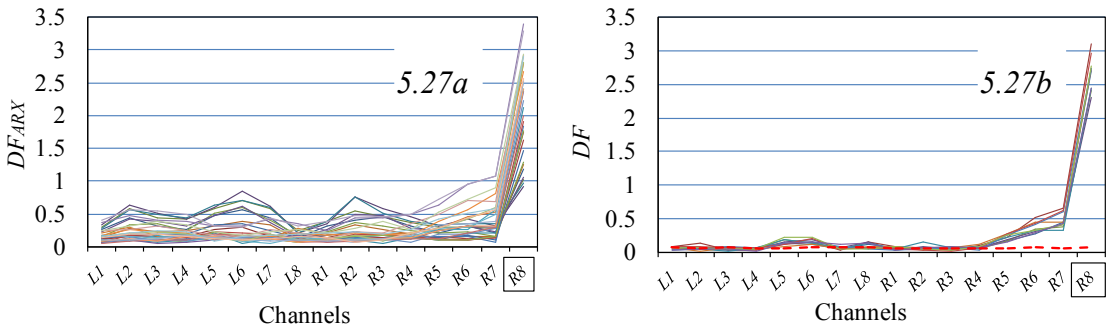

Figure 5.27. DC3 with 3% noise diagrams – (a) DF_{ARX} with damage and temperature effects; (b) Final values of *DFs* after correction using DF_{ANN}

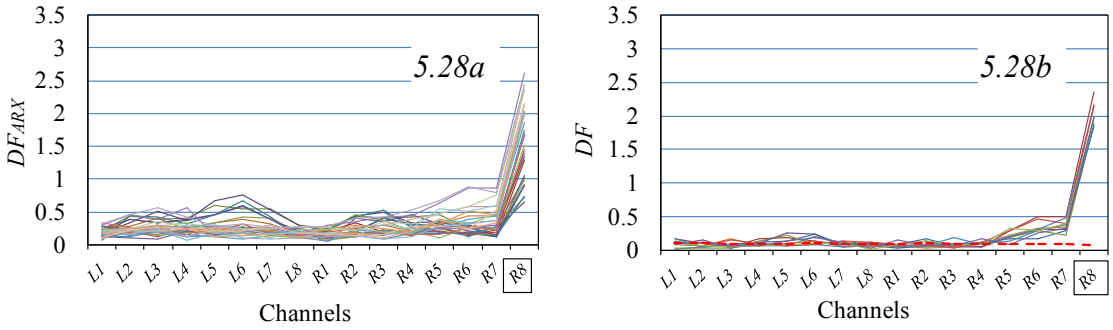

Figure 5.28. DC3 with 5% noise diagrams – (a) DF_{ARX} with damage and temperature effects; (b) Final values of *DFs* after correction using DF_{ANN}

5.7 Damage case 4 (DC4): Reduction of steel elastic modulus of 20% for all steel beams between channels L6 & L7 and R6 & R7 – symmetric case to DC1

5.7.1 DC4 with 0% noise

Damage case 4 is identical to the DC1, except the location of the damage is symmetrical in regards to the middle supports of the bridge. This means that the damage is located between channels L6 & L7 and R6 & R7. Figure 5.29a presents appropriate DF_{ARX} values, which are successfully indicating the location and extent of the damage. Figure 5.29b & 5.29c follow the same pattern as for DC1. Finally, in the Figure 5.29d, it is shown that *DF* values are corresponding to the DF_{ARX} values in Figure 5.29a, and to appropriate values in DC1. Also, it is shown that the diagram is not fully symmetric, as in DC1. This is explained by the fact that the damage location in this case is much closer to the location of the triggering forces, which are not symmetrical compared to the longitudinal axis of the footbridge. Therefore, the final graph in Figure 5.29d is not totally symmetric as in DC1. The effect of the triggering force location is further investigated in section 5.9.

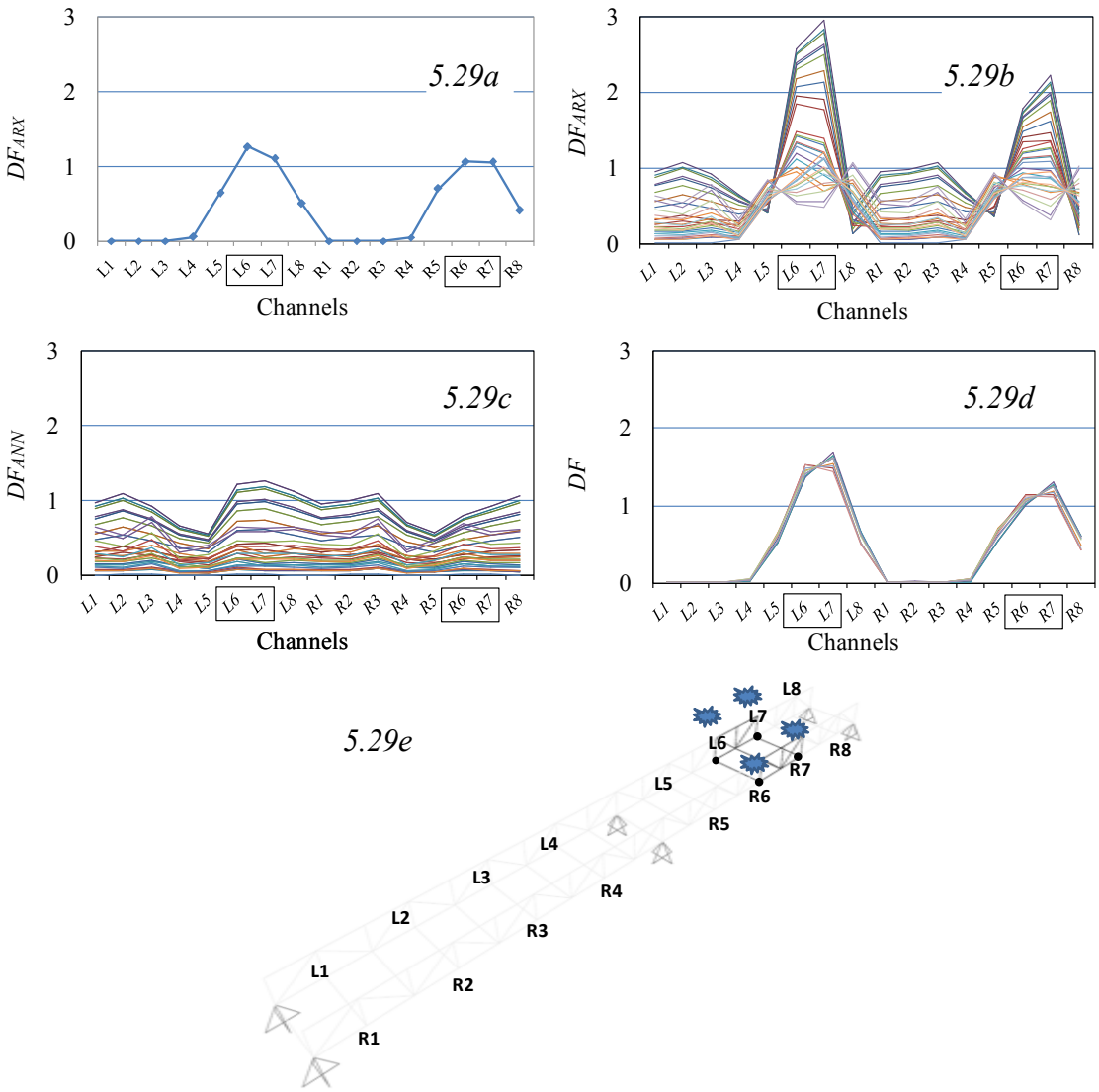

Figure 5.29. DC4 with 0% noise diagrams – (a) DF_{ARX} with damage only; (b) DF_{ARX} with damage and temperature effects; (c) Neural network output (DF_{ANN}); (d) Final values of *DFs* after correction using DF_{ANN}; (e) Damage location

5.7.2 DC4 with 1%, 3% & 5% noise

Figure 5.30a, Figure 5.31a & Figure 5.32a indicate the noise influence on the graphs with temperature effect in the structure. These figures correspond to the appropriate figures in DC1. It can be concluded that the effect of the triggering forces on these diagrams is not so pronounced as for the case with 0% noise. This damage case confirms the robustness of this damage detection method, considering that it can detect damage at various parts of the footbridge structure. It is indicated that for the adjacent span, all the damage features

have smaller values than the threshold, which confirms that there is no damage present in the mentioned span.

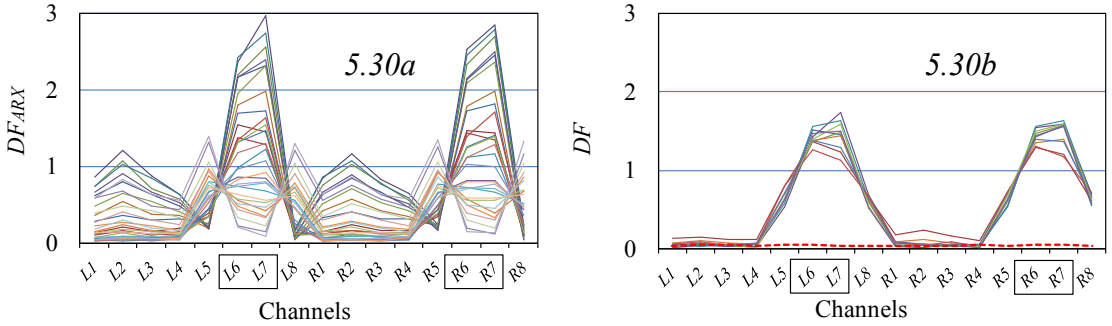

Figure 5.30. DC4 with 1% noise diagrams – (a) DF_{ARX} with damage and temperature effects; (b) Final values of *DFs* after correction using DF_{ANN}

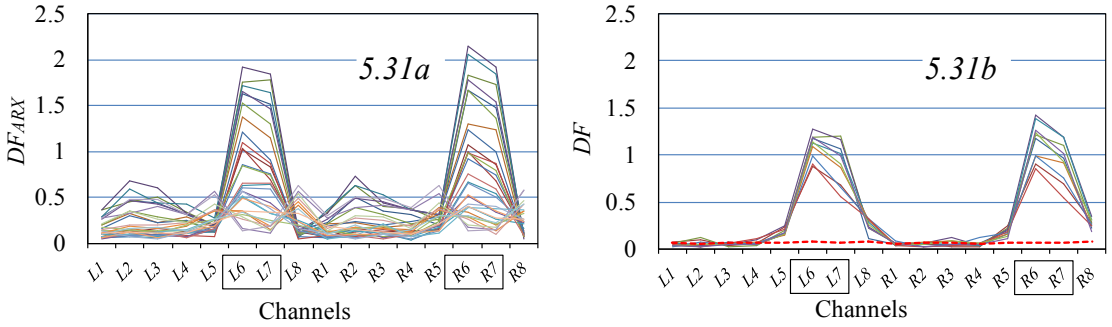

Figure 5.31. DC4 with 3% noise diagrams – (a) DF_{ARX} with damage and temperature effects; (b) Final values of *DFs* after correction using DF_{ANN}

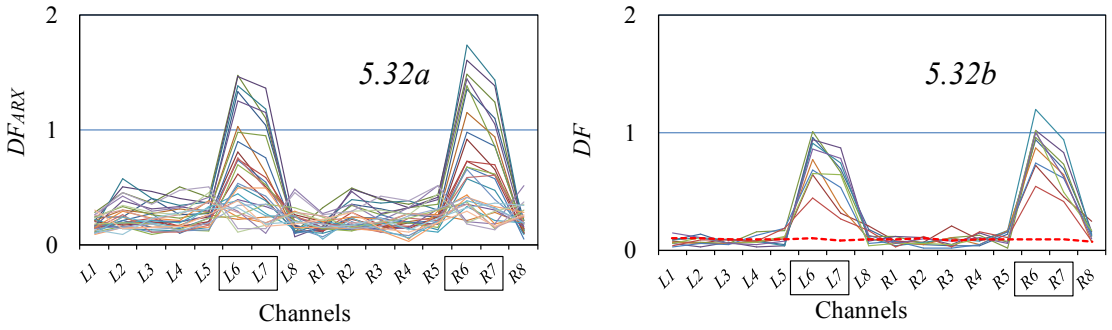

Figure 5.32. DC4 with 5% noise diagrams – (a) DF_{ARX} with damage and temperature effects; (b) Final values of *DFs* after correction using DF_{ANN}

5.8 Damage case 5 (DC5): Reduction of concrete elastic modulus of 25% for concrete deck between channels L2 & L3 and R2 & R3

5.8.1 DC5 with 0% noise

This damage case was adopted in order to investigate how temperature variability affects damage detection process due to the stiffness change of concrete material. Damage Features DF_{ARX} for the damage case only have smaller values compared to the other damage cases. This indicates that the extent of the damage in this damage case is smaller than in other damage cases. In order to verify this, frequency change analysis, due to the different applied damage cases, was conducted. Table 5.1 confirms that the smallest change in the frequency occurs in this damage case. Change in the value of the first natural frequency for DC5 is only 0.147%, compared to the DC2 where this change is 0.9%. It can also be concluded that if the concrete modulus reduces to 0%, change in first 4 modes is below 5%. This indicates that concrete slab is not contributing significantly in the structure's stiffness as the steel elements. It is indicated how this difference progresses as damage is being increased.

Considering that damage features in Figure 5.33a were not as high as in the other damage, temperature variability has bigger effect on the DF_{ARX} shown in Figure 5.33b, compared to the other damage cases. However, Figure 5.33d indicates that this damage detection procedure can successfully detect damage even with smaller values of damage features, and with change in the first natural frequency of only 0.147%.

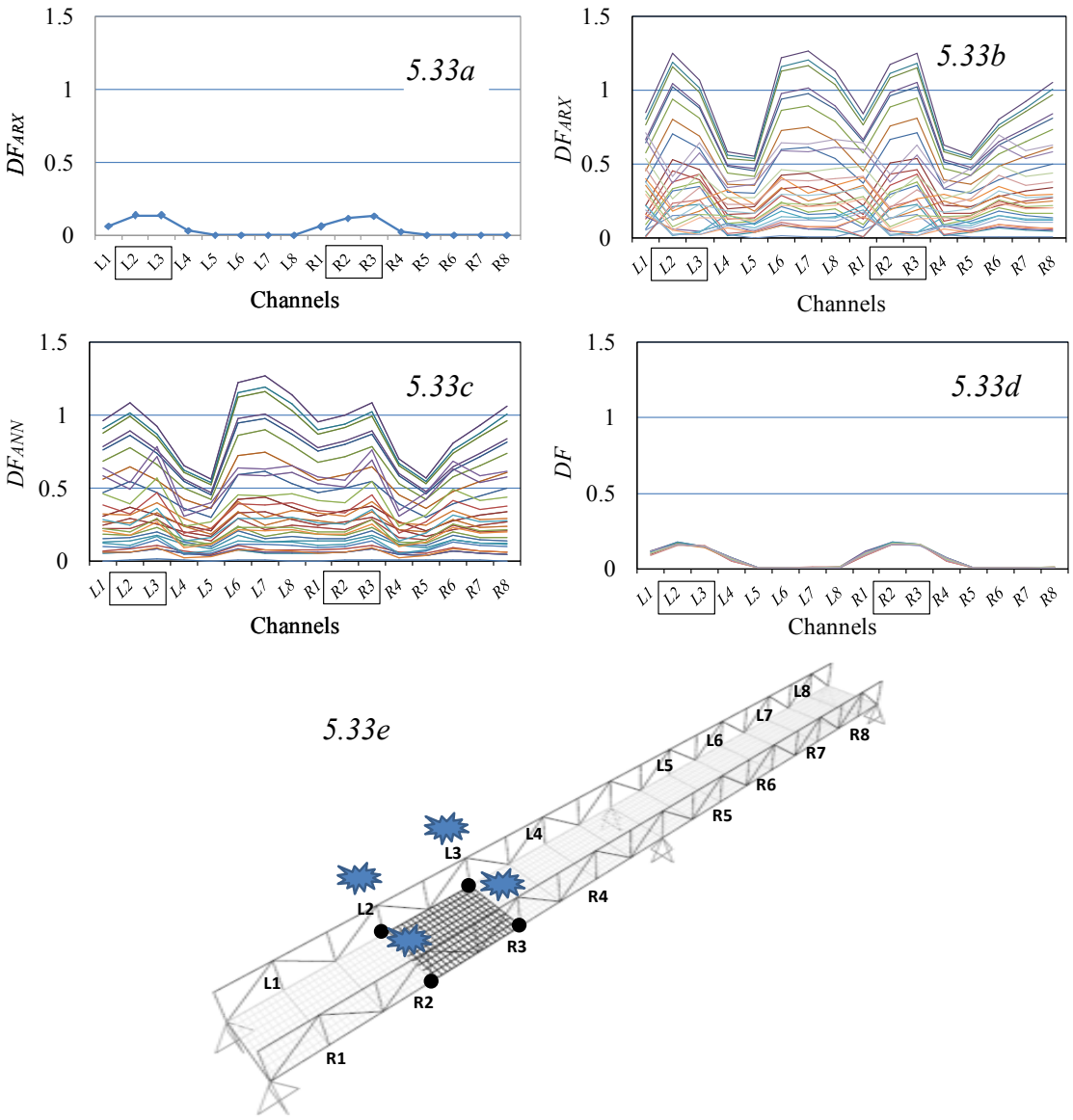

Figure 5.33. DC5 with 0% noise diagrams – (a) DF_{ARX} with damage only; (b) DF_{ARX} with damage and temperature effects; (c) Neural network output (DF_{ANN}); (d) Final values of *DFs* after correction using DF_{ANN}; (e) Damage location

5.8.2 DC5 with 1%, 3% & 5% noise

Considering that the values of the damage features are much smaller than for the other damage cases, it is presented in Figure 5.34, Figure 5.35 & Figure 5.36 that the noise has significant effect on the damage features. Therefore, this algorithm was not able to successfully determine the correct location and severity of the damage for majority of the cases with 3% and 5% noise. This is explained by the fact that concrete slab does not contribute to the stiffness of the structure as much as the other steel elements. Therefore, reduction of the stiffness in the slab is not so pronounced in the damage detection procedure as in other damage cases.

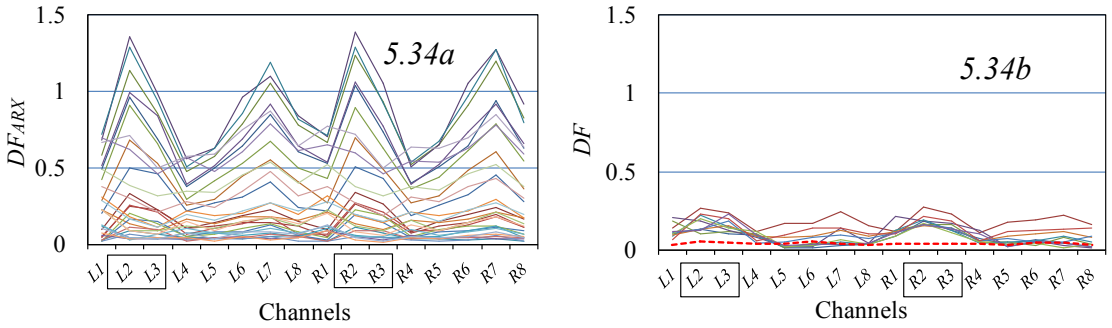

Figure 5.34. DC5 with 1% noise diagrams – (a) DF_{ARX} with damage and temperature effects; (b) Final values of *DFs* after correction using DF_{ANN}

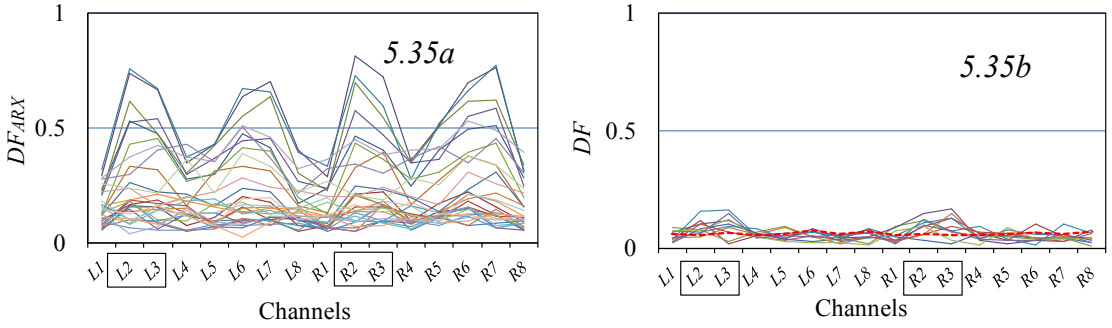

Figure 5.35. DC5 with 3% noise diagrams – (a) DF_{ARX} with damage and temperature effects; (b) Final values of *DFs* after correction using DF_{ANN}

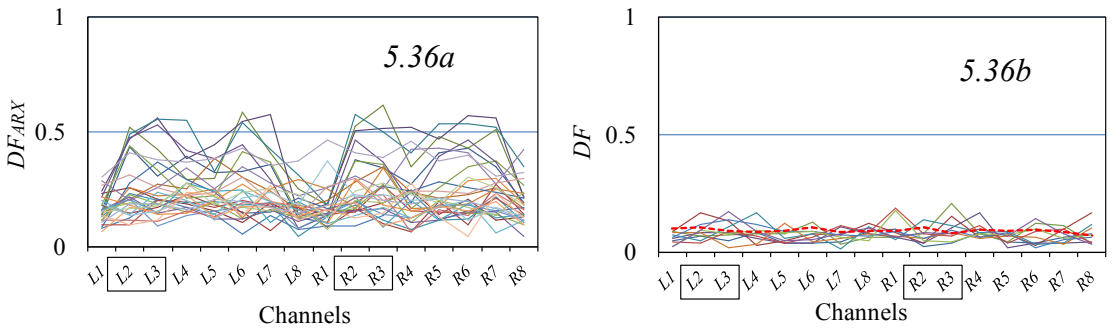

Figure 5.36. DC5 with 5% noise diagrams – (a) DF_{ARX} with damage and temperature effects; (b) Final values of *DFs* after correction using DF_{ANN}

5.9 Influence of the Impact Location

In the analysis of DC4 it was mentioned that final *DF* values were not fully symmetric, as in DC1. It was also indicated that this was due to the fact that the damage in that damage case was much closer to the location of the triggering forces. These forces by themselves are not symmetric in regards to the longitudinal bridge axis, which causes final *DFs* to be asymmetric. In order to confirm this, different impact locations of the triggering forces were used for comparison (Figure 5.37).

In Figure 5.38 it is shown that for all locations of the triggering forces, damage features diagrams follow similar pattern, with maximum values at channels L2 & L3 and R2 & R3 locations. However, as the force location becomes closer to the damage location, difference between the damage features at opposite sides of the bridge increases. This is confirmed in Table 5.2, which shows differences between the damage features of channels L3 & R3: $\frac{(DF_{L3} - DF_{R3})}{DF_{L3}} \times 100$.

This data confirms that the location of the triggering forces can alter the values of the damage features, especially if the location of the forces is close to the damage. However, effect of the location of these impact forces is not significant for the final values of damage features.

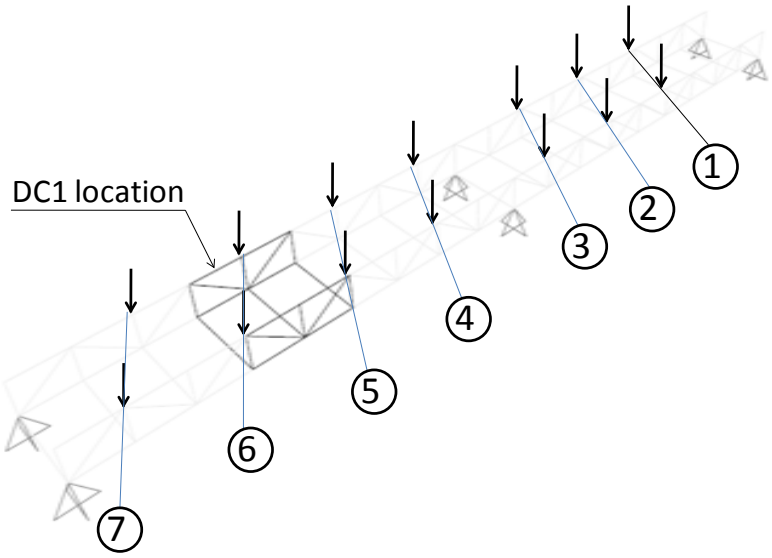

Figure 5.37. Different impact locations of the triggering forces

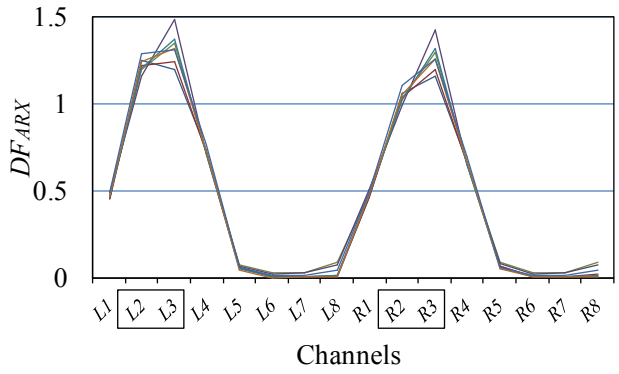

Figure 5.38. DF_{ARX} for different impact locations of the triggering forces

Table 5.2. Difference between DF_{ARX} between channels L3 & R3 for different impact locations of the triggering forces

[redacted]

CHAPTER 6:CONCLUSIONS AND RECOMMENDATIONS

6.1 Conclusions

In this thesis, a new framework to compensate detrimental temperature effects in damage detection process is presented. For the proposed framework, a time series analysis based damage detection method is employed along with backpropagation artificial neural networks for damage detection.

A finite element model of a steel footbridge structure with concrete deck and with two equal spans is used for verification of the developed methodology. Five damage cases are applied to the model, along with variable temperature effects with a range of -25°C and 55°C. These temperature effects cause change of elastic modulus for steel and concrete material, as well as additional axial forces in the structure. These two factors then alter the dynamic response of the structure.

In the time series analysis part of the method, vibration data of the structure is used to define ARX models with sensor clustering methodology, where neighbour sensors in particular cluster are used to predict the vibration behaviour of the reference sensor. Considering that time series analysis part of this method employs vibration data for damage detection, temperature variability affects the output of this method. It is demonstrated in Chapter 5 that damage features from the time series analysis part of the methods (DF_{ARX}) clearly indicate the location and extent of the damage for all five damage cases without the temperature effects. However, when temperature effects are assigned to the system, it is shown that damage is not clearly indicated with these damage features.

In order to compensate the temperature effects, backpropagation algorithm for neural networks is then applied as a next step. Neural networks are first trained with the DF_{ARX} from the healthy state with different temperature effects, where the input data consists of temperature values for three groups of elements at the bridge structure. The output of the ANN then produces damage features (DF_{ANN}) for the healthy state, at specific element

temperatures. These features represent damage features from the time series analysis based method, for temperature values acting in the damage case, but without the damage effects. Final damage features (*DF*) are then determined as absolute values of the difference between DF_{ARX} and DF_{ANN}. Temperature effects are therefore compensated with subtraction of DF_{ANN} from DF_{ARX} values.

It is presented in Chapter 5 that this methodology can successfully compensate temperature effects for all damage cases introduced to the footbridge finite element model without the noise effects and for most of the cases with the introduction of the noise effect. To the best of knowledge of the author, it is the first methodology capable of identifying and locating damage under temperature effects by using output only vibration data.

6.2 Recommendations

As already mentioned in the literature review chapter, several issues that can affect damage detection procedure in bridge structures under variable temperature effects exist. One of these issues is the change of the boundary conditions under different temperature conditions. Another important issue is the bilinear behaviour of the frequency change under different temperature effects, mostly due to the increasing stiffness of the asphalt layer at freezing temperatures. Both of these issues should be considered in the future research with this methodology. Also, for cases where the damage is small, final damage features (*DF*) become less effective when noise effects are significant. Considering that noise effects are always present in real type structures, future research should focus on minimization of the noise effects on damage detection methodology explained in this thesis.

In order to prove effectiveness and robustness of the introduced methodology, additional numerical models, as well as real type structures should be analyzed for damage detection with the same methodology. Although this methodology employed only vibration data for this study, it can also be modified for use of other type of data, such as strain data – solely or in conjunction with vibration data. Different numerical models should be included in order to include different types of structural systems under the temperature effects. Thermal gradient in longitudinal direction of the bridge can also vary, besides the

transverse gradient, which is included in this study. Real type structures include other environmental and operational effects, besides the temperature, where this issue becomes more complex. In order to prove full effectiveness of the proposed methodology, these effects should be included in the analysis. Some of the points discussed in this section are already being investigated by other members of author's research team.

REFERENCES

"AASHTO LRFD Bridge Design Specifications, Customary U.S. Units.", (2010) 5th Edition, Loose Leaf

Aktan, A.E., Tsikos, C.J., Catbas, F.N., Grimmelsman K. and Barrish R. (1999) "Challenges and opportunities in bridge health monitoring." *Proceedings of the 2nd international workshop on structural health monitoring*, CA, USA: Stanford.

Alampalli, S., (1998) "Influence of in-service environment on modal parameters.", Proc. IMAC 16 (Santa Barbara, CA) pp 111–16

Bakhary, N., Hao, H. and Deeks, A.J., (2007) "Neural network based damage detection using a substructure technique." Proceedings of the 5th Australasian congress on applied mechanics.

Balmes, E., Basseville, M., Bourquin, F., Mevel, L., Nasser, H. and Treyssede, F., (2008) "Merging sensor data from multiple temperature scenarios for vibration monitoring of civil structures." *Structural Health Monitoring*, 7:129-142.

Bandara, R.P., Chan, T.H.T. and Thambiratnam, D.P., (2014) "Frequency response function based damage identification using principal component analysis and pattern recognition technique", *Engineering Structures*, Volume 66, 116-128

Baptista, F.G., Budoya, D.E., de Almeida, V.A.D., Ulson, J.A.C., (2014) "An experimental study on the effect of temperature on piezoelectric sensors for impedance-based structural health monitoring.", *Sensors (Switzerland)*, Volume 14, Issue 1, 1208-1227

Basseville, M., Bourquin, F., Mevel, L., Nasser, H., and Treyssède, F., (2010) "Handling the temperature effect in vibration monitoring: Two subspace-based analytical approaches." *Journal of Engineering Mechanics*, 136(3), 367–378.

Box, G.E., Jenkins, G.M. and Reinsel, G.C. (2013) "Time Series analysis: Forecasting and Control." 4th Edition, John Wiley & Sons, Hoboken, NJ, USA.

Breccolotti, M,,Franceschini, G. and Materazzi, A.L., (2004) “Sensitivity of dynamic methods for damage detection in structural concrete bridges.”, *Shock and Vibration*, 11: 383–394

Brownjohn, J.M.W., de Stefano, A., Xu, Y.L., Wenzel, H. and Aktan, A.E., (2011) “Vibration-based monitoring of civil infrastructure: Challenges and successes.”, *Journal of Civil Structural Health Monitoring*, Volume 1, Issue 3-4, 79-95

“BS 5400-2: Steel, concrete and composite bridges. Specification for loads.” (2006), BSI Group

“CAN/CSA-S6-06, Canadian Highway Bridge Design Code” (2006)

Catbas, F.N., Susoy, M. and Frangopol, D.M., (2008) “Structural health monitoring and reliability estimation: Long span truss bridge application with environmental monitoring data.”, *Engineering Structures*, 30, 2347-2359.

Cornwell, P., Farrar, C.R., Doebling, S.W. and Sohn, H., (1999) “Environmental variability of modal properties,” *Experimental Techniques*, 39(6), pp. 45-48.

Cross, E.J., Koo, K.Y., Brownjohn, J.M.W. and Worden, K., (2013) “Long-term monitoring and data analysis of the Tamar bridge.” *MechSyst Sig Process* ;35:16–34.

Dackermann, U., Li, J. and Samali, B., (2013) “Identification of member connectivity and mass changes on a two-storey framed structure using frequency response functions and artificial neural networks.” *Journal of Sound and Vibration*; 332(16):3636–53.

Demuth, H. and Beale, M. (2002) “Neural Network Toolbox - For Use with MATLAB “, MathWorks

Deraemaeker, A. , Reynders, E., De Roeck, G., Kullaa, J. (2008) “Vibration-based structural health monitoring using output-only measurements under changing environment.”, *Mechanical Systems and Signal Processing*, Volume 22, Issue 1, 34-56

“DIN 1072: Road and foot bridges - design loads.”, (1985) Deutsches Institut Fur Normung E.V. (German National Standard)

Doebling, S.W., Farrar, C.R., Prime, M.B. and Shevitz, D.W. (1996) "Damage identification and health monitoring of structural and mechanical systems from changes in their vibration characteristics: a literature review.", *Los Alamos National Laboratory Report LA-13070-MS*

Doebling, S.W., Farrar, C.R., Prime, M.B. and Cornwell, P.J., (2000) "Structural Health Monitoring Studies of the Alamosa Canyon and I-40 Bridges.", *Los Alamos National Laboratory Report LA-13635-MS*

Emerson, M. (1976a) "Bridge temperatures estimated from the shade temperature", TRRL Report LR 696, Transport and Road Research Laboratory, Department of Environment, UK

Emerson, M. (1976b) "Extreme values of bridge temperatures for design purposes.", Report LR744, Transport and Road Research Laboratory, Department of Environment, London

Fan, W. and Qiao, P. (2011) "Vibration-based Damage Identification Methods: A Review and Comparative Study.", *Structural Health Monitoring*, Volume 10, Issue 1, 83-111

Farrar, C.R. and Jauregui, D.A. (1998a) "Comparative study of damage identification algorithms applied to a bridge: I. experiment.", *Smart Materials and Structures*, 7(5):704-719

Farrar, C.R. and Jauregui, D.A. (1998b) "Comparative study of damage identification algorithms applied to a bridge: II. numerical study", *Smart Materials and Structures*, 7(5):720-731

Farrar, C. R. and Worden, K. (2007) "An introduction to structural health monitoring", Phil. Trans. R. Soc. A 365, 303–315.

Fassois, S.D. and Kopsaftopoulos, F.P., (2013) "Statistical Time Series Methods for Vibration Based Structural Health Monitoring.", New Trends in Structural Health Monitoring, CISM International Centre for Mechanical Sciences

Figueiredo, E., Park, G., Farrar, C.R., Worden, K. and Figueiras, J., (2011) "Machine learning algorithms for damage detection under operational and environmental variability", *Structural Health Monitoring*, Volume 10, Issue 6, 559-572

Freeman, J.A., Skapura, D.M., (1991) "Neural networks: algorithms, applications, and programming techniques." Addison Wesley Longman Publishing Co., Inc. Redwood City, CA, USA

Fritzen, C.P., Kraemer, P. and Buethe, I., (2013) "Vibration-based Damage Detection under Changing Environmental and Operational Conditions.", *Advances in Science and Technology,* Vol 83, 95-104

Fu, Y., DeWolf, J.T., (2001) "Monitoring and analysis of a bridge with partially restrained bearings." *Journal of Bridge Engineering*, Volume 6, Issue 1, 23-29

Fujino, Y., Abe, M., Shibuya, H., Yanagihara, M. and Sato, M., (2000) "Monitoring of Hakucho suspension bridge using ambient vibration.", Workshop on Research and Monitoring of Long Span Bridges, Hong Kong, pp. 142–149.

Giraldo, D.F., Dyke, S.J., Caicedo, J.M., (2006) "Damage detection accommodating varying environmental conditions." *Structural Health Monitoring* 5:155-172.

Guan, H., (2006) "Vibration-based structural health monitoring of highway bridges.", Ph.D. Dissertation, University of California, San Diego

"Guidelines for Structural Health Monitoring – Design Manual no. 2" (2001), ISIS - Canada

Gül, M. (2009) "Investigation of damage detection methodologies for structural health monitoring." Ph.D. Dissertation, University of Central Florida, Orlando, FL, USA.

Gül, M. and Catbas, F. N. (2009) "Statistical pattern recognition for structural health monitoring using time series modeling: theory and experimental Verifications." *Mechanical Systems and Signal Processing*, 23(7), 2192-2204.

Gül, M. and Catbas, F.N. (2011) "Structural health monitoring and damage assessment using a novel time series analysis methodology with sensor clustering." *Journal of Sound and Vibration*, 330(6): 1196-1210.

Hagan, M.T. and Demuth, H.B., (1996) “Neural Network Design”, PWS Publishing Company

Hamey, C. S., Lestari, W., Qiao, P. Z., and Song, G. B. (2004) "Experimental damage identification of carbon/epoxy composite beams using curvature mode shapes." *Structural Health Monitoring*, 3(4), 333-353.

He, X., (2008) “Vibration-based damage identification and health monitoring of civil structures.”, Ph.D. thesis, Department of Structural Engineering, University of California, San Diego.

Heaton, J., (2008) “Introduction to Neural Networks for Java.”, 2nd Edition, Heaton Research, Inc.

Hios, J.D. and Fassois, S.D., (2014) “A global statistical model based approach for vibration response-only damage detection under various temperatures: A proof-of-concept study.”, *Mechanical Systems and Signal Processing*, Volume 49, Issue 1-2, 77-94

Hong, D.S., Nguyen, K.D., Lee, I.C., Kim and J.T., (2012) “Temperature-Compensated Damage Monitoring by Using Wireless Acceleration-Impedance Sensor Nodes in Steel Girder Connection.”, *International Journal of Distributed Sensor Networks*, Volume 2012, Article number 167120

Hsu, T.Y., Loh, C.H., (2010) “Damage detection accommodating non-linear environmental effects by non-linear principal component analysis”. *Structural Control and Health Monitoring* 17: 338-354.

Hu, Y.H. and Hwang, J.N., (2000) “Handbook of Neural Network Signal Processing.“ CRC Press

Hu, W.H., Mountinho, C., Magalhaes, F., Caetano, E. and Cunha, A., (2009) “Analysis and extraction of temperature effect on natural frequencies of a footbridge based on continuous dynamic monitoring.” In Proceedings of the 3rd International Operational Modal Analysis Conference. Portonovo, Italy, pp. 55–62.

Hu, W.H., Thöns, S., Rohrmann, R.G., Said, S. and Rücker, W., (2015) “Vibration-based structural health monitoring of a wind turbine system Part II:

Environmental/operational effects on dynamic properties", *Engineering Structures*, in press.

Jagannathan, S., (2006) "Neural Network Control of Non-linear Discrete-Time Systems", CRC Press

Jenkins, C.H., Kjerengtroen, L. and Oestensen, H. (1997) "Sensitivity of parameter changes in structural damage detection.", *Shock and Vibration*, 4(1): 27–37.

Karbhari, V. M. and Ansari, F., (2009) "Structural health monitoring of civil infrastructure systems." CRC Press

Kessler, S. S., (2002) "Piezoelectric-based in-situ damage detection of composite materials for structural health monitoring systems." Ph.D. Thesis, MIT, Cambridge, MA

Khanukhov, K.M., Polyak, V.S., Avtandilyan, G.I. and Vizir, P.L., (1986) "Dynamic elasticity modulus for low-carbon steel in the climactic temperature range.", Central Scientific-Research Institute of designing steel structures, Moscow, translated from *Problemy Prochnosti* 7 55–58.

Kim, C. Y., Jung, D. S., Kim, N. S. and Yoon, J. G., (1999) "Effect of vehicle mass on the measured dynamic characteristics of bridges from traffic-induced test." IMAC XIX, Kissimmee, FL, pp. 1106–1110.

Kim, J., Park, J., Lee, B., (2007) "Vibration-based damage monitoring in model plate-girder bridges under uncertain temperature conditions." *Engineering Structures*, Vol. 29, No. 7, pp. 1354–1365.

Ko, J.M., Chak, K.K., Wang, J.Y., Ni, Y.Q., Chan, T.H.T., (2003) "Formulation of an uncertainty model relating modal parameters and environmental factors by using long-term monitoring data", Proceedings of SPIE - The International Society for Optical Engineering, Volume 5057, 298-307

Ko, J.M., Ni, Y.Q., (2005) "Technology developments in structural health monitoring of large-scale bridges.", *Engineering Structures*, Volume 27, Issue 12 SPEC. ISS., 1715-1725

Koo, K.Y., Brownjohn, J.M.W., List, D.I. and Cole, R., (2013) "Structural health monitoring of the Tamar suspension bridge.", *Structural Control and Health Monitoring*, Volume 20, Issue 4, Pages 609-625

Kostić, B. and Gül, M. (2014) "Damage assessment of a Laboratory Bridge model using time series analysis.", 9th International Conference on Short and Medium Span Bridges, Calgary, Alberta, Canada

Kromanis, R. and Kripakaran, P., (2014) "Predicting thermal response of bridges using regression models derived from measurement histories", *Computers and Structures*, Volume 136, 64-77

Krose, B.J.A., P. and van der Smagt, P., (1994) "An Introduction to Neural Networks.", University of Amsterdam, Faculty of Mathematics & Computer Science

Kullaa, J. (2002) ''Elimination of Environmental Influences From Damage-sensitive Features in a Structural Health Monitoring System,'' First European Workshop on Structural Health Monitoring, pp. 742–749, DEStech Publications, Paris, Onera.

Kullaa, J. (2004) ''Latent Variable Models to Eliminate the Environmental Effects in Structural Health Monitoring.", Proceedings of the Third European Conference on Structural Control, Vol. 2, pp. S5–55–S5–58, Vienna University of Technology, Vienna, Austria.

Kullaa, J. (2005) ''Damage Detection Under a Varying Environment using the Missing Data Concept,'' Proceedings of the 5th International Workshop on Structural Health Monitoring, Stanford, CA, Stanford University, DEStech Publications, pp. 565–573.

Kullaa, J., (2009) "Eliminating Environmental or Operational Influences in Structural Health Monitoring using the Missing Data Analysis.", *Journal of Intelligent Material Systems and Structures*, Volume 20, Issue 11, 1381-1390

Kullaa, J., (2014) "Structural Health Monitoring under Non-linear Environmental or Operational Influences.", *Shock and Vibration*, Volume 2014, Article number 863494

Laory, I., Trinh, T.N., Smith, I.F.C., Brownjohn, J.M.W., (2014) "Methodologies for predicting natural frequency variation of a suspension bridge.", *Engineering Structures*, Volume 80, 211-221

Li, H., Li, S.L., Ou, J.P. and Li, H.W., (2010) "Modal identification of bridges under varying environmental conditions: Temperature and wind effects." *Structural Control and Health Monitoring* 17: 499-512

Li, J., Dackermann, U., Xu, Y.L. and Samali, B. (2011) "Damage identification in civil engineering structures utilizing PCA compressed residual frequency response functions and neural network ensembles." Structural Control and Health Monitoring; 18(2):207–26.

Liu, C., Harley, J.B., Bergés, M., Greve, D.W., Oppenheim, I.J., (2015) "Robust ultrasonic damage detection under complex environmental conditions using singular value decomposition", *Ultrasonics*, Volume 58, 75-86

Ljung, L. (1999) "System Identification: Theory for the User.", second ed., Prentice Hall, Upper Saddle River, New Jersey.

Lourakis, M.I.A., (2005) "A Brief Description of the Levenberg-Marquardt Algorithm Implemened by levmar.", Institute of Computer Science Foundation for Research and Technology - Hellas

Mehrjoo, M., Khaji, N., Moharrami, H. and Bahreininejad, A., (2008) "Damage detection of truss bridge joints using artificial neural networks." *Expert Systems with Applications*; 35(3):1122–31.

Mehrotra, K., Mohan, C.K., Ranka, S., (1997) "Elements of artificial neural networks.", MIT Press Cambridge, MA, USA

Meruane, V. and Heylen, W., (2011) "Structural damage assessment with antiresonances versus mode shapes using parallel genetic algorithms." Structural Control and Health Monitoring, Volume 18, Issue 8, 825-839

Meruane, V. and Heylen, W., (2012) "Structural damage assessment under varying temperature conditions." *Structural Health Monitoring*, Volume 11, Issue 3, 345-357

Min, J., Park, S., Yun, C. B., Lee, C. G. and Lee, C. (2012) "Impedance-based structural health monitoring incorporating neural network technique for identification of damage type and severity." *Engineering Structures*, *39*, 210-220.

Moaveni, B. and Behmanesh, I., (2012) "Effects of changing ambient temperature on finite element model updating of the Dowling Hall Footbridge," *Engineering Structures*, vol. 43, pp. 58–68.

Monnier, T., Guy, P., Jayet, Y., Baboux, J. C. and Salvia, M., (2000) "Health monitoring of smart composite structures using ultrasonic guided waves." Proc. SPIE 4073, 173-181.

Moorty, S. and Roeder, C. W. (1992) "Temperature-dependent bridge movements." ASCE, *Journal of Structural Engineering*. 118, 1090–1105.

Mosavi, A. A., Dickey, D., Seracino, R. and Rizkalla, S. (2012) "Identifying damage locations under ambient vibrations utilizing vector autoregressive models and Mahalanobis distances." *Mechanical Systems and Signal Processing*, 26, 254-267.

Moser, P. and Moaveni, B., (2011) "Environmental effects on the identified natural frequencies of the Dowling Hall Footbridge," *Mechanical Systems and Signal Processing*, vol. 25, no. 7, pp. 2336–2357.

Moyo, P., Brownjohn, J., (2002) "Detection of anomalous structural behaviour using wavelet analysis." *MechSyst Sig Process*; 16:429–45.

Nakamura, M., Masri, S. F., Chassiakos, A. G. and Caughey, T. K. (1998) "A method for non-parametric damage detection through the use of neural networks." *Earthquake engineering & structural dynamics*, 27(9), 997-1010.

Ni, Y. Q., Hua, X. G., Fan, K. Q. and Ko, J. M., (2005) "Correlating modal properties with temperature using long-term monitoring data and support vector machine technique." *Engineering Structures*, vol. 27, no. 12, pp. 1762–1773.

Ni, Y.Q., Zhou, H.F., Chan, K.C. and Ko, J.M., (2008) "Modal Flexibility Analysis of Cable-Stayed Ting Kau Bridge for Damage Identification.", *Computer-Aided Civil and Infrastructure Engineering*, 23, 223-236.

Ni, Y.Q., Zhou, H.F. and Ko, J.M., (2009) “Generalization capability of neural network models for temperature - frequency correlation using monitoring data.” *Journal of Structural Engineering*; 135:1290.

NRCC (2013) “Critical Concrete Infrastructure: Extending the life of Canada’s bridge network”, Volume 18, Number 1

Oh, C.K. and Sohn, H., (2009) “Damage diagnosis under environmental and operational variations using unsupervised support vector machine”, *Journal of Sound and Vibration*, Volume 325, Issue 1-2, 224-239

Pandey, A. K., Biswas, M., and Samman, M. M. (1991) "Damage Detection from Changes in Curvature Mode Shapes." *Journal of Sound and Vibration*, 145(2), 321-332.

Peeters, B. and De Roeck, G., (2001) “One-year monitoring of the Z24-Bridge: environmental effects versus damage events.”, *Earthquake Engineering and Structural Dynamics,* 30 (2) 149–171.

Pham, T., (2009) “The Influence of Thermal Effects on Structural Health Monitoring of Attridge Drive Overpass.” Master's thesis, Department of Civil Engineering, University of Saskatchewan, Saskatoon, Canada.

Report Card for America’s Infrastructure (2013); *(ASCE)*

Reynders, E., Wursten, G. and De Roeck, G., (2014) “Output-only structural health monitoring in changing environmental conditions by means of non-linear system identification”, Structural Health Monitoring, Volume 13, Issue 1, 82-93

Rumelhart, D.E., Hinton, G.E., Williams, R.J., (1986) “Learning representations by back-propagating errors.”, *Nature*, Volume 323, Issue 6088, 533-536

Rytter, T., (1993) “Vibration based inspection of civil engineering structure”, Ph.D. Dissertation, Department of building technology and structure engineering, Aalborg University, Denmark.

Sabeur, H., Colina, H. and Bejjani, M., (2007) “Elastic strain, Young’s modulus variation during uniform heating of concrete.”, *Magazine of Concrete Research,* 59 (8) 559–566.

Samali, B., Dackermann, U. and Li, J., (2012) "Location and severity identification of notch-type damage in a two-storey framed structure utilising frequency response functions and artificial neural networks." Advances in Structural Engineering; 15(5):743–57

Schulz, J.L., Command, B., Goble, G.G. and Frangopol, D.M. (1995) "Efficient field testing and load rating of short-and medium-span bridges.", *Structural Engineering Review*, 7(3): 181–194

Sepehry, N., Shamshirsaz, M. and Bastani, A., (2011) "Experimental and theoretical analysis in impedance-based structural health monitoring with varying temperature", *Structural Health Monitoring*, Volume 10, Issue 6, 573-585

Shiradhonkar, S. R. and Shrikhande, M. (2011) "Seismic damage detection in a building frame via finite element model updating." *Computers and Structures*, 89(23), 2425-2438.

Shoukry, S. N., Riad, M. Y. and William, G. W. (2009) "Longterm sensor-based monitoring of an LRFD designed steel girder bridge." *Engineering Structures*, Volume 31, Issue 12, 2954-2965

Shu, J., Zhang, Z., Gonzalez, I. and Karoumi, R. (2013) "The application of a damage detection method using Artificial Neural Network and train-induced vibrations on a simplified railway bridge model." *Engineering structures*, *52*, 408-421.

Siddique, A. B., Sparling, B. F. and Wegner, L. D. (2007) "Assessment of vibration-based damage detection for an integral abutment bridge." *Canadian Journal of Civil Engineering*, vol. 34, no. 3, pp. 438–452,

Simonsen, E., Janoo, V.C., Isacsson, U., (2002) "Resilient properties of unbound road materials during seasonal frost conditions." *Journal of Cold Regions Engineering*, Volume 16, Issue 1, 28-50.

Sohn, H., Dzwonczyk, M., Straser, E.G., Kiremidjian, A.S., Law, K. and Meng, T., (1999) "An experimental study of temperature effect on modal parameters of the Alamosa canyon bridge.", *Earthquake Engineering and Structural Dynamics*; 28:879-97

Sohn, H. and Farrar, C.R., (2000) “Statistical Process Control and Projection Techniques for Structural Health Monitoring.”, European COST F3 Conference on System Identification & Structural Health Monitoring, Madrid, Spain.

Sohn, H., Worden, K. and Farrar, C.R., (2002) “Statistical damage classification under changing environmental and operational conditions.” *Journal of Intelligent Material Systems and Structures* 13: 561-574.

Sohn, H., Park, G., Wait, J. R., Limback, N. P. and Farrar, C. R., (2003) “Wavelet-based active sensing for delamination detection in composite structures.” *Smart Materials and Structures*, 13, 153–160.

Sohn, H., (2007) “Effects of environmental and operational variability on structural health monitoring.”, Philosophical Transactions of the Royal Society A: Mathematical, Physical and Engineering Sciences Volume 365, Issue 1851, 539-560

Sohn, H. and Oh, C.K. (2009) “Statistical pattern recognition in structural health monitoring.”, *Encyclopedia of Structural Health Monitoring* (England: Wiley)

Torres-Arredondo, M.-A. , Sierra-Pérez,J., Tibaduiza, D.-A., Mcgugan, M., Rodellar, J., Fritzen, C.-P., (2015) “Signal-based non-linear modelling for damage assessment under variable temperature conditions by means of acousto-ultrasonics.”, *Structural Control and Health Monitoring*.

Wahab, M.A, De Roeck, G., (1997) “Effect of temperature on dynamic system parameters of a highway bridge,” *Structural Engineering International*, 7, pp. 266-270.

Wenzel, H. (2009) “Health Monitoring of Bridges”, John Wiley & Sons

Wood, M. G. (1992) “Damage analysis of bridge structures using vibrational techniques.” Ph.D. Thesis, Department of Mechanical and Electrical Engineering, University of Aston, Birmingham, UK

Worden, K. & Manson, G. (2007) “The application of machine learning to structural health monitoring”. Phil. Trans. R. Soc. A 365, 515–537.

Worden, K., Farrar, C.R., Manson, G., Park, G. (2007) "The fundamental axioms of structural health monitoring.", Proceedings of the Royal Society A: Mathematical, Physical and Engineering Sciences, Volume 463, Issue 2082, 1639-1664

Xia, Y., Hao, H., Zanardo, G. and Deeks, A.J., (2006) "Long term vibration monitoring of a RC slab: Temperature and humidity effect." *Engineering Structures* 28:441-452.

Xia, Y., Xu, Y.L., Wei, Z.L., Zhu, H.P. and Zhou, X.Q., (2011) "Variation of structural vibration characteristics versus non-uniform temperature distribution." *Engineering Structures* 33: 146-153.

Xia, Y., Chen, B., Weng, S., Ni, Y.Q. and Xu, Y.L. (2012) "Temperature effect on vibration properties of civil structures: A literature review and case studies.", *Journal of Civil Structural Health Monitoring*, Volume 2, Issue 1, 29-46

Xu, Z.D., and Wu, Z., (2007) "Simulation of the effect of temperature variation on damage detection in a long-span cable-stayed bridge," *Structural Health Monitoring*, vol. 6, no. 3, pp. 177–189.

Yam, L. H., Yan, Y. J. and Jiang, J. S. (2003) "Vibration-based damage detection for composite structures using wavelet transform and neural network identification." *Composite Structures*, 60(4), 403-412.

Yan, A.M., Kerschen, G., De Boe, P. and Golinval, J.C., (2005a) "Structural damage diagnosis under changing environmental conditions – Part 1: linear analysis." *Journal of Mechanical Systems and Signal Processing* 19: 847-864.

Yan, A.M., Kerschen, G., De Boe, P. and Golinval, J.C., (2005b) "Structural damage diagnosis under changing environmental conditions – Part 2: local PCA for non-linear cases." *Journal of Mechanical Systems and Signal Processing* 19: 865-880.

Yarnold, M.T. and Moon, F.L., (2015) "Temperature-based structural health monitoring baseline for long-span bridges", *Engineering Structures*, Volume 86, 157-167

Zhou, H.F., Ni, Y.Q. and Ko, J.M., (2010) "Constructing input to neural networks for modeling temperature - caused modal variability: Mean temperatures, effective

temperatures, and principal components of temperatures." *Engineering Structures*; 32:1747-59

Zhou, H.F., Ni, Y.Q., Ko, J.M., (2012) "Eliminating Temperature Effect in Vibration-Based Structural Damage Detection.", *Journal of Engineering Mechanics*, Volume 137, Issue 12, 785-796

Zhou, G.D. and Yi, T.H., (2014) "A Summary Review of Correlations between Temperatures and Vibration Properties of Long-Span Bridges", *Mathematical Problems in Engineering*, Volume 2014, Article number 638209

Zhu, X. and Rizzo, P., (2013) "Guided waves for the health monitoring of sign support structures under varying environmental conditions.", *Structural Control and Health Monitoring*, Volume 20, Issue 2, 36-52